Universität Bremen

Creation and optimization of a genetically encoded sensor for studying the serotonergic system

---

Dissertation des Fachbereichs 2 Biologie/Chemie

der Universität Bremen

Dezember 2022

Zur Erlangung des Doktorgrades der Naturwissenschaften

-Dr. rer. nat-

Vorgelegt von

Martin Claus Maria Kubitschke

in der Abteilung Synthetische Biologie

Betreut von

Prof. Dr. Olivia Masseck

Reviewers

1. Reviewer: Prof. Dr. Olivia Masseck

2. Reviewer: Prof. Dr. Janine Kirstein

3. Reviewer: Prof. Dr. Thomas Günther-Pomorski

Date of oral examination: 15.02.2023

Examination commission

1. Examiner: Prof. Dr. Michael Koch

2. Examiner: Prof. Dr. Olivia Masseck

3. Examiner: Prof. Dr. Janine Kirstein

4. Examiner: Prof. Dr. Andreas Dotzauer

Attending Students

1. Jana Ottens

2. Kristin Carolin Claussen

Acknowledgment

Versicherung an Eides Statt

Ich, **Martin Claus Maria Kubitschke,**

versichere an Eides Statt durch meine Unterschrift, dass ich die vorstehende Arbeit selbständig und ohne fremde Hilfe angefertigt und alle Stellen, die ich wörtlich dem Sinne nach aus Veröffentlichungen entnommen habe, als solche kenntlich gemacht habe, mich auch keiner anderen als der angegebenen Literatur oder sonstiger Hilfsmittel bedient habe.

Ich versichere an Eides Statt, dass ich die vorgenannten Angaben nach bestem Wissen und Gewissen gemacht habe und dass die Angaben der Wahrheit entsprechen und ich nichts verschwiegen habe.

Die Strafbarkeit einer falschen eidesstattlichen Versicherung ist mir bekannt, namentlich die Strafandrohung gemäß § 156 StGB bis zu drei Jahren Freiheitsstrafe oder Geldstrafe bei vorsäzlicher Begehung der Tat bzw. Gemäß § 161 Abs. 1 StGB bis zu einem Jahr Freiheitsstrafe oder Geldstrafe bei fahrlässiger Begehung.

Ort, Datum

Unterschrift

Summary

The molecule serotonin sparks the interest of scientists for over half a century. Research of the molecule led to the discovery that this molecule is important for a variety of different functions. Among other things, serotonin is released in the brain, acting as a neurotransmitter and neuromodulator. Interestingly, alterations of the brain areas where serotonin is released or synthesized in, seem to be associated to different neurological diseases like depression, fear related diseases or alzheimers.

Therefore, the ability to monitor serotonin within these neurological circuits is of great importance to understand how the changes occur, and if so, what could be done to prevent or reverse them.

In this work, a genetically encoded fluorescent biosensor for the detection of serotonin was produced. The sensor consists of two proteins, cpGFP and the 5-HT$_{1A}$ receptor, a GPCR involved in the transmission of extracellular signals into the intracellular lumen across the plasma membrane. Ultimately, the substitution of a large part of the third intracellular loop of the 5-HT$_{1A}$ receptor with cpGFP as well as various mutations in specific linker domains between the two proteins, led to the genetically encoded serotonin sensor *sDarken*.

The sensor *sDarken* is able to detect serotonin by a strong reduction of its fluorescence after binding of serotonin. Although not predominantly expressed in the membrane, the fluorescence was most intense in the membrane portions of HEK cells where *sDarken* was expressed. The sensor *sDarken* is able to detect multiple sequential applications of serotonin and showed no changes in its fluorescence response, while the cells were embedded within media with different pH values. Furthermore, other chemicals failed to induce a similar reduction in fluorescence, with the exception of the 5-HT$_{1A}$ receptor agonist 8-OH-DPAT as well as the 5-HT$_{1A}$ receptor antagonist WAY-100635, suggesting a specificity of the sensor for serotonin.

Measurement of the affinity to serotonin show that *sDarken* is capable to measure serotonin within physiological relevant concentrations. Furthermore, the introduction of a single point mutation within the 5-HT$_{1A}$ receptor as well as the substitution of cpGFP for sfcpGFP showed that it is possible to modify the

sensor's affinity to serotonin while measuring a comparable fluorescence response.

While further investigations are needed for a full characterization of *sDarken*, this sensor shows to be a promising tool for future efforts to understand serotonin and its involvement in various diseases.

Zusammenfassung

Das Molekül Serotonin weckt seit über einem halben Jahrhundert das Interesse von Wissenschaftlern. Forschung im Hinblick auf dieses Molekül führte zu den Entdeckungen, dass es für eine Vielzahl unterschiedlicher Funktionen wichtig ist. Unter anderem wird Serotonin im Gehirn ausgeschüttet, wo es Aufgaben als Neurotransmitter und Neuromodulator erfüllt. Interessanterweise wurde gezeigt, dass Veränderungen in Hirnarealen in die Serotonin ausgeschüttet oder synthetisiert wird, mit verschiedenen neurologischen Erkrankungen wie Depressionen, Angstörungen oder Alzheimer in Verbindung stehen.

Daher ist die Fähigkeit, die Ausschüttung von Serotonin in eben jenen neurologischen Schaltkreisen sichtbar zu machen, von großer Bedeutung, um die genauen Auswirkungen dieser Veränderungen zu verstehen sowie zu verstehen, wie die Veränderungen entstehen oder wodurch man sie gegenbenfalls verhindern oder rückgängig machen könnte.

In dieser Arbeit wurde ein genetisch codierter fluoreszierender Biosensor zum Nachweis von Serotonin hergestellt. Der Sensor besteht aus zwei Proteinen, cpGFP und dem 5-HT$_{1A}$-Rezeptor, einem GPCR, der an der Übertragung von extrazellulären Signalen in das intrazelluiläre Lumen durch die Membranen beteiligt ist. Letztlich führte die Substitution eines großen Teiles des dritten intrazellulären Loops des 5-HT$_{1A}$-Rezeptors durch cpGFP, sowie verschiedene Mutationen in spezifischen Linkerdomänen zwischen den beiden Proteinen zum genetisch encodierten Serotonin Sensor *sDarken*. Der Sensor *sDarken* ist in der Lage, Serotonin durch eine starke Reduktion seiner Fluoreszenz nach Bindung von Serotonin nachzuweisen. Obwohl nicht überwiegend in der Membran exprimiert, zeigte sich die Fluoreszenz in den Membranteilen von HEK-Zellen in denen *sDarken* exprimiert wurde am stärksten. Der Sensor *sDarken* ist in der Lage, mehrfache Applikation von Serotonin nachzuweisen und zeigte keine Veränderungen in der Fluoreszenzreaktion, während unterschiedliche pH-Werte im Medium der Zellen vorlagen. Darüber hinaus konnten andere Chemikalien keine ähnliche Fluoreszenzreduktion auslösen, mit Ausnahme des 5-HT$_{1A}$-Rezeptor Agonisten 8-OH-DPAT sowie des 5-HT$_{1A}$-

Rezeptor Antagonisten WAY-100635, was für eine Spezifität des Sensors für Serotonin spricht.

Messungen der Affinität von *sDarken* zu Serotonin zeigt, dass *sDarken* in der Lage ist, Serotonin in physiologisch relevanten Konzentrationen zu messen. Darüber hinaus zeigte die Einführung einer einzelnen Punktmutation innerhalb des 5-HT$_{1A}$-Rezeptors sowie die Substitution von cpGFP durch sfcpGFP, dass es möglich ist, die Affinität des Sensors zu Serotonin zu modifizieren, während eine vergleichbar hohe Fluoreszenzreaktion gemessen werden konnte. Während für eine vollständige Charakterisierung von *sDarken* weitere Untersuchungen erforderlich sind, erweist sich dieser Sensor als vielversprechendes Werkzeug für zukünftige Bemühungen, Seroronin und seine Beteiligung an verschiedenen Krankheiten zu verstehen.

Table of Contents

Table of Figures

Index of Tables

List of Abbrevations

5-HIAA	5-hydroxyindole acetic acid
5-HT	5-Hydroxytryptamine (Serotonin)
5-HTP	5-hydroxytryptophan
8-OHDPAT	7-(Dipropylamino)-5,6,7,8-tetrahydronapthalen-1-ol
AC	adenylyl cyclase
AADC	aromatic L-amino acid decarboxylase
AD	aldehyde dehydrogenase
AP-2	adapter protein-2
Arg	arginine
ATP	adenosine triphosphate
BSM	brain sphingomyelin
cAMP	cyclic adenosine monophosphate
cGMP	cyclic guanosine monophosphate
CHO cells	chinese hamster ovary cells
CHOL	Cholesterol
CniFER	cell-based neurotransmitter fluorescent engineered reporters
CNS	central nervous system
cpGFP	circular permuted Green fluorescent protein
Cys	cysteine
DA	Dopamine
DAG	diacylglycerine
DR	Dorsal raphe
EDTA	ethylenediaminetetraacetic acid
eGFP	enhanced green fluorescent protein
ERK	extracellular signal-regulated kinase
FRET	förster resonance energy transfer
GABA	gamma-aminobutyric acid
GAP	GTPase-activating proteins
GDP	guanine nucleotide diphosphate
GEF	guanine nucleotide exchange factor
GFP	Green fluorescent protein
GIRK	inward rectifying potassium channel

Gly	glycine
GPCR	G-protein coupled receptor
G-protein	Guanine nucleotide binding protein
GRK	G-protein receptor kinase
GTP	Guanin nucleotide triphosphate
HEK cells	human embryonic kidney cells
ICL3	Intracellular loop 3
JNK	c-Jun N-terminal kinase
MAO	monoamine oxidase
MAOI	monoamine oxidase inhibitors
MAP kinases	mitogen-activated protein kinases
MDD	major depressive disorder
MR	median raphe
NADH	nicotinamide adenine dinucleotide
NE	Norephinephrine
NMDAR	N-methyl-D-aspartate receptor
OCT	organic cation transporter
PBP	periplasmic binding protein
PCR	polymerase chain reaction
PEI	polyethylenimine
PH domain	pleckstrin homology domain
Phe	phenylalanine
PI3K	phosphoinosite 3 kinase
PKA	protein kinase A
PLC	phospholipase C
PnO	pontine reticular formation
POPC	(2R)-3-(Hexadecanoyloxy)-2-{[(9Z)-octadec-9-enoyl]oxy}propyl-2-(trimethylazaniumyl)ethylphosphate
Rmg	raphe magnus nucleus
Rpa	raphe pallidus nucleus
RoB	raphe obscurus nucleus
RT	Room temperature
SDS	sodium dodecyl sulfate
Src	Proto-oncogene tyrosine-protein kinase Src
SSRI	selective serotonin reuptake inhibitor

TCA	tricyclic antidepressants
Thr	Threonine
TM	transmembrane
TPH	tryptophan hydroxylase
Tris	2-Amino-2-(hydroxymethyl)propane-1,3-diol
Trp	tryptophan
Tyr	tyrosine
VDCC	voltage dependent ca^{2+} channel
WAY-100635	N-[2-[4-(2-Methoxyphenyl)-1-piperazinyl]ethyl]-N-(2-pyridyl)cyclohexanecarboxamide

1 Introduction

1.1 Serotonin

Serotonin (5-HT, 5-Hydroxytryptamine) is a molecule involved in many functions inside the organisms. Initially found as a constrictor of smooth muscle cells in the gastrointestinal tract and as a vasoconstrictor in blood it is also known for its role as a neurotransmitter/neuromodulator. (Rapport et al., 1948b; Twarog & Page, 1953; Vialli & Erspamer, 1937).

Intensive investigations linked the molecule to cognition, mood, adaptation to stress, neurogenesis, learning and memory, vasodilation, hemostasis, intestinal mobility, wound healing and inflammatory response (Gershon, 2013; Lin et al., 2014; Lucki, 1998; Mann & Oakley, 2013; Mauler et al., 2016). Additionally Serotonin is associated with different psychological disorders such as addiction, schizophrenia, depression, anxiety, Alzheimers and Parkinsons disease (Amato, 2015; Geldenhuys & Van der Schyf, 2011; Müller & Homberg, 2015; Politis & Niccolini, 2015).

In the following sections, the discovery, chemistry and the location of serotonin producing cells in the CNS (central nervous system) are presented. Afterwards the implications of serotonin in various illnesses is elucidated. Then, specific types of proteins, G-protein coupled receptors and their interaction partners are introduced. Later a closer look into the 5-HT_{1A} receptor and fluorescence proteins is given. Lastly an overview of genetically encoded biosensors is laid out.

1.1.1 The discovery of Serotonin

The initial discovery of serotonin was achieved 1937 by Vialli and Erspamer, who isolated an unknown substance which they called "enteramine" from enterchromaffine cells of the rabbit gastric mucosa. In their work, they could show that this substance is able to induce the smooth muscle contraction of the gut in rats and mice and also in the rats uterus (Vialli & Erspamer, 1937).

Eleven years later (1948) a second discovery of serotonin was made by M.M. Rapport with the help of A.A. Green, both working in the group of I.H. Page. During their work, they isolated a substance from bovine blood which acts as a vasoconstrictor. They named the substance "serotonin" (Rapport et al., 1948b, 1948a). The structure of this molecule was published one year afterwards (Rapport, 1949). Three years later, the analysis of the structure of the earlier found molecule "enteramine" showed that this substance had in fact the same chemical structure as the later found serotonin (Erspamer & Asero, 1952).

Next it was found that serotonin, in addition to its effects in the gastrointestinal tract and in the blood, acts as a neurotransmitter in invertebrates and vertebrates (Twarog & Page, 1953). After identifying serotonin in brain tissue, new research investigating serotonin as a neurotransmitter begun.

Since then, tremendous research had been done unfolding a variety of functions in the organism where serotonin is involved in. One of the latest discovered is the posttranslational modification of histones by serotonin in serotonergic cells, a process called serotonylation (Farrelly et al., 2019).

1.1.2 Chemistry of Serotonin

In animals and humans, serotonin is synthesized in a two-step reaction out of tryptophan (Fig. 1). These steps are catalyzed by the enzymes tryptophan 5-hydroxylase (TPH) and aromatic L-amino acid decarboxylase (AADC) (Azmitia, 2020).

In the first step of serotonin synthesis, tryptophan is hydroxylated at the C5 position of the aromatic ring to 5-hydroxytryphtophan (5-HTP) (Fig. 1). The catalytic enzyme TPH requires for this reaction molecular oxygen and the cofactor tetrahydrobiopterin. This reaction is the rate limiting step of serotonin biosynthesis (Welford et al., 2016).

The enzyme TPH is present in two different isoforms: TPH1 which is expressed in the periphery and pineal gland and TPH2 which seems to be mostly expressed in the brain (Walther et al., 2003). The expression of TPH is specific for cells producing 5-HT (Joh et al., 1975).

In the second step of serotonin synthesis, the enzym AADC, decarboxylates 5-HTP with the help of the cofactor pyridoxal phosphate to 5-Hydroxytryptamin (5-HT).

Serotonin is metabolized by mono amine oxidases A (MAO-A) and aldehyde dehydrogenase (AD) which leads to H_2O_2 and 5-hydroxyindole acetic acid (5-HIAA). Furthermore, it is used for the synthesis of melatonin in the pineal gland (Ganguly et al., 2002).

Tryptophan   5-Hydroxytryptophan   5-Hydroxytryptamine (5-HT, Serotonin)
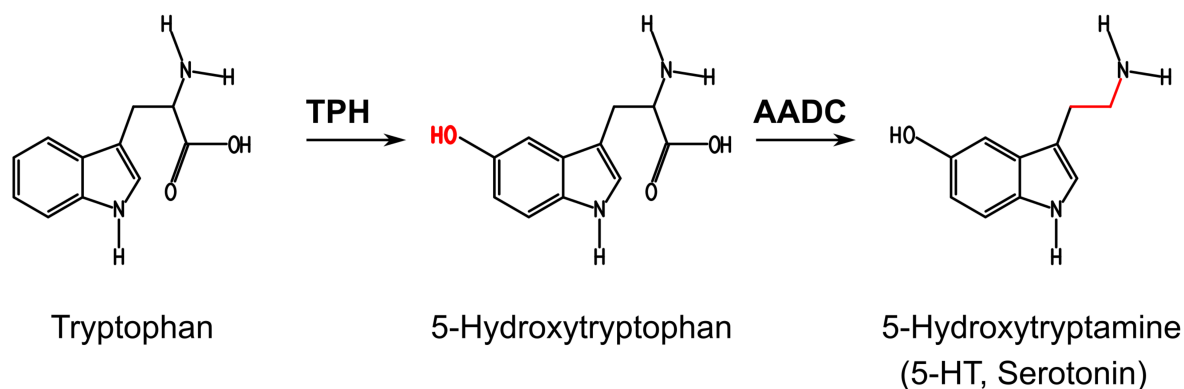
Figure 1: Serotonin Synthesis

1.1.3 Serotonergic System

In the first extensive mapping study done by Dahlström and Fuxe to find neuronal cells which contain and release serotonin, they found cellular locis flanking the midline, mostly in the raphe areas of the pons and the midbrain located in 9 groups which are designated B1-B9 (Dahlström & Fuxe, 1964).

The loci can be put together into two groups, the rostral group which is situated in the mesencephalon and rostal pons and project into the forebrain and the caudal group, which is located in the medulla oblongata and project down the spinal cord. Both groups are separated by a gap in the pons which contains non serotonergic neurons (Fig. 2).

Single cell analyses of different cells in the B1-B9 regions showed, that there are differences of serotonergic neurons within and between the nuclei, exhibiting a more complex interconnection of the serotonergic system (Calizo et al., 2011; Crawford et al., 2013; Fernandez et al., 2016; Okaty et al., 2015). Furthermore, cells in the nuclei are not

exclusively serotonergic neurons (Baker et al., 1991; Descarries et al., 1982). For example, in the region B6 and B7, which are both located in the dorsal raphe nucleus (DRN), research found dopaminergic, GABAergic, glutamatergic, peptidergic and nitergic neurons (Vasudeva et al., 2011). Serotonergic neurons seem to form true synapses in only a minority of cases and releasing serotonin non synaptically (Descarries et al., 2010). Therefore the majority of serotonergic signaling is done via volume transmission (Fuxe et al., 2010; Umbriaco et al., 1995). The different effects of serotonin are transmitted by the 14 different 5-HT receptors which show differential expression in specific areas of the brain (Mengod et al., 2010).

To complicate things further, serotonergic neurons were also shown to co release other transmitters as well as serotonin upon activation. This is suggested for glutamate (Okaty et al., 2019), gamma-aminobutyric acid (GABA) (Shikanai et al., 2012) and substance P (Hennessy et al., 2017; Okaty et al., 2015).
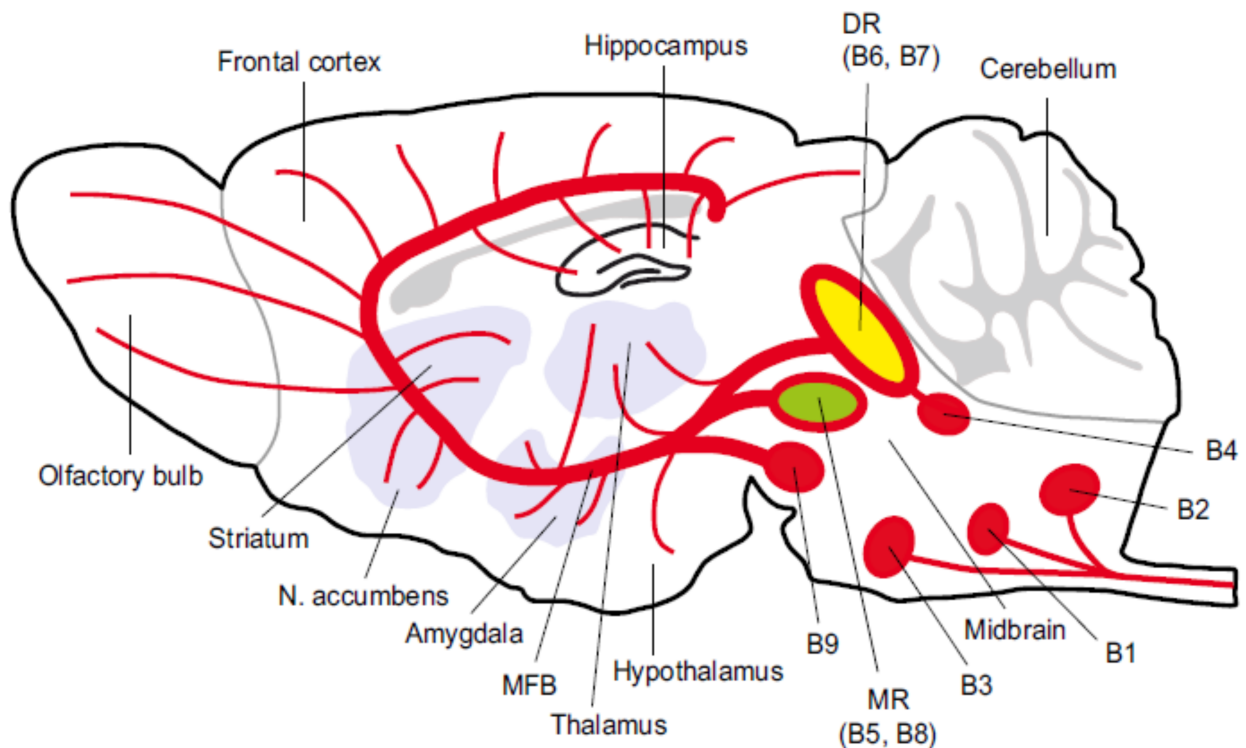
Figure 2: Overview of the serotonergic system in rodents (Lesch & Waider, 2012)

While the efferent and afferent connections of the serotonergic systems are well known, there is still lacking knowledge on how the system is functioning, due to its complex signaling mechanisms. Furthermore, changes in the serotonergic system are implicated in a variety of different diseases. One of them is major depressive disorder, a disease where after decades of research there is still lacking knowledge preventing an effective treatment of this disease. But there are hints, some of which are presented in the next paragraph, that the serotonergic system contributes in the pathology of depression.

1.1.4 Serotonin in depression

Major depressive disorder (MDD) is a severe illness affecting over 280 million people worldwide (World Health Organization 2017), across all races and socioeconomic groups.

While research was carried out over decades, the cause of depression is still not found and an effective treatment working successfully for all people is still not available, while most treatments show side effects.

One of the earliest theory regarding the cause of depression is the monoamine hypothesis, which linked deficits of the monoamines serotonin, dopamine and noradrenalin to depression (Coppen, 1967; Yohn et al., 2017).

This theory was reinforced by different findings. For example reserpine, an anti-hypertensive used in the mids 20th century led to depression in people undergoing hypertension therapy. Withdrawal of the substance led to a full recovery from symptoms of depression (Freis, 1954). Also, investigations showed that acute tryptophan depletion can lead to a recurrence of depression symptoms in patients that demonstrated remission with 5-HT antidepressants (Delgado et al., 1999; Neumeister et al., 2004) and that the cerebrospinal fluid levels of 5-HIAA, the metabolite of 5-HT, of a subset of patients with MDD appear to be lower than the control group (Asberg, 1997; Placidi et al., 2001).

First drugs which were found to treat MDD in the 1950s are the monoamine oxidase inhibitors (MAOIs), which were initially developed for the treatment of tuberculosis, as well as the tricyclics antidepressants (TCAs).

Inhibiting the monoamine oxidase by MAOIs, leads to the inhibition of the metabolization of monoamines (e.G. serotonin [5-HT], norepinephrine [NE] and dopamine [DA]) while TCAs

assumable work by inhibiting the reuptake of NE and 5-HT. The effects of both compound classes therefore are leading to the increase of synaptic levels of monoamines.

Later on, more specific drugs, namely serotonin reuptake inhibitors (SSRIs) were developed blocking the serotonin reuptake by inhibition of the serotonin transporter (SERT), increasing the synaptic levels of serotonin.

While it could be shown that depletion of monoamines by depletion of dopamine and tryptophan did not cause depressive symptoms (Salomon et al., 1997), serotonin transporter deficient mice show depressive symptoms (Ansorge et al., 2004), indicating a role of 5-HT in depression that is much more complex than only a deficit of monoamines.

One major breakthrough in the research of depression was the finding, that administration of a single dose of ketamine leads to an antidepressant response (Berman et al., 2000). While ketamine and its metabolites mainly interact with the glutamatergic system, changes affecting the serotonergic system were identified, which could explain the antidepressant response. There is evidence, that the antidepressant response is caused by stimulation of projections of the prefrontal cortex to the dorsal raphe nucleus, which stimulates serotonin release (López-Gil et al., 2019). Another group proposed, that the fast antidepressant effect of ketamine is due to blockage of N-methyl-D-aspartate receptors (NMDAR) and T-type calcium channels, inhibiting neuronal bursts of the lateral habenula, an inhibitor of the dorsal raphe nucleus, which seem to be overactive in depression (Y. Yang et al., 2018).

Depression is just one of many diseases which is accompanied with changes in the serotonergic signaling. This shows that there is an urgent need for the development of new tools which are capable of measuring serotonin dynamics. Direct measurement of serotonin dynamics could lead to new findings in the research of these diseases, which could open up new possibilities in terms of treatments or new pharmaceutical approaches. Direct measurement of serotonin is challenging but possible. There are a variety of techniques established which have been used, that are presented in the next paragraph.

1.1.5 Detecting serotonin

Different approaches have been utilized to detect serotonin in the brain. In earlier experiments, serotonin was measured by a spectromeric method, determining serotonin in the brain via a reaction of serotonin with o-pthalaldehyde. This generates highly fluorescent products which are measured for serotonin concentration determination (Maickel et al., 1968). This technique was further improved by the addition of cysteine (Curzon & Green, 1970). Other approaches utilized gas chromatography (Maruyama & Takemori, 1971) or high-performance liquid chromatography (Sasa & Blank, 1977) which was coupled to mass spectrometry (Park et al., 2013), to measure serotonin in brain tissue. Additionally, the measurement of serotonin is possible through an enzyme immunoassay, which was used to detect serotonin in the cerebrospinal fluid in the time of 3h (Chauveau et al., 1991).

To achieve higher spatial resolution to detect serotonin concentration in smaller areas and release of serotonin with single cell resolution other approaches were developed.

One technique measures the uptake of serotonin indirectly. This is done via the use of fluorescent false neurotransmitters, which are acting as substrates for serotonin transporters and vesicular monoamine transporter 2 (Henke et al., 2018).

An approach to directly measure serotonin is via the use of three photon microscopy which makes use of the autofluorescence of serotonin. With that technique the serotonin content and the release kinetics of somatic serotonergic vesicles could be investigated in dorsal raphe neurons of rats (Kaushalya et al., 2008). Furthermore, it is possible to measure serotonin *in vivo* by microdialysis, where a microdialysis probe pumps a perfusate into the brain and collects a dialysate from which the serotonin contents are measured (X. Sun et al., 2002). In a different approach direct serotonin measurement can be carried out *in vivo* by the help of fast scan cyclic voltammetry. In this technique, a microelectrode is positioned inside the brain in the area of interest and the analyte e.g. serotonin is oxidized, generating a measurable current. This technique was used to directly measure serotonin release in the substentia nigra pars reticulata in rats (Hashemi et al., 2011). Due to advancements within the field of electrode manufacturing, single synapse measurements of neurotransmitters are possible (Y.-T. Li et al., 2014). Still this technique has different drawbacks. Dependent on the molecules it is hard to distinguish between them, if they do not exhibit redox activity at different potentials for example dopamine, epinephrine and

norephinephrine (Roberts & Sombers, 2018). Furthermore reduction of sensitivity due to electrode fouling can occur over time from molecules like serotonin (Jackson et al., 1995). And for measuring serotonin release with nanoelectrodes, the limit of detection was 77 µM (Colombo et al., 2015).

In this thesis, a new genetically encoded biosensor (*sDarken*) for serotonin is developed, to measure serotonin with high spatial and temporal resolution. To understand the mechanism of action of this biosensor, within the next paragraphs, the involved proteins are described. This includes mechanism of activation and known interactions, which are briefly discussed.

1.2 G-Protein coupled receptors (GPCRs)

The term G-protein coupled receptor (GPCR) defines a family of around 600 integral membrane proteins in the human genome, which make up one of the biggest protein superfamily (International Human Genome Sequencing Consortium et al., 2001; Venter et al., 2001).

Proteins of the GPCR family are divided into the different classes A-F based on phylogenetics analysis (Fredriksson et al., 2003). Of these classes, the biggest and best investigated is the class A (rhodopsin like) GPCR family with over 650 known receptors (Gloriam et al., 2007), which are further subdivided into four main groups α, β, γ and δ.

Each class has a distinctive characteristics, for example Class A GPCRs contain mostly the NsxxNPxxY motif in the transmembrane VII or the D(E)-R-Y(F) motif in the second intracellular loop (Fredriksson et al., 2003).

One feature of all GPCRs is, that they consist of an extracellular N-terminus with seven transmembrane domains spanning through the membrane, bound together by three extracellular and three intracellular loops, ending in an intracellular C-terminus (Fig. 3).

There is an extreme variability of ligands of different GPCRs. Ligands for GPCRs can be anything from single photons to ions, lipids, nucleotides, amines, peptides, or even proteins (Fredriksson et al., 2003). Ligands can either bind at the binding site of the endogenous transmitter of the receptor, which is called the ortosteric site or to other sites within the receptor which are called allosteric sites. Ligands of GPCRs which are binding

to the ortosteric binding site act either by stimulating a submaximal to maximal activation of the receptor (agonists), blocking the activation of the agonist (competitive antagonist) or by inhibiting the endogenous activity of the GPCR (inverse agonist). Ligands binding to the allosteric binding sites of the receptor have little to no effect on the receptor activity by themselves, but they are able to amplify or diminish the effect of ligands binding at the ortosteric binding site (Jensen & Spalding, 2004; Wingler & Lefkowitz, 2020).

The activation of GPCRs by their agonists can lead to activation of three different classes of proteins, leading to different intracellularly activated signaling cascades. These proteins include Heteromeric Guanine nucleotide-binding proteins, G-protein-coupled receptor kinases (GRKs) and β-Arrestin (Kahsai et al., 2018).
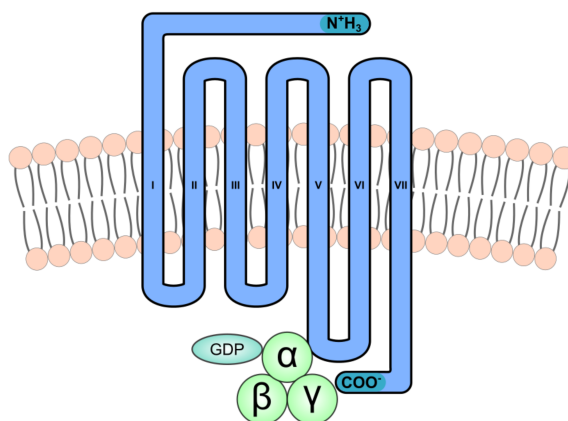
Figure 3 The basic GPCR structure with bound G-protein

Even in the absence of any GPCR ligand, the GPCR is in constant motion. There are fast fluctuations occurring, in the timeframes of femto- to nanoseconds, by changes in the lengths of chemical bonds, changes of angles between chemical bonds and changes by motions of the amino acid side chains. Also, there are slower movements occurring, within nano- to milliseconds, which involves motions in the helices, the receptor loops or rearrangements of side chains which are embedded in the interior of the protein. While the

conformation is changing fast and constantly, the transition between conformational states is slow. But due to the fast small movements within the conformational states, the protein can adopt a large number of closely related structures (Henzler-Wildman & Kern, 2007).

The stabilization of specific conformational states can be affected by ligands, binding of intracellular proteins, by dimerization occurring with other GPCRs, by post translational modifications and by changes in pH or lipid composition in the membrane where the GPCR is embedded (Latorraca et al., 2017).

When activated by a ligand and subsequent switching of the conformational state of the GPCR to an active conformation, the receptor undergoes specific rearrangements which seems to be particular important for its functionality. Ligand binding induces a shift in transmembrane domain 3 (TMD) with a rearrangement of TMD3-5, which form new contacts with TMD5-TMD6. This causes a rearrangement of TMD6 resulting in a large rotation (Venkatakrishnan et al. 2013). It rotates and swings around, away from the center of the helix bundle, with a different extent dependent on the receptor (Deupi & Standfuss, 2011). This can be the magnitude of 14 Å, which is the case for the β_2-Adrenergic Receptor in complex with a G-protein (Rasmussen et al., 2011).

1.3 Heteromeric G-Proteins

Heteromeric guanine nucleotide binding proteins (G Proteins) are major players in the intracellular signalling cascades which are activated by the activation of GPCRs by their respective agonists. These proteins are composed of three subunits named Gα, Gβ and Gγ.

The Gα proteins are classified on their sequence homology and divided into four major groups: Gs, Gi/0, Gq/11, G12/13. In total there are 21 human Gα isotypes which are encoded by 16 genes (Downes & Gautam, 1999; Simon et al., 1991).

The different families of Gα subunits have been shown to regulate adenylyl cyclases (AC), cGMP phosphodiesterases, phospholipase C (PLC) and RhoGEFs (Kristiansen, 2004; Milligan & Kostenis, 2006).

For the Gβ/γ subunit, there are 5 Gβ (Clapham & Neer, 1997) and 12 Gγ (Huang et al., 1999; Simon et al., 1991) isoforms identified in the human and mouse genome.

The different Gβ/γ subunits have been shown to regulate the recruitment of GRKs to the membrane (GRK2/3), they are involved in the regulation of different channels like the inward rectifier potassium channel (GIRK) or voltage-dependent Ca^{2+} channels (VDCC), and are able to regulate ACs, PLC, phosphoinosite 3 kinase (PI3K) and mitogen-activated protein kinases (Map Kinases) (Khan et al., 2013; Smrcka, 2008)(Fig. 4).

The subunits Gα and Gγ are attached to the plasmamembrane by post translational modifications. The Gα subunit is N-myristoylated at the N-terminus, a process which is amplified by N-palmitoylation (C. A. Chen & Manning, 2001). The Gγ subunit is anchord to the membrane through C-terminal prenylation of a specific CAAX motif. The CAAX motif determines the type of prenylation (Wedegaertner et al., 1995).

In the inactive state the GDP is bound to the Gα subunit, which is associated with the Gβ/γ subunit, forming an heterotrimer which is inactive. Ligand binding to GPCR and subsequent structural rearrangements induce conformational changes within the G-protein, bound to the GPCR. This promotes the dissociation of guanosine diphosphate (GDP) from the Gα subunit (Toyama et al., 2017). Then Guanosine triphosphate (GTP) is bound to the GDP free binding site of the GPCR-G-protein complex, which results in a conformational change of the G-protein triggering the dissociation of Gα and the Gβ/γ dimer. Both subunits are now active, interacting with different proteins, triggering a variety of intracellular pathways.

The Gα subunit possesses an intrinsic GTPase activity which triggers the re-association of the Gα subunit with the Gβ/γ dimer through hydrolysation of GTP to GDP, inactivating both subunits. Modulating proteins which are able to interact with Gα subunits like GTPase-activating proteins (GAPs) can increase the intrinsic GTPase activity, terminating the activity of the G-protein subunits faster (Kimple et al., 2011; Ross & Wilkie, 2000).
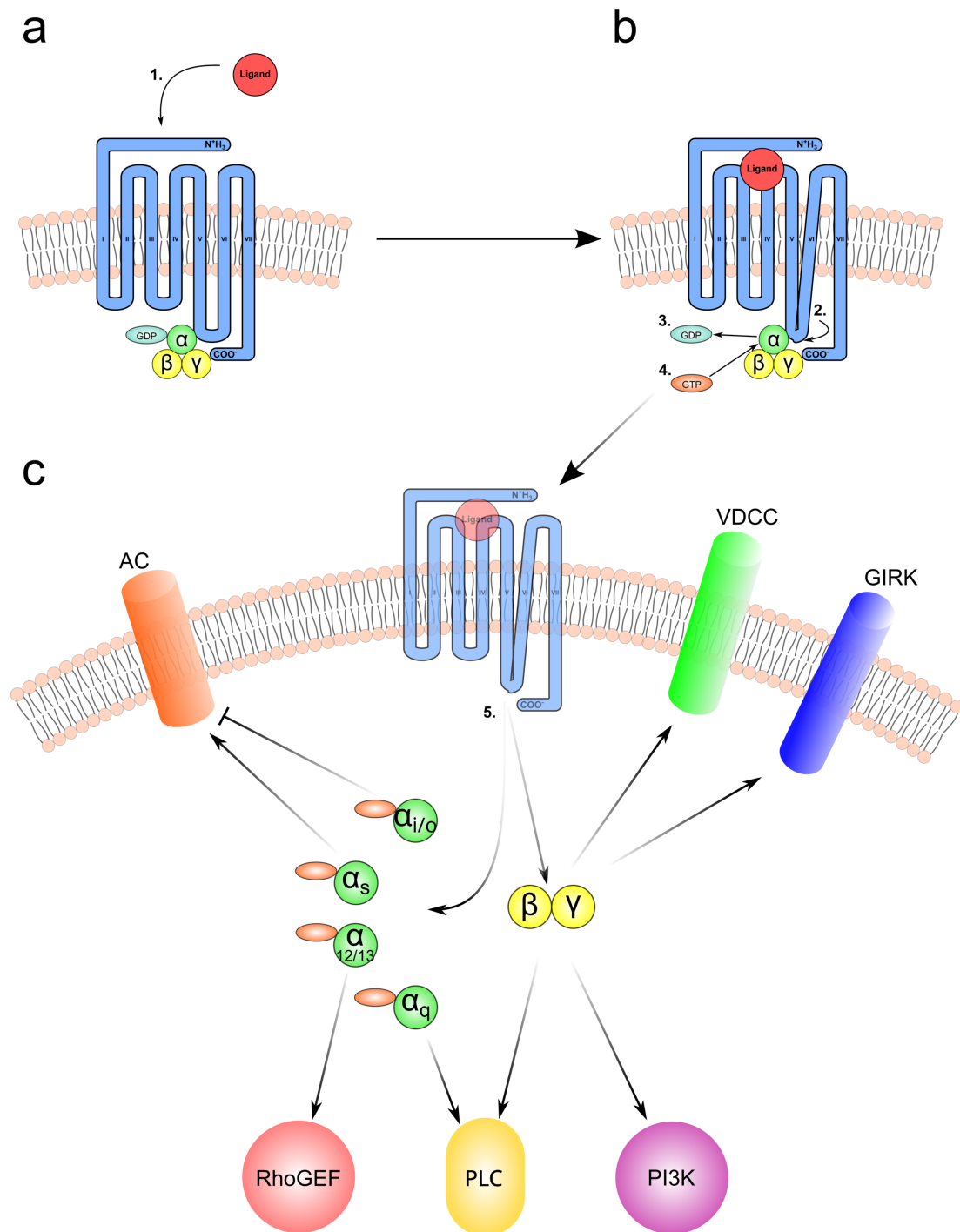
Figure 4: Activation of G-protein signaling cascades triggered by GPCR ligand binding;

After ligand binding (a, 1.) the GPCR undergoes a conformational change (b, 2.). This leads to dissociation of GDP (b, 3.) and association of GTP (b, 4.) within the Gα subunit of the G-protein. The α and β/γ subunits dissociated (c, 5.) and activate different intracellular pathways dependent on the subunits activated.

1.4   G protein coupled receptor Kinases

G protein coupled receptor kinases (GRKs) phosphorylate intracellular domains of GPCRs regulating their downstream signaling through G protein dependent and independent pathways.

This protein family consists of GRK1 (Weller et al., 1975), GRK2 (Benovic et al., 1986), GRK3 (Benovic et al., 1991), GRK4 (Ambrose et al., 1992), GRK5 (Kunapuli & Benovic, 1993), GRK6 (Benovic & Gomez, 1993) and GRK7 (Hisatomi et al., 1998; E. R. Weiss et al., 1998). The expression of GRKs 1 and 7 is mostly limited to rod and cone photoreceptors and pinealocytes (Pugh & Lamb, 2000; Somers & Klein, 1984; X. Zhao et al., 1997), while isoforms of the other GRKs are expressed in every mammalian cell (E. V. Gurevich et al., 2012).

GRKs are associated to the membrane differently between subfamilies. GRKs can be prenylated at their c-terminal end (GRK1 and 7), recruited to the membrane through their pleckstrin homology (PH) domain (GRKs 2 and 3), or are membrane associated by palmitoylation of cysteins in their c-terminal end (GRKs 4, 5 and 6) or through an amphipathic helix which interacts with membrane phospholipids (GRKs 4, 5 and 6).

GRKs remain in inactive form and are activated due to their interaction with active GPCRs. Once activated they are able to phosphorylate proteins in particular GPCRs, using adenosine triphosphate (ATP), at side chains of serine or threonine residues. The occurrence of GPCR phosphorylation can lead to inactivation of G-protein mediated signaling of GPCRs through binding of β arrestins (V. V. Gurevich & Gurevich, 2019).

1.5   β-Arrestin

The arrestin family is composed of 4 proteins named arrestin 1-4. Two of these proteins, arrestin 1 and 4 are expressed in the retina while arrestin 2 and 3 are universally expressed and are generally referred to as "β-arrestin 1" and "β arrestin 2" (Alvarez, 2008; Ferguson, 2001). Characteristic for the arrestin family is their capability to interact with activated G-protein coupled receptors (Peterson & Luttrell, 2017).

When GPCRs are active, GRKs are able to phosphorylate intracellular aminoacids of the GPCR. This generates a binding site for β-arrestins within the active GPCR. The binding of

β-arrestins stabilizes the GPCRs active conformation with high agonist affinity, which is similar to the complex of ligand-GPCR-heteromeric G-protein in the absence of GTP (De Lean et al., 1980; V. V. Gurevich & Benovic, 1997). This complex leads to an exclusion of G-proteins to interact with the GPCR, a process called desensitization (Attramadal et al., 1992; Lohse et al., 1992). Furthermore, both β-arrestins are directly interacting with the clathrin heavy chain and the β2 adaptin subunit of the adapter protein-2 (AP-2) which leads to clustering of the receptor in clathrin coated pits ultimately leading to receptor endocytosis (Fig. 6) (Goodman et al., 1996; Krupnick et al., 1997; Laporte et al., 1999, 2000). Dependent on specific phosphorylated serine residues in the carboxyterminal tail of the receptor, GPCRs are either slowly or fastly dephosphorylated, recycled and resensitized (Oakley et al., 1999).

Interaction of β-arrestins with different proteins were found, showing a possible heteromeric G-protein independent signaling by GPCRs. Proteins which exhibit interactions with β-arrestin include Src family tyrosine kinases (Barlic et al., 2000; Luttrell et al., 1999), extracellular signal-regulated kinase 1 and 2 (ERK1/2), (DeFea et al., 2000), Ser/Thr protein phosphatase (PP)2A (Beaulieu et al., 2005), E3 ubitiquin ligases and deubiquitinases (Shenoy et al., 2001, 2008, 2009), second messenger degrading cAMP phosphodiesterases (cyclic adenosine monophosphate, PDE) (Perry et al., 2002),diacylglycerol kinase (Nelson et al., 2007), elements of the nuclear factor κB (NfκB) signaling pathway (Witherow et al., 2004) and regulators of small GTPase activity (Bhattacharya et al., 2002; Claing et al., 2001).
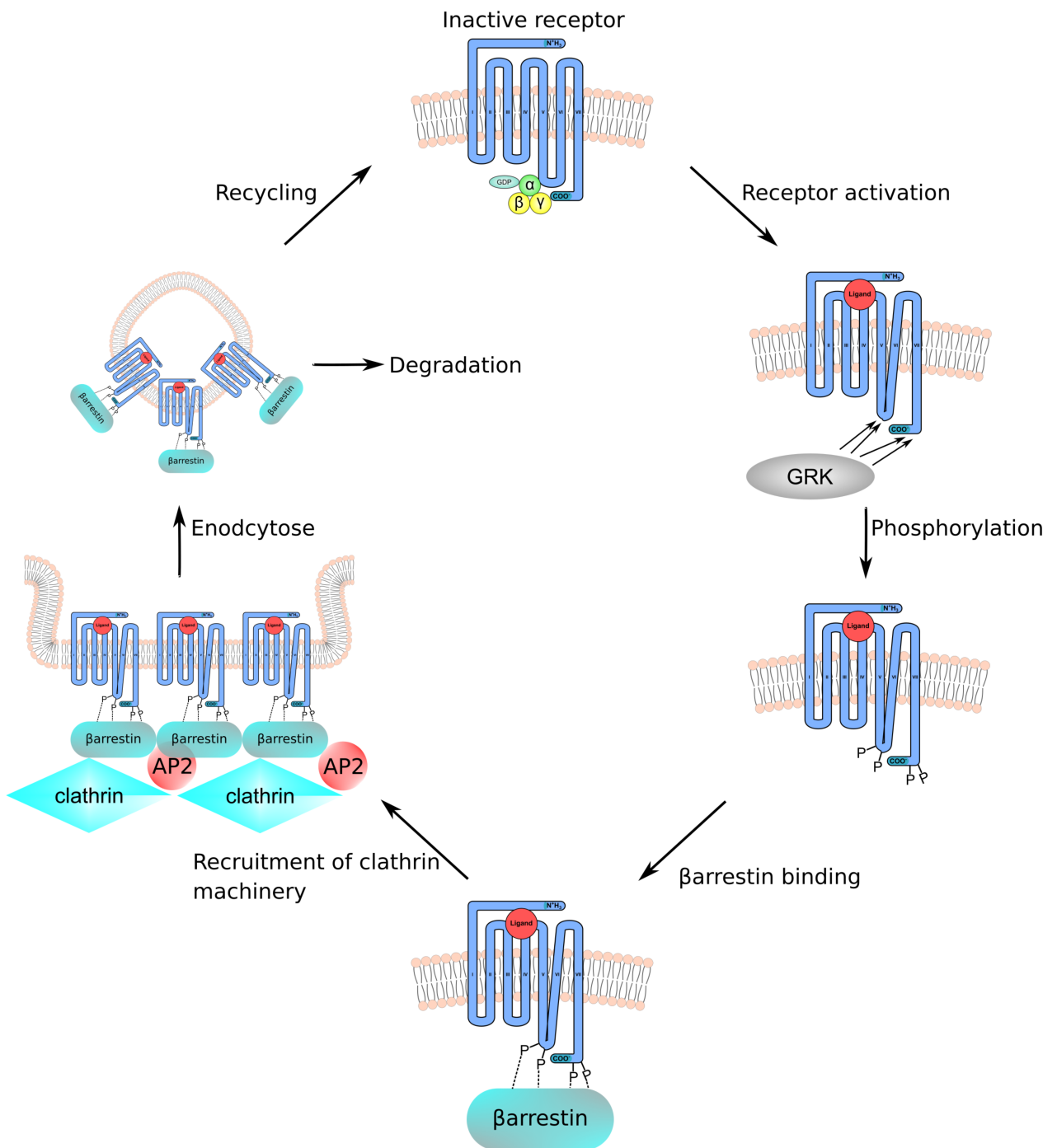
Figure 5: Scheme of β-arrestin binding and receptor internalization of active GPCRs.

1.6 5-HT$_{1A}$ Receptor

The 5-HT$_{1A}$ receptor is one of 14 receptors of the 5-HT receptor family. With the exception of the 5-HT$_3$ receptor, which is a cation channel, all 5-HT receptors are found in the amine group cluster of class A GPCRs (rhodopsin like) (Fredriksson et al., 2003).
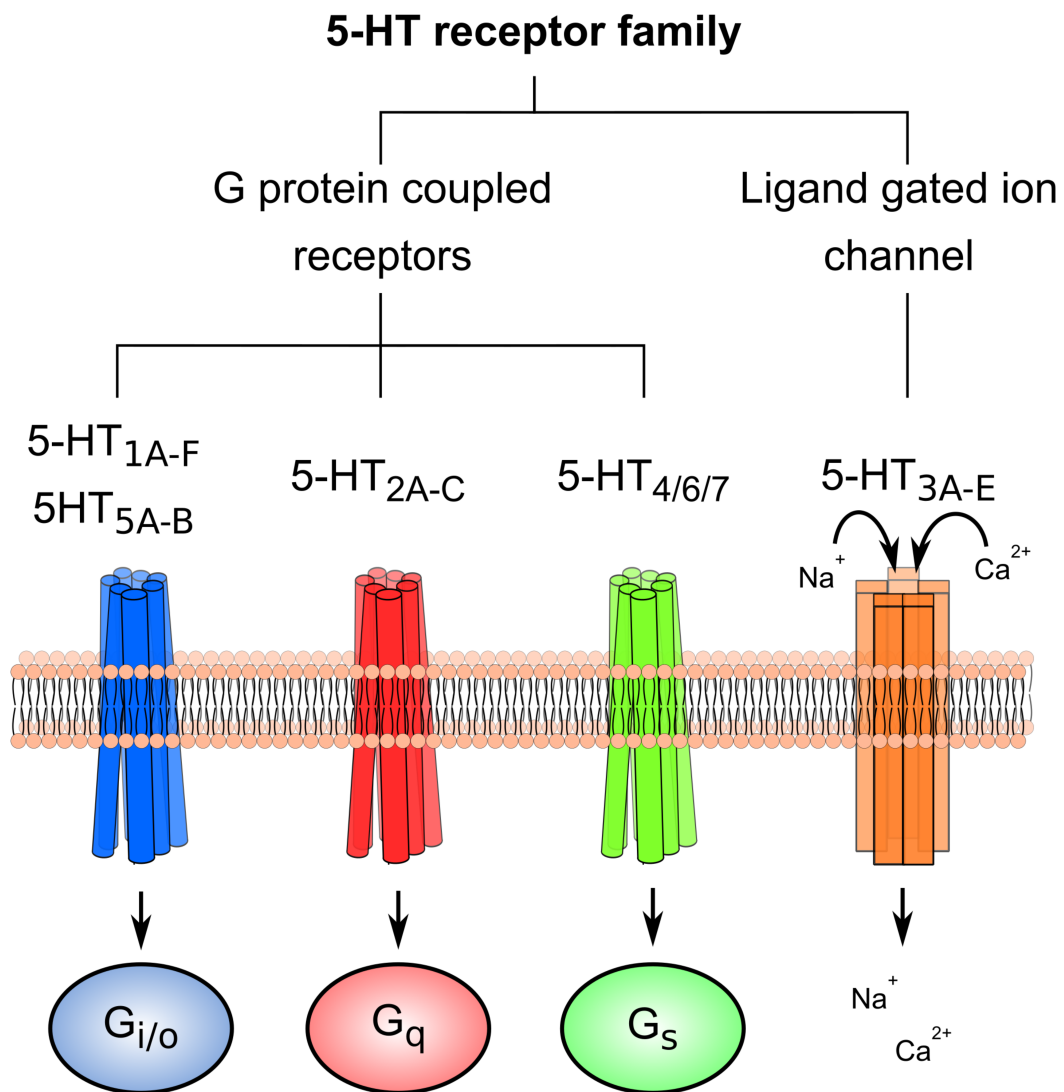
Figure 6: The 5-HT receptor family.

The receptors are expressed in the central and peripheral nervous system, in the blood, in the intestines, in the endocrine system and in the cardiovascular system.

In the brain, these receptors are mediating the effects of serotonin that is released in the nervous system. Upon activation different 5-HT receptors can activate distinct intracellular pathways. Among them are the stimulation of adenylyl cyclase by activation of heteromeric Gs proteins (5-HT$_4$, 5-HT$_6$, 5-HT$_7$), inhibition of adenylyl cyclase by activation of heteromergic Gi/o proteins (5-HT$_{1A-F}$, 5-HT$_{5A}$ and 5-HT$_{2B}$) activation of phospholipase C by activation of heteromeric Gq proteins (5-HT$_{2A-C}$) or permeabilization of the cell plasma membrane for cations (5-HT$_3$) (Fig. 6).

The first successfully cloned receptor of this important family was the 5-HT$_{1A}$ receptor (Kobilka et al., 1987). Intensive research could link this receptor to aggression (Miczek et al., 1998), sexual activity (Maswood et al., 1998), food intake (Gilbert et al., 1988), the regulation of the sleep cycle, memory formation (Edagawa et al., 1998), thermoregulation (Seletti et al., 1995) and immune function (Iken et al., 1995).

The 5-HT$_{1A}$ receptor is a class A receptor of the GPCR family. Like the other class A GPCRs, the 5-HT$_{1A}$ receptor is composed of three extracellular and three intracellular loops as well as seven TM domains. In addition, the 5-HT$_{1A}$ receptor is palmitoylated at two cysteins found at the end of the C-terminus leading to a membrane association of the C-terminal end forming a fourth intracellular pseudoloop (Papoucheva et al., 2004) (Fig. 7).

In the nervous system, the 5-HT$_{1A}$ receptor is expressed presynaptically in serotonergic neurons, acting as an autoreceptor or post synaptically on dendrites of non serotonergic neurons acting as a heteroreceptor (Albert, 2012; Altieri et al., 2013; Riad et al., 2000). As autoreceptor, the 5-HT$_{1A}$ receptor directly regulates serotonin release of serotonergic neurons by a negative feedback loop diminishing serotonin release (Blier et al., 1998; Innis & Aghajanian, 1987; Liu et al., 2005).

The 5-HT$_{1A}$ receptor couples in neurons mainly to the Gi/o pathway leading to the inhibition of adenylyl cyclase and therefore to a reduction of cAMP synthesis via Gα proteins (De Vivo & Maayani, 1986; Fargin et al., 1989; Raymond et al., 1989; S. Weiss et al., 1986). Furthermore, its activation leads to activation of GIRK channels and inhibition of voltage dependent calcium channels Ca^{2+} channels by activity of the Gβ/γ subunits in hippocampal neurons and dorsal raphe nucleus neurons (Andrade et al., 1986; Colino & Halliwell, 1987; Karschin et al., 1991; Penington & Kelly, 1990; Zgombick et al., 1989). Furthermore, 5-

HT$_{1A}$ receptor activation can lead to stimulation of adenylyl cyclase (Markstein et al., 1986; Shenker et al., 1985) and to inhibition of Phospholipase C activation (Claustre et al., 1988). Stimulation of adenylyl cyclase by the 5-HT$_{1A}$ receptor seems to happen, when the receptor is co expressed with adenyly cyclase II (Albert et al., 1999). The 5-HT$_{1A}$ receptor shows high affinity to serotonin with an Kd of 1,8nM ± 0,3 (Ho et al., 1992), underlying its excellent use as a candidate to generate a genetically encoded biosensor.

To study the receptor, different selective substances have been developed, leading to an activation, partial activation or inhibition of the 5-HT$_{1A}$ receptor. One of the agonist, which activate the 5-HT$_{1A}$ receptor is 8-OH-DPAT (Hoyer et al., 1985), which is a non-selective agonist, activating also the 5-HT$_7$ receptor (Lovenberg et al., 1993; Ruat et al., 1993). A selective inhibitor of the 5-HT$_{1A}$ receptor is WAY-100635 which is specific for the 5-HT$_{1A}$ receptor, able to inhibit its action (Forster et al., 1995).
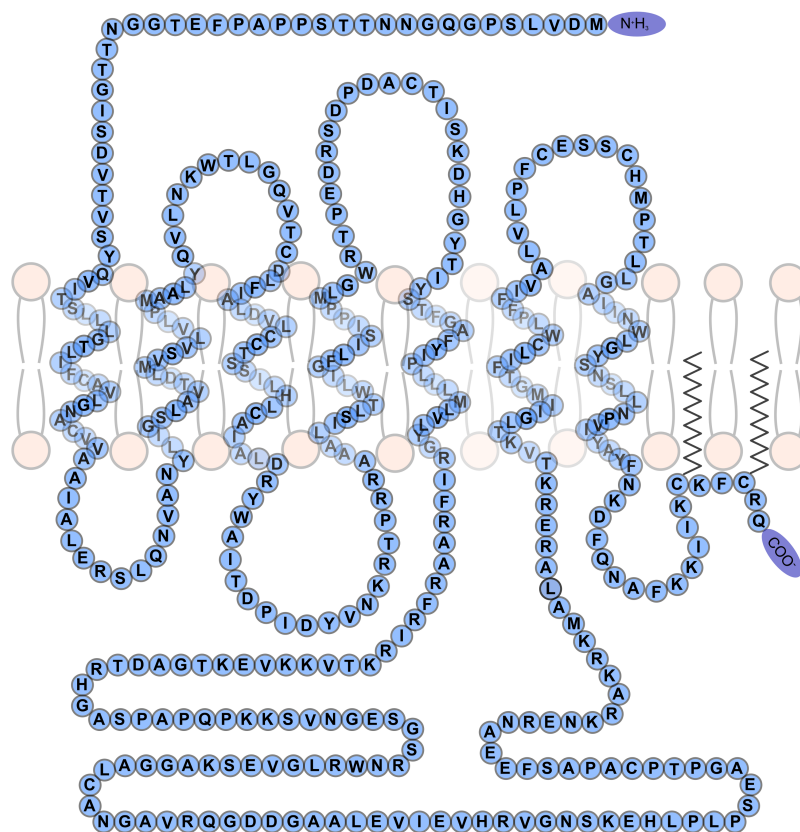
Figure 7: Sequence of the 5-HT1A receptor.

1.7   Green fluorescence protein (GFP)

The green fluorescence protein (GFP) of *Aequorea victoria* was discovered by O. Shimomura 1962 (Shimomura et al., 1962). Much later, the cDNA was cloned (Prasher et al., 1992) and it was successfully expressed in living organisms (Chalfie et al., 1994; Inouye & Tsuji, 1994). Soon after that, the X-ray structure was solved (Ormö et al., 1996; F. Yang et al., 1996). The N- and C-termini of GFP are flexible and are outside of the GFP formed structure. GFP consists of 11 beta-strands forming a barrel like structure. They surround an alpha-helix in its core which contains the chromophore in its center (Fig. 8).

The chromophore of GFP consists of Ser/Thr^{65} – Tyr^{66} – Gly^{67} which maturates due to several autocatalytic steps which involves cyclization and dehydration of Ser/Thr^{65} and Gly67 and dehydrogenation of Tyr^{66} by molecular oxygen. The autocatalytic steps and structural rearrangements within the protein maturation process are possible without involvement of external cofactors (Tsien, 1998).

Native GFP forms weak dimers, which could lead to aggregation of proteins fused to GFP. This can be prevented by a single point mutation A206K (Zacharias et al., 2002). Native GFP consists of two chemically different populations. One has a neutral chromophore and is excitable at 395 nm and one has an anionic chromophore which is excitable at 475 nm. Both of them emit light in the green color spectrum at 505 nm (Brejc et al., 1997; Cubitt et al., 1995; Heim et al., 1994).

Mutational studies led to the development of GFP variants containing mostly the anionic forms of the chromophore suitable for live cell imaging also because of their high folding efficiency at 37°C. These variants were called eGFP and Emerald (Cormack et al., 1996; Heim et al., 1995). Additional mutational studies produced new fluorescence proteins with different brightness, photostability and shifted absorption and emission spectra (Delagrave et al., 1995; Ehrig et al., 1995; Griesbeck et al., 2001; Mena et al., 2006, p. 2; Nagai et al., 2002; A. W. Nguyen & Daugherty, 2005; Tsien, 1998; T.-T. Yang et al., 1998).

The rise of fluorescence proteins able to emit light in the full range of visible light led to the development of fluorescence sensors, able to detect changes in proteins or protein-protein interactions by a process called förster resonance energy transfer (FRET). In this process a FRET donor, which has an overlapping emission spectrum with the excitation spectrum of a FRET acceptor, transfers its energy after excitation radiation less to the acceptor

which emits the taken-up energy via light. Since this process is strongly dependent on proximity and orientation of the two proteins to each other, a high amount of genetically encoded sensors were developed using it.

The fluorescence of GFP and its derivatives, as well as the fluorescence of other fluorescence proteins, could remain when there is a break at specific positions in the aminoacid sequence (Baird et al., 1999). In this case, the native N- and C-terminus of the protein is fused together via a linker sequence to generate a circular permuted fluorescence protein. This circular permuted fluorescence proteins are more sensitive to their physiochemical environment compared to their native counterpart. Changes in pH, the temperature or structural changes in proteins linked to this circular permuted fluroescent proteins, can lead to changes in the fluorescence intensity (Baird et al., 1999). This circular permutation gave rise to the creation of biosensors, capable to detect structural rearrangements in different proteins.
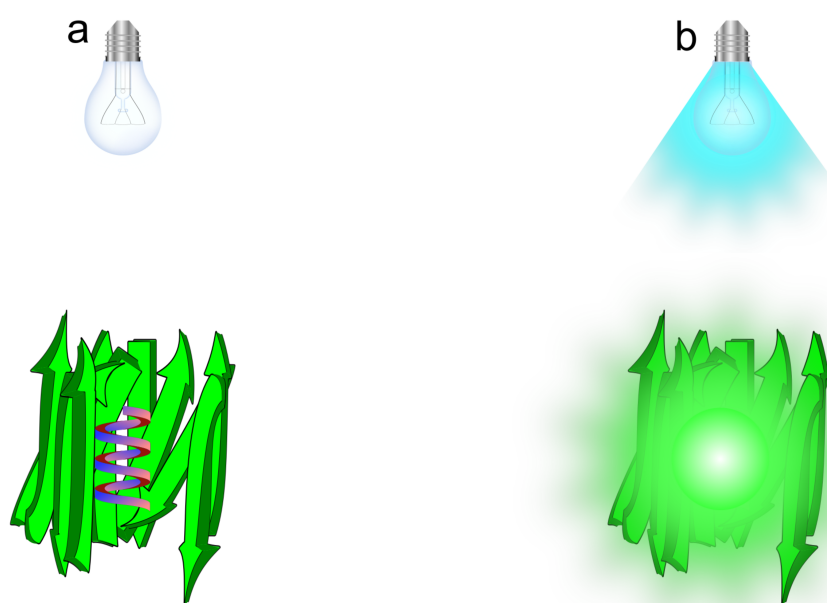
Figure 8: Structure of the Green fluorescence protein;
The protein is composed of 11 beta strands forming a barrel like structure. Embedded in
its core is an alpha helix containing the chromophore which shows no fluorescence (a)
but upon illumination emits green light (b).

1.8 Genetically encoded Biosensors

Genetically encoded biosensors are developed to convert a molecular event into a detectable optical signal. Therefore, genetically encoded biosensors have incredible potential for new breakthroughs in basic understanding of cellular processes and understanding mechanisms behind diseases.

Genetically encoded biosensor rely on two main components. One which is capable of binding to a molecule or active/inactive state of a protein, and a second one which is able to generate a detectable change in a signal.

The first component of the genetically encoded sensors is often derived from endogenous proteins acting in the signaling pathway of interest. They are sensitive to the targeted event and therefore are great candidates for the basis of a genetically encoded biosensor.

As for the second component, the use of fluorescence proteins, as the readout of cellular events is extremely beneficial. Their absorption and emission of light is occurring in nanoseconds, thus genetically encoded sensors based on fluorescence proteins are able to monitor cellular events which are extremely fast. Furthermore, the use of fluorescence proteins enables to detect changes in high spatial resolution, enabling measurements of processes in cellular and even subcellular resolution. Moreover, fluorescence proteins do not need application of exogenous chemicals for their function and are a rather nontoxic technique to be used in cells. They can be expressed randomly in cellular populations or their expression can be directed in specific subsets of cellular populations via the use of cell specific promoters. With the help of different tags, they are able to label specific compartments within the cells or even specific microdomains within the same compartments of a single cell (Kim et al., 2019; Tenner et al., 2021). For detection either fluorescence protein fragments, a complete protein or multiple different variants of fluorescence proteins are used, which are coupled to the sensing component of genetically encoded biosensors, changing their fluorescence behavior by signal induced changes in the sensing component.

Today, there are a plethora of different genetically encoded biosensors available, able to detect different targets. With them, it is possible to measure different pathways or cellular behaviors, ranging from detecting phases of the cell cycle (Bajar et al., 2016; Hahn et al., 2009; Sakaue-Sawano et al., 2017; Sugiyama et al., 2009), molecular crowding inside the

cell (Boersma et al., 2015), changes in pH (Awaji et al., 2001; Mahon, 2011), changes in membrane voltage (Han et al., 2013; Hochbaum et al., 2014; Piatkevich et al., 2018), concentration of molecules like ATP (Saito et al., 2012; Yaginuma et al., 2014; Yoshida et al., 2016), cAMP (Mukherjee et al., 2016; Odaka et al., 2014; Ohta et al., 2018), cGMP (Bhargava et al., 2013; Niino et al., 2010), carbon monoxide (Wang et al., 2012), glucose (Fehr et al., 2003; Veetil et al., 2010), NADH (Y. Zhao, Jin, et al., 2011), O_2 (Erapaneedi et al., 2016), concentration of ions like Ca^{2+} (Nakai et al., 2001; Ohkura et al., 2012; Y. Zhao, Araki, et al., 2011), Cl^- (Kuner & Augustine, 2000), Mg^{2+} (Lindenburg et al., 2013), Zn^{2+} (Evers et al., 2007), the activity of enzymes like akt (Yoshizaki et al., 2006), ERK (Harvey et al., 2008), JNK (Fosbrink et al., 2010), PKA (J. Zhang et al., 2001), caspase 3 (Tyas et al., 2000), lipids like DAG (Sato et al., 2006), reduction oxidation events measuring H_2O_2 (Belousov et al., 2006), H_2S (S. Chen et al., 2012), post translational modifications like βArrestin2 ubiquitation (Perroy et al., 2004), histone acetylation (Sasaki et al., 2009) or ubitiquination (Ganesan et al., 2006).

For measuring neurotransmitters, different approaches have been successfully employed (Fig. 9a-c).

One of the earliest approaches to detect neurotransmitters was the utilization of periplasmic binding proteins (PBPs) from bacteria. Started in 2005, the PBPs ybeJ and MglB were used with the combination of FRET to generate genetically encoded biosensors capable to detect glutamate (Deuschle et al., 2005; Hires et al., 2008; Okumoto et al., 2005). These sensors were further optimized (Okada et al., 2009) or altered, that instead of FRET, the fluorescence change of cpGFP was utilized to generate a measurable fluorescence response upon binding of glutamate (Marvin et al., 2013). Further improvements have led to the development of sensors with faster kinetics capable of measuring high frequency burst of glutamate release (Helassa et al., 2018).

Besides the tremendous improvements of glutamatergic genetical encoded sensors based on PBPs, further PBP sensors were built for glycine (W. H. Zhang et al., 2018), acetylcholine (Borden et al., 2020), GABA (Marvin et al., 2019), and serotonin (Unger et al., 2020).

Apart from PBPs, another strategy to measure the release from neurotransmitters via genetical encoded sensors, is the usage of cell-based biosensors, CNiFERs (cell-based neurotransmitter fluorescent engineered reporters). In this technique, cells expressing a

chosen Gq coupling metabotropic receptor are used in tandem with a genetically encoded Ca^{2+} indicator as the detector of neurotransmitter releasing events. These cells are implanted into the brain areas of interest for investigation of specific neurotransmitters. This technique was successfully employed for acetylcholine (Q.-T. Nguyen et al., 2010), norepinephrine and dopamine (Muller et al., 2014). Furthermore, its use was expanded by generating CNiFERs expressing ligand-gated ion channels in tandem with genetically encoded FRET sensor for detection of neurotransmitter release (Yamauchi et al., 2011).

Beside CNiFERs and PBPs, in a different approach to detect the release of neurotransmitters, genetically encoded biosensors based on GPCRs are developed. First studies investigated GPCR receptor activation mechanism with the use of FRET (Malik et al., 2013; Vilardaga et al., 2003). FRET capable fluorescence proteins were either inserted into the third intracellular loop and fused to the C-terminus of the receptor (Vilardaga et al., 2003), or fused in series to the C-terminus of the receptor with the addition of the alpha helix forming C-terminus of a G-protein (Malik et al., 2013). Later the circular permuted version of GFP (cpGFP) was used, where substitution of the third intracellular loop by cpGFP led to the development of sensors capable of detection of dopamine (Patriarchi et al., 2018; F. Sun et al., 2018), acetylcholine (Jing et al., 2018), norepinephine (Feng et al., 2019) and serotonin (Wan et al., 2021).

To complement the possibilities arising from genetically encoded biosensors, red shifted versions are developed (Patriarchi et al., 2020) enabling dual color imaging or new combinations using simultaneous stimulation via optogenetics.

a) PBPs based sensors
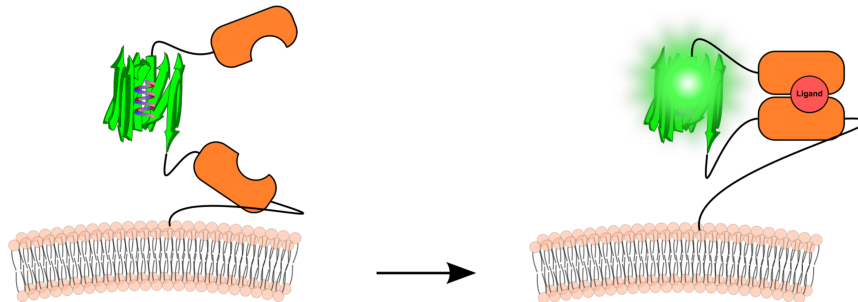
b) GPCRs based sensors
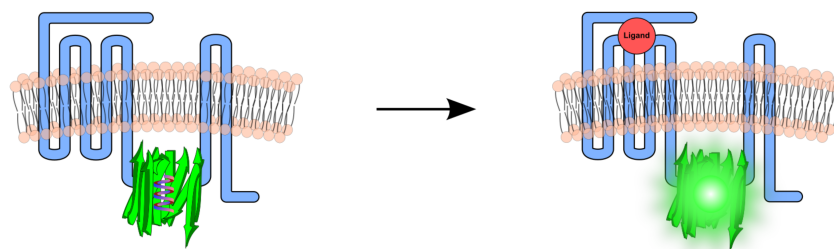
c) CNiFERs
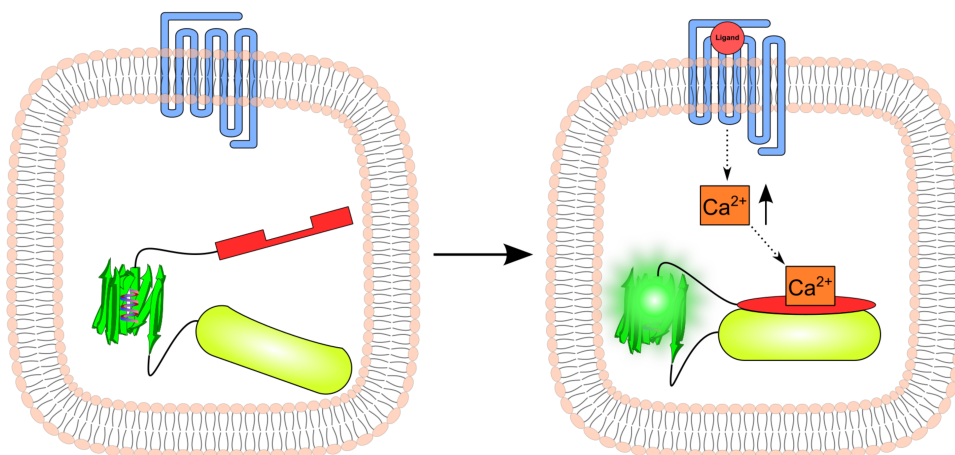
Figure 9: Genetically encoded biosensor to monitor neurotransmitter release;

Based on a) bacterial periplasmic binding proteins (PBPs), b) G protein coupled receptors (GPCRs), c) cell-based neurotransmitter fluorescent engineered reporters (CniFERs).

1.9   Generation of a serotonin sensor

In my thesis, the generation of a genetically encoded serotonin sensor *sDarken* is discussed. In the beginning random substitution of the third intracellular loop o the 5-HT$_{1A}$ receptor with cpGFP were carried out. The cpGFP was either directly inserted or flanked by linkers. Later, the approach published by Patriachi et al. 2018 was used. The sensor was created by substitution of the third intracellular loop of the 5-HT$_{1A}$ receptor with circular permuted GFP (cpGFP) flanked by linker sequences which are five aminoacids long. Mutations of specific aminoacid sequences in the linker sequences led to a generation of protein libraries of which some candidates showed changes in fluorescence upon application of serotonin. Of these initial mutations, one was chosen which exhibit high baseline fluorescence while still showing a great response upon serotonin application. This mutant was called *sDarken*.

sDarken showed high binding affinity to serotonin in the nanomolar range. Repetitive stimulation of *sDarken* with serotonin was able to generate a repetitive response. Further investigation showed, that *sDarken* is highly specific for serotonin compared to other neurotransmitters and the precursor and metabolite of serotonin. Also, because of the 5-HT$_{1A}$ receptor backbone, the agonist 8-OH-DPAT as well as the 5-HT$_{1A}$ receptor antagonist Way-100635 could effectively initiate the sensor response, or inhibit responses elicit by serotonin respectively.

Substitution of cpGFP with a circular permuted form of superfolder GFP, cpsfGFP was able to show an even higher affinity for serotonin. This mutant was also able to show repetitive responses and was highly specific for serotonin. Furthermore, single point mutations within the 5-HT$_{1A}$ receptor backbone of the sensor protein led to a new sensor, with lower affinity for serotonin (micromolar range).

2   Materials and Methods

2.1   Materials

2.1.1 Chemicals

The 1Kb DNA Ladder plus and Midori Green advanced DNA Stain was purchased from Nippon Genetics Europe GmbH. Agarose was purchased from Biozym. 5-Hydroxyindole-3-acetic acid (5-HIAA), (±)-8-Hydroxy-2-(dipropylamino)-tetralin-hydrobromid (8-OH-DPAT), Acetylcholine chloride, Dopamine hydrochloride, Histamin dyhydrochloride, L-Glutamic acid, L-Norepinephrine hydrochloride, L-Trypthophan, WAY-100365 maleate salt (WAY-100635) and Y-Aminobutric acid (GABA) were purchased from Sigma Aldrich. Carbenicilin disodium salt, Chloramphenicol, Ethanol ≥99,8%, p.a., Kanamycinsulfate, 750 I.U./mg, LB-Agar (Luria/Miller), LB-Medium (Luria/Miller), Penicillin, Serotonin Hydrochloride and Streptomycin were purchased from Carl Roth. Purple Gel loading dye and fetal bovine serum were purchased from Thermo Fischer Scientific. Isopropanol was purchased from VWR chemicals. Polyethylenimine (PEI, branched, average Mw ~25000) was purchased from Aldrich chemistry.

2.1.2 Kits for Molecular biology

The GeneJET Plasmid Miniprep Kit was purchased from Thermo Fisher Scientific. The In-Fusion® HD Cloning Kit was purchased from Takara Bio USA. The NucleoSpin® Gel and PCR Clean-up, NucleoBond® Xtra Midi, NucleoBond® Xtra Midi EF and NucleoBond® Xtra Maxi EF kits were purchased from Macherey-Nagel.

2.1.3 Cells

Human Embryonic Kidney Cells SV40 transformed (293tsA1609neo) were purchased from Sigma Aldrich. Competent Stellar Cells (E.Coli, HST08 strain, chemically competent) were purchased from Takara Bio USA.

2.1.4 Enzymes

NotI-HF, HindIII-HF and EcoRI-HF were purchased from New England Biolabs GmbH (NEB). PrimeSTAR MAX DNA polymerase and In-Fusion Master Mix were included in the In-Fusion® HD Cloning Kit purchased from Takara Bio USA.

2.1.5 Programs used

Nippon Genetics CameraStudio (Nippon Genetics) was used for taking pictures in the gel documentation system. HoKAWO 3.0 (Hamamatsu Photonics Deutschland GmbH) was used for camera control in the measurements carried out. ImageJ FiJi (ImageJ Community) was used for image processing. Inkscape (Inkscape Community) was used for figure creation. LibreOffice (The document foundation) was used for word processing. Rstudio (Rstudio PBC) was used for plot generation. SnapGene Viewer (Insightful sience) was used to built and visualize DNA plasmids. Zotero (Corporation for Digital Scholarship, previously Center for History and New Media at George Mason University) was used for managing citations and bibliography.

2.1.6 Buffers

PBS 1x

2,7 mM	KCl
138 mM	NaCl
0,5 mM	$MgCl_2$
0,9 mM	$CaCl_2$
1,47 mM	KH_2PO_4
8 mM	Na_2HPO_4

TAE 1x

40 mM	Tris base
1 mM	EDTA
20 mM	glacial Acetic acid

2.1.7 Solutions for DNA Isolation (Mini preparation)

Solution I (100 mL)

50 mM	Tris base
10 mM	$Na_2EDTA \times H_2O$
10mg	RNAse A
pH 8	

Solution II (200 mL)

| 200 mM | NaOH |
| 35 mM | SDS |

Solution III (200 mL)

| 3 M | potassium acetate |

glacial acetic acid to pH 5.5

2.2 Methods

2.2.1 Polymerase chain reaction

DNA fragment amplification was done by polymerase chain reactions (PCR). Primers for PCRs were synthesized by Thermofischer scientific. Components needed for the PCRs were purchased from Takara Bio USA as the PrimeStar® Max Premix, which contained Buffer, dNTPs, Ions and the polymerase (PrimeSTAR Max DNA Polymerase). PCR reactions containing premix, template and primers were incubated in a PCR cycler (FastGene Thermocycler, Nippon Genetics Europe GmbH). A standard PCR procedure was done following the next schemes:

Table 1: PCR pipetting scheme

PCR Premix (Takara) 2x	5µL
Primer 1	1 µL (1 µmol)
Primer 2	1 µL (1 µmol)
Template	1 µL (1 ng/µL)
Water	2 µL
Total Volume	10 µL

Table 2: PCR program settings

	Denaturation	1 min	94°C
30x	Denaturation	20 sec	94°C
	Annealing	20 sec	60°C
	Elongation	15 sec/kb	72°C
	Elongation	5 min	72°C
	Incubation	Infinite	4°C

Products generated with PCR were used in downstream cloning applications namely In-Fusion cloning. Therefore primers often contained overhangs in their 5'-end, complementary to ends of other PCR products or the ends of the restricted plasmids.

2.2.2 Plasmid restriction

Plasmids were digested by restriction enzymes (NotI-HF, HindIII-HF, EcoRI-HF; New England Biolabs GmbH) using following standard restriction scheme:

Table 3: Restriction pipetting scheme

	Restriction	Control
Template	5 µL	5 µL
Restriction Enzyme 1	1 µL	-
Restriction Enzyme 2	1 µL	-
Buffer (CutSmart 10x)	3 µL	3 µL
Water	20 µL	22 µL
Total Volume	30 µL	30 µL

Samples were incubated at 37°C shaking at 300 rpm (New Brunswick TM Innova® 42/42R Incubator, Eppendorf).

The two vectors used as a backbone for the generation of the constructs are shown in the appendix (see 6.2). The pAAV-vector was restricted using EcoRI-HF and HindIII-HF opening the multiple cloning site for the insertion of genes of interest downstream of the promoter region (CMV promoter). The pN1-Vector was restricted using the enzymes HindIII-HF and NotI-HF, cutting out the mCherry coding sequence, generating an insertion site for the DNA of interest downstream of the promoter region (CMV promoter).

Inserts generated via PCR as well as restricted plasmids were separated using gel electrophoresis.

2.2.3 Gel electrophoresis

DNA was separated by gel electrophoresis using gels containing 1,5% Agarose (Biozym) and visualized by Midori green advanced DNA Stain (Nippon Genetics Europe GmbH), which was added according to the manufacturer information. The gels were placed in a electrophoresis chamber (Horizontal Gel Electrophorese Chamber EV1450, LTF Labortechnik) containing 1x TAE buffer (40 mM Tris base, 1 mM EDTA, 20 mM acetic acid) and a voltage of 120 V was applied for 35 min separating DNA fragments according to their length.

Afterwards gels were transferred to the FAS-Digi PRO Gel Documentation System (Nippon Genetics Europe GmbH) and DNA visualized by blue light excitation. Pictures were taken using the attached camera (EOS200D, Canon). DNA bands were cut out and transferred into a 1,5 mL reaction tube for subsequent DNA extraction.

2.2.4 Gel extraction

Gel slices were purified using the NucleoSpin® Gel and PCR Clean-up kit (Macherey Nagel) according to the protocol of the manufacturer.

200 µL Buffer NTI per 100 mg of gel was added to the reaction tube containing the gel with the DNA of interest, The reaction tube was incubated at 50°C for ~15 min until the gel was completely dissolved. The solution was loaded into a NulceoSpin® Gel and PCR Clean-up Column which was placed onto a 1,5 mL reaction tube. The sample was centrifuged for 30 s at 11000 x g and the flow-through discarded. Afterwards the tube was washed twice by adding 600 µL Buffer NT3 with subsequent centrifugation for 30 s at 11000 x g. The flow-through was discarded. Next, the tube was dried via centrifugation for 1 min at 11000 g. The column was placed into a new 1,5 mL reaction tube and 30 µL of Buffer NE was added to the column. Afterwards the reaction tube was incubated for 1 min at RT (room temerature). Following, the tube was centrifuged for 1 min at 11000 x g and the eluate stored at - 20°C for further use.

2.2.5 Cloning

In-Fusion cloning (Takara Bio USA) was used to fuse the DNA fragments with complementary overlapping ends together. In the In-Fusion reaction, DNA Fragments and a linearized vector containing complementary ends are hybridizing to each other promoted by the vaccinia virus DNA polymerase. They are ultimately joined through the repair mechanisms available in *E.Coli (Irwin et al., 2012)* (Fig. 10).
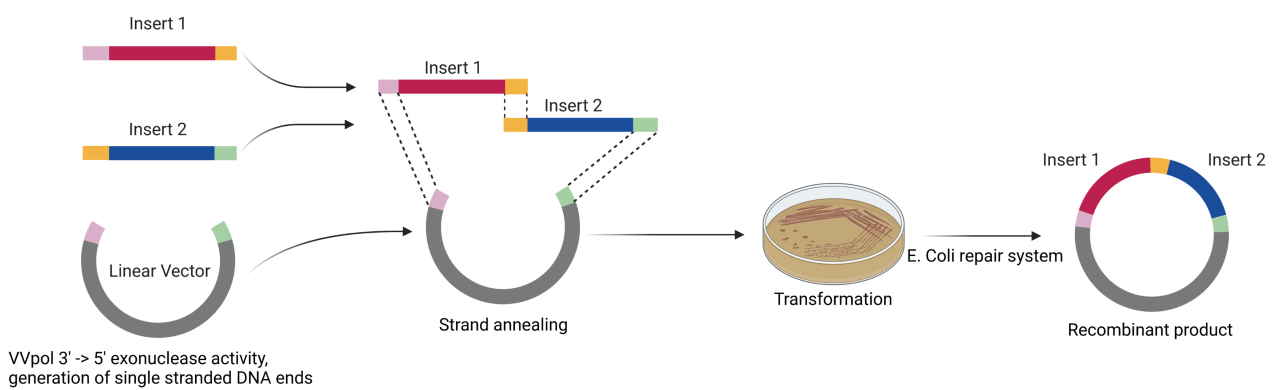
Figure 10: In Fusion cloning, made with Biorender.

The In-Fusion reactions were prepared using following standard scheme:

Table 4: In-Fusion pipetting scheme

In Fusion Master Mix (5x)	0,5 µL
DNA Fragments	~10 ng/µL per Fragment
Linearized vector	~5 ng/µL
Water	Fill up to 2,5 µL
Total Volume	2,5 µL

2.2.6 Cloning of plasmids

In an In-Fusion reaction, a linearized vector and multiple DNA fragments were assembled into an plasmid. The overhangs needed for this reaction were introduced by the primers used for the PCR reactions of the DNA fragments. For the generation of plasmids containing the pAAV backbone, the vector pAAV-CMV-MCS was restricted with EcoRI-HF and HindIII-HF. For the generation of plasmids containing the pN1 backbone, the plasmid pN1-mApple was restricted with the restriction enzymes HindIII-HF and NotI-HF.

As the template for the amplification of the $5-HT_{1A}$ receptor, the open reading frame (ORF) for the Human $5-HT_{1A}$ receptor (Uniprot: P08908) which was present on a pENTR vector (pENTR-5-HT$_{1A}$.mCerulean) was used. Furthermore other plasmids, used in the cloning procedures were purchased from Addgene: sfGFP-N1 was a gift from Michael Davidson & GeoffreyWaldo (Addgene plasmid #54737; RRID:Addgene_54737), mApple-N1 was a gift from Michael Davidson (Addgene plasmid #54567; RRID:Addgene_54567), pN1-GCaMP6m-XC was a gift from Xiaodong Liu (Addgene plasmid #111543; RRID: Addgene_111543), pAAV-Syn-ChrimsonR-tdT was a gift from Edward Boyden (Addgene plasmid #59171; RRID: Addgene_59171), pMSCV-IRES-mCherry FP was a gift from Dario Vignali (Addgene plasmid # 52114; RRID:Addgene_52114) and the pAAV-CMV plasmid was brought from Takara Bio.

The primers sequence of primers used throughout the cloning procedures are present in the appendix (see 6.1).

2.2.6.1   Cloning of pAAV-CMV-1AcpGFPS I

The vector pAAV-CMV-1AcpGFPS I was generated by an In-Fusion reaction carried out using three inserts combined with a restricted pAAV-MCS vector.

The first insert was ampliefied by PCR using the primers "For-pAAV-5-HT1As" and "S1A3LcGIII R" with the plasmid pENTR 5-HT$_{1A}$.mCerulean as the template.

The second insert was amplified using the primers "cpGFP F" and "cpGFP R" with the template pN1-GCaMP6m-XC.

The third insert was amplified using the primers "S1A3LcGIII F" and "5HT1Ae-Rev-pAAV". The vector pENTR 5-HT$_{1A}$.mCerulean was used as the template.

2.2.6.2 Cloning of pAAV-CMV-1AcpGFPS II

The vector pAAV-CMV-1AcpGFPS II was built using three PCR products combined with a restricted pAAV-MCS vector joined together in an In-Fusion reaction.

The first piece was generated by PCR amplification using the primers "For-pAAV-5-HT1As" and "S1A3LcG IV R" with the plasmid pENTR 5-HT$_{1A}$.mCerulean as the template.

The second PCR product was created using the primers "cpGFP F" and "cpGFP R" with the template pN1-GCaMP6m-XC.

The third PCR product was built using the primers "S1A3LcG IV F" and "5HT1Ae-Rev-pAAV". The vector pENTR 5-HT$_{1A}$.mCerulean served as the DNA template in this reaction.

2.2.6.3 Cloning of pAAV-CMV-1AcpGFPS III

The vector pAAV-CMV-1AcpGFPS III was generated by In-Fusion reaction each carried out using three inserts combined with a restricted pAAV-MCS vector.

The first insert was produced by PCR using the primers "For-pAAV-5-HT1As" and "S1A3LcG IV FL R" with the plasmid pENTR 5-HT$_{1A}$.mCerulean as the template.

The second insert was amplified using the primers "cpGFP F" and "cpGFP R" with the template pN1-GCaMP6m-XC.

The third inserts were amplified using the primers "S1A3LcG IV FL F" and "5HT1Ae-Rev-pAAV". The vector pENTR 5-HT$_{1A}$.mCerulean was as the template.

2.2.6.4 Cloning of pAAV-CMV-1AcpGFPS IV

The vector pAAV-CMV-1AcpGFPS IV was generated by In-Fusion reaction each carried out using three inserts combined with a restricted pAAV-MCS vector.

The first insert was produced by PCR using the primers "For-pAAV-5-HT1As" and "S1A3LcG VI FL R" with the plasmid pENTR 5-HT$_{1A}$.mCerulean as the template.

The second insert was amplified using the primers "cpGFP F" and "cpGFP R" with the template pN1-GCaMP6m-XC.

The third inserts were amplified using the primers "S1A3LcG VI FL F" and "5HT1Ae-Rev-pAAV". The vector pENTR 5-HT$_{1A}$.mCerulean was as the template.

2.2.6.5 Cloning of pAAV-CMV-S1A3LcG splitG I

The vector pAAV-CMV-S1A3LcG splitG I was generated in an In-Fusion reaction containing the restricted pAAV-MCS and four inserts created by PCR reactions.

The first insert was amplified by PCR using the primers "For-pAAV-5-HT1As" and "S1A3LsplitG II FL R" and the pENTR 5-HT$_{1A}$.mCerulean as a template.

The second insert was generated via PCR using the primer pair "FP F" and "cpGFP R" with the template eGFP in a PCR reaction.

The third insert was generated via PCR using the primer pair "S1A3LcGIII FL F" and "S1A3LsplitG II dou FL 1AFP 2 R" with the template pENTR 5-HT$_{1A}$.mCerulean.

The fourth insert was generated via PCR using the primer pair "cpGFP F" and "GFP pAAV R" with the template eGFP.

2.2.6.6 Cloning of pAAV-CMV-S1A3LcG splitG II

The generation of vector pAAV-CMV-S1A3LcG splitG II was similar to the generation of the vector pAAV-CMV-S1A3LcG splitG.

The vector was created in an In-Fusion reaction containing the restricted pAAV-MCS and four inserts created by PCR reactions.

The first insert was amplified by PCR using the primers "For-pAAV-5-HT1As" and "S1A3LcGIII FL R" and the plasmid pENTR 5-HT$_{1A}$.mCerulean as a template.

The second insert was generated via PCR using the primer pair "cpGFP F" and "FP R" with the template eGFP in a PCR reaction.

The third insert was generated via PCR using the primer pair "S1A3LsplitcG I FL F" and "S1A3LsplitcG IdouFL R" with the template pENTR 5-HT$_{1A}$.mCerulean.

The fourth insert was generated via PCR using the primer pair "FP F" and "hacpGFP-pAAV" with the template eGFP.

2.2.6.7 Cloning of pN1-CMV-dLight M#

The vectors pN1-CMV-dlight M# were generated by random mutations. The vector library was created in an In-Fusion reaction containing the restricted pN1-mApple vector and three inserts, two of which containing radnom mutations in specific linker regions.

The first insert was generated via PCR with the primers "N1 1A HIII F" and "1A Li cG DL1 M R". As a template, the plasmid pENTR 5-HT$_{1A}$.mCerulean was used.

The second insert was generated with the primer pair "cpGFP F" and "cpGFP R", using the template pN1-GCaMP6m-XC.

The third insert was generated with the primers "1A Li cG DL1 M F" and "1A N1 NI R" also using the plasmid pENTR 5-HT$_{1A}$.mCerulean as a template.

2.2.6.8   Cloning of pN1-CMV-2AS-M#

The vectors pN1-CMV-dlight M# were generated by random mutations. The vector library was created in an In-Fusion reaction containing the restricted pN1-mApple vector and three inserts with two containing the random mutations.

The first insert was generated via PCR with the primers "N1 1A HIII F" and "S1A Li 2AS M R". As a template, the plasmid pENTR 5-HT$_{1A}$.mCerulean was used.

The second insert was generated with the primer pair "cpGFP F" and "cpGFP R", using the template pN1-GCaMP6m-XC.

The third insert was generated with the primers "S1A Li 2AS M F" and "1A N1 NI R" also using the plasmid pENTR 5-HT$_{1A}$.mCerulean as a template.

2.2.6.9   Cloning of pN1-CMV-TC

The In-Fusion reaction was used to generate a plasmid library with plasmids named pN1-CMV-TC M#. These plasmids contained different mutations at specific positions within their sequence.

The In-Fusion reaction contained 2 inserts and the restricted vector.

The first insert was amplified using the primer pairs "N1 1A HIII F" and "cpGFP R". As a template, the plasmid pN1-CMV-2AS-M24 was used.

For the second insert the primer pairs "S1A Li 2AS M F" "1A N1 NI R" were used. The plasmid pENTR 5-HT$_{1A}$.mCerulean served as the DNA template.

2.2.6.10 Cloning of pN1-CMV-RR

The In-Fusion reaction was used to generate a plasmid library with plasmids named pN1-CMV-RR M#. These plasmids contained different mutations at specific positions within the n-terminal linker sequence.

The In-Fusion reaction contained 2 inserts and the restricted vector.

For the first insert the primer pairs "N1 1A HIII F" and "S1A Li 2AS M R" were used in a PCR reaction containing the plasmid pENTR 5-HT$_{1A}$.mCerulean as a template.

For the second insert the primer pairs "cpGFP F" and "1A N1 NI R" were used. As a template, the plasmid pN1-CMV-2AS-M24 was used.

2.2.6.11 Cloning of pN1-CMV-CF

The In-Fusion reaction was used to generate a plasmid library with plasmids named pN1-CMV-CF M#. These plasmids contained different mutations at specific positions within the n-terminal linker region.

The In-Fusion reaction contained three inserts and the restricted vector.

For the first insert the primer pairs "N1 1A HIII F" and "S1A Li 2AS M R" were used in a PCR reaction containing the plasmid pENTR 5-HT$_{1A}$.mCerulean as a template.

The second insert was generated with the primer pair "cpGFP F" and "cpGFP R", using the template pN1-GCaMP6m-XC.

For the third insert the primer pairs "2AS CF F" and "1A N1 NI R" were used. As a template, the plasmid pENTR 5-HT$_{1A}$.mCerulean was used.

2.2.6.12 Cloning of pN1-CMV-CW

The In-Fusion reaction was used to generate a plasmid library with plasmids named pN1-CMV-CW M#. These plasmids contained different mutations at specific positions within the n-terminal linker region.

The In-Fusion reaction contained three inserts and the restricted vector.

For the first insert the primer pairs "N1 1A HIII F" and "S1A Li 2AS M R" were used in a PCR reaction containing the plasmid pENTR 5-HT$_{1A}$.mCerulean as a template.

The second insert was generated with the primer pair "cpGFP F" and "cpGFP R", using the template pN1-GCaMP6m-XC.

For the third insert the primer pairs "2AS CW F" and "1A N1 NI R" were used. As a template, the plasmid pENTR 5-HT$_{1A}$.mCerulean was used.

2.2.6.13   Cloning of pN1-CMV-L2ASCF

The In-Fusion reaction was used to generate a plasmid library with plasmids named pN1-CMV-L2ASCF M#**.** These plasmids contained different mutations and a changed substitution site in the n-terminal linker region.

The In-Fusion reaction contained two inserts and the restricted vector.

For the first insert the primer pairs "N1 1A HIII F" and "1A Li cG DL1 M R" were used in a PCR reaction containing the plasmid pENTR 5-HT$_{1A}$.mCerulean as a template.

For the second insert the primer pairs "cpGFP F" and "1A N1 NI R" were used. As a template, the plasmid pN1-CMV-2AS-M34 was used.

2.2.6.14   Cloning of pN1-CMV-NG*N*

The In-Fusion reaction was used to generate a plasmid library with plasmids named pN1-CMV-M34-NGN#**.** These plasmids contained mutations at aminoacids of the n-terminal linker region, not mutated in earlier mutation rounds.

The In-Fusion reaction contained two inserts and the restricted vector.

For the first insert the primer pairs "N1 1A HIII F" and "M34 NG Mut R" were used in a PCR reaction containing the plasmid pENTR 5-HT$_{1A}$.mCerulean as a template.

For the second insert the primer pairs "cpGFP F" and "1A N1 NI R" were used. As a template, the plasmid pN1-CMV-2AS-M34 was used.

2.2.6.15   Cloning of pN1-CMV-NG*C*

The In-Fusion reaction was used to generate a plasmid library with plasmids named pN1-CMV-M34-NGC#**.** These plasmids contained mutations at aminoacids of the c-terminal linker region, not mutated in earlier mutation rounds.

The In-Fusion reaction contained two inserts and the restricted vector.

For the first insert the primer pairs "N1 1A HIII F" and "cpGFP R" were used in a PCR reaction containing the plasmid pENTR 5-HT$_{1A}$.mCerulean as a template.

For the second insert the primer pairs "M34 NG Mut F" and "1A N1 NI R" were used. As a template, the plasmid pN1-CMV-2AS-M34 was used.

2.2.6.16   Cloning of pN1-CMV-H-sDarken

The In-Fusion reaction was used to generate pN1-CMV-H-sDarken. This plasmid contained a circular permuted form of superfolderGFP. In an In-Fusion reaction four inserts and the restricted pN1 vector were joined together.

Therefore, for generating the first insert, the primer pairs "N1 1A HIII F" and "M34 sfcpGFP R" were used in a PCR reaction containing the plasmid pENTR 5-HT$_{1A}$.mCerulean as a template.

For the second insert the primer pair "sfcpGFP F" and "FP R" was used to amplify a specific DNA fragment of the template plasmid sfGFP-N1.

For the third insert, the primers "sfcpGFP builder F" and "sfcpGFP R" were used in a PCR reaction also containing the sfGFP-N1 as a template.

The fourth piece was generated via PCR with primer "M34 sfcpGFP F" and "1A N1 NI R" and the plasmid pENTR 5-HT$_{1A}$.mCerulean.

2.2.6.17   Cloning of pN1-CMV-M34-D116N

For the introduction of the single point mutation in the coding sequence of sDarken, PCRs and a subsequent In-Fusion reaction were carried out. In the In-Fusion reaction, PCR products were integrated into a restricted pN1 plasmid. For the reaction two inserts were generated via PCR with the plasmid pN1-CMV-2AS-M34 as a template. The first insert was amplified using the primer "N1 1A HindIII F" together with the primer "M34KDMut2 R". The second insert was amplified using the primer "M34KDMut2 F" combined with the reverse primer "1A N1 NI R". For both reactions the plasmid pN1-CMV-2AS-M34 served as a template. Both inserts were integrated into a restricted pN1 plasmid (HindIII-HF, NotI-HF) using In-Fusion cloning.

2.2.6.18   Cloning of pN1-CMV-sDarken-m*Cherry*

For attachment of mCherry to the ORF of *sDarken*, the *sDarken* coding sequence was amplified excluding the stop codon, using the plasmid pN1-CMV-2AS-M34 and the primers "N1 1A HindIII F" and "1A mCh R". The DNA sequence coding for mCherry was amplified using primers "mCherry F" and "mCh N1 R" with pMSCV-IRES-mCherry FP as a template. Both amplificates were incorporated into a restricted pN1 vector using the In-Fusion reaction.

2.2.7 Transformation

2 μL of In-Fusion reaction product was added to 20 μL of chemically competent stellar cells (Takara Bio USA). Next, cells were incubated on ice for 20 min, following a 45 sec heat shock at 42°C. Then, cells were incubated for 2 min on ice. Afterwards 200 μL SOC medium (Takara Bio USA) was added and the cells were incubated for 1 h at 37°C. After incubation, cells were plated on Agar plates containing Kanamycin (Kanamycinsulfate, Carl Roth) if the pN1 vector backbone was used, or Carbinicilin (Carbenicilin disodium salt, Carl Roth) if the pAAV vector backbone was used. Plates were incubated over night at 37°C (New Brunswick TM Innova® 42/42R Incubator, Eppendorf).

After incubation, colonies were picked with a sterile pipette tip and transferred into cell culture tubes containing LB-Broth media (LB-Medium [Luria/Miller], Carl Roth). Cells were incubated over night at 37°C shaking with 300 rpm (New Brunswick TM Innova® 42/42R Incubator).

2.2.8 Mini Preparations

2.2.8.1   Commercial Mini Preparation for mutant screening

Plasmid DNA Purification of *E.Coli* was carried out using the GeneJET Plasmid Miniprep Kit (ThermoFisher Scientific) according to the protocol provided by the manufacturer.

8 mL of overnight culture was centrifuged with 6000 x g for 5 min and the supernatant discarded. Cells were completely resuspended in 250 μL Resuspension Solution and

transferred into a 1,5 mL reaction tube. Next 250 µL Lysis Solution was added and the tube inverted five times. Following, 350 µL Neutralization Solution was added and the tube was inverted again five times. The tubes were centrifuged for 5 min at 13000 x g and the resulting supernatant was transferred onto the GeneJET spin columns. The columns were centrifuged for 1 min and the flow through discarded. The columns were washed two times by adding 500 µL Wash solution to the tubes with subsequent centrifugation for 60 sec at 13000 x g. The flow-through was discarded. Next, the column was centrifuged again at 13000 x g for 1 min and afterwards the GeneJET spin column was transferred onto a new 1,5 mL reaction tube. Lastly, 50 µL of Eluation buffer was added onto the tube, incubated at RT for 2 min and the DNA eluted via centrifugation at 13000 x g for 2 min. The DNA was stored at -20 °C for further use.

2.2.8.2   Mini preparation for correct vector assembly screening

Mini preparation to screen colonies for the correct assembly of plasmid DNA were done using following protocol.

1,5 mL of overnight colonies were centrifuged at 6000 g for 5min. The supernatant was discarded and the remaining pellet resuspended in 100 µL Solution I (50mM Tris base, 10 mM Na$_2$EDTA x H$_2$O, RNAse A, pH 8). Afterwards the cells were lysed with 100 µL Solution II (200 mM NaOH, 35 mM SDS) and the lysis stopped after around 10 sec with the admission of solution III (3 M potassium acetate, conc. acetic acid to ph 5.5). Afterwards, the samples were centrifuged and the supernatant transferred into reaction tubes containing 500 µL 96% EtOH and incubated at -20°C for 15 min. After incubation, samples were vortexed briefly and centrifuged at 15000 g for 5 min. The supernatant was discarded and 500 µL 70% EtOH was added to the samples. The samples were centrifuged for 3 min at 15000 g, the supernatant was discarded and the remaining pellets were dried. Afterwards pellets were resuspended in 30 µL ddH$_2$O. Lastly each sample was checked for correct vector assembly by DNA restriction using the resuspended pellet as a template and the two restriction enzymes flanking the inserted DNA sequence.

Overnight colonies of samples identified containing the correct insert were used to prepare new overnight colonies by inoculate 100 mL of LB-Broth media with the samples following incubation at 37°C and shaking with 300 rpm until the next day.

2.2.9 Midi Preparation

Larger Scale Plasmid DNA purification was carried out using the NucleoBond® Xtra Midi Kit (Macherey Nagel) according to the protocol provided by the manufacturer.

100 mL of over night cultures were transferred into 2x 50 mL Falcon tubes and centrifuged with 6000 x g for 10 min at 4°C (Centrifuge 5804-R, Eppendorf). The flow-through was discarded and the pellets resuspended with a total of 8 mL Buffer RES. Next, cells were lysed adding 8 mL Buffer LYS, inverting the tube 5 times and incubating for 5 min. While lysis, NucleoBond® Xtra Columns were equilibrated by adding 12 mL Buffer EQU applying the buffer onto the rim of the filter. The lysis was stopped using 8 mL Buffer NEU and inverting the tube until solution was completely colorless. The homogeneous solution was directly loaded onto the Column filter. The flow-through was discarded and the column filter washed with 5 mL Buffer EQU. The filter was removed and the column washed with 8 mL Buffer WASH. The DNA was eluded using 5 mL Buffer ELU and collected in a new 50 mL Falcon tube. DNA was precipitated by adding 3,5 mL isopropanol to the solution with subsequent vortexing of the sample. The solution was centrifuged at 4°C for 30 min at 15000 x g. The resulting flow-through was discarded and the pellet was washed by adding 2 mL 70% EtOH and centrifugation at 15000 x g for 5 min at RT. Last, the pellet was dried, dissolved in 300 µL ddH$_2$O and stored at -20°C for further use.

2.2.10   DNA concentration measurement

DNA concentration was measured using a BioPhotometer (D30 Photometer, Eppendorf; µCuvette G1.0, Eppendorf). The system was blanked against 1µl of puffer used for DNA resuspension. Afterwards, DNA sample were loaded onto the µCuvette and the DNA concentration was measured.

2.2.11   Sequencing

Sequencing was carried out by LGC genomics GmbH using Sanger sequencing. Samples were prepared as requested by the company. Specific primers which were flanking the DNA regions of interest were provided by the company. Results of sequencing were aligned with estimated maps of the vectors using the online multiple sequence alignment

tool Clustal Omega from EMBL-EBI (Madeira et al. 2022) and correct assembly and sequence information of generated vectors were verified.

2.2.12   Cell Culture

2.2.12.1   Splitting

Human embryonic kidney cells were splitted 2 times a week. Old media was aspirated and cells were detached by force, using 5 mL fresh preheated (37°C) media (Roti Cell DMEM High Glucose, sterile, with glutamine, without pyruvate, Carl Roth). An appropriate volume of the Cell suspension was transferred to a new T25 flask (Sarstedt) containing 5 mL medium. Afterwards, cells were incubated at 37°C at 5% CO_2 (CellXpert C170i Incubator, Eppendorf) until confluence of ~80% was reached for the next splitting cycle.

2.2.12.2   Transfection

Cells were splitted into tissue culture treated 35 mm microscope dishes (µ-Dish 35 mm, Ibidi) or tissue culture treated 60 mm cell culture dishes (Sarstedt). After reaching a confluency of 70%, cells were transfected using Polyethylenimine (PEI, Polyethylenimine, branched, average Mw ~25000, Aldrich chemistry).

For 35 mm microscope dishes, 1 µg DNA were added to 100 µL of DMEM (Roti Cell DMEM High Glucose, Carl Roth). To this solution, 4 µL PEI was added and thoroughly mixed. For 60 mm cell culture dishes, 3 µg DNA and 12 µL PEI was used.

In both cases the solution was incubated for 15 min at RT. Afterwards the solutions were added drop wise to the cell dishes and the dishes were carefully shaken for an equal distribution of the mixture. Transfected cells were transferred to the incubator and incubated at 37°C at 5% CO_2 for 12-36h until they were measured.

2.2.13   Preparation of Chemicals

Stock solutions of chemicals used for the investigation of the sensor were prepared fresh on the day of the measurements.

Therefore a small amount of the chemicals were weight in using a precision balance (Practum® Analytical and Precision Balances Scale, Sartorius). Volume needed for preparation of stock solutions were calculated, and afterwards the chemicals were dissolved in the calculated volumes of PBS (2,7 mM KCl, 138 mM NaCl, 0,5 mM MgCl$_2$, 0,9 mM CaCl$_2$, 1,47 mM KH$_2$PO$_4$, 8 mM Na$_2$HPO$_4$). Needed volumes of PBS for preparing specific concentrations of stock solutions were calculated using the following formula:

$$(\frac{m}{M})*(\frac{1}{c})=V$$

m = weight of chemical

M = Molecular mass of chemical

c = wanted concentration of chemical

V = Volume of puffer needed

Different concentrations used in the experiments were prepared by dilution of the stock solutions using PBS.

2.2.14   Measurements

2.2.14.1   Mutant screening

The media on the cells was aspirated and the cells washed with PBS (2,7 mM KCl, 138 mM NaCl, 0,5 mM MgCl$_2$, 0,9 mM CaCl$_2$, 1,47 mM KH$_2$PO$_4$, 8 mM Na$_2$HPO$_4$) three times. 3 mL PBS was added to the cells and the cells were placed under the microscope setup (BX51 Fluorescent microscope, LUMPlanFL N 40x Objective, Olympus).

For screening of serotonin sensor mutants, serotonin was applied using a syringe containing serotonin (Serotonin Hydrochloride, Carl Roth) in high concentration (100 µM). The syringe was connected to a cannula via a polypropylen tube. The cannula was placed on a manipulator unit (Mini 25-ZL, Luigs & Neumann Feinmechanik + Elektrotechnik GmbH) connected to a micromanipulator (SM-10-V2.0, Luigs & Neumann Feinmechanik + Elektrotechnik GmbH). The cannula was positioned right above the surface level of the

PBS solution in the culture dish. A series of pictures were acquired over 2 min for each mutant which showed promising fluorescence (camera used: Orca-Spark, Hamamatsu Photonics; light source: pE-300, CoolLED; Excitation filter: ET470/40 X, Chroma Technology Corporation; Emission filter: ET525/50 M, Chroma Technology Corporation), controlled by the program HoKAWO (Verison 3.0, Hamamatsu Photonics Deutschland GmbH). While recording, after around the 30 s mark, ~3 mL of serotonin solution was added to the bath solution.

2.2.14.2 Measurements of specificity and affinity

The media on the cells was aspirated and the cells washed with PBS three times. 3 mL PBS (2,7 mM KCl, 138 mM NaCl, 0,5 mM $MgCl_2$, 0,9 mM $CaCl_2$, 1,47 mM KH_2PO_4, 8 mM Na_2HPO_4) was added to the cells and the cells were placed under the microscope setup (BX51 Fluorescent microscope, LUMPlanFL N 40x Objective, Olympus).

To measure the affinity or specificity of possible serotonin sensors, chemicals were applied using a selfmade gravity driven perfusion system, which contained two reservoirs for solutions. In one of the reservoirs, PBS was filled, while the other reservoir contained the solution with the chemical of interest. The output of the reservoirs was a fine cannula, which was placed via a micromanipulator ((Mini 25-ZL + SM-10-V2.0, Luigs & Neumann Feinmechanik + Elektrotechnik GmbH) directly beside the cells, with the opening of the cannula facing the cells.

Cells were continuously perfused with PBS of the first reservoir. A series of pictures were acquired over 2 min for each measurement (Orca-Spark, Hamamatsu Photonics; Excitation filter: ET470/40 X, Chroma Technology Corporation; Emission filter: ET525/50 M, Chroma Technology Corporation), controlled by the program HoKAWO (Verison 3.0, Hamamatsu Photonics Deutschland GmbH). While recording, chemicals were applied by switching the perfusion system output to the reservoir, containing PBS with the chemical of interest. Each measurement was repeated three times.

2.2.14.3 Confocal imaging

35 mm microscope dishes (Ibidi) containing transfected cells were washed using 3x 1 mL PBS (2,7 mM KCl, 138 mM NaCl, 0,5 mM $MgCl_2$, 0,9 mM $CaCl_2$, 1,47 mM KH_2PO_4, 8 mM

Na$_2$HPO$_4$). Afterwards 2 mL of PBS was added and the dishes transferred to a confocal microscope (LSM 880, Zeiss). Fluorescence was measured using laser excitation at 488 nm. Photons were detected in the range between 493 nm-574 nm.

2.2.14.4   Determination of pH influence

Possible influence of different pH values to the fluorescence change of a fluorescence sensor was determined by measuring maximal fluorescence responses of the sensor at various pH values of the buffer used in the experiment. Measurements were carried out using the procedure described under 2.2.14.1 Mutant screening, with PBS buffers of different pH values (6.2, 6.6, 7.0, 7.4, 7.8). Each pH values was measured with replicates of three.

Measurements were compared using a one way analysis of variance (one-way anova). Normal distribution was tested using the Shapiro-Wilk test.

2.2.14.5   Determination of binding affinity

Measurements of binding affinity of different versions of a genetically encoded serotonin sensor were fitted using a four parameter sigmoidal fit (SigmaPlot):

$$y = y_0 + \left(\frac{a}{\left(1 + e^{-\left(\frac{x - x_0}{b}\right)}\right)} \right)$$

With y0 = minimal response value, a = minimal response value – maximal response value, x0 = infliction point (IC50/EC50), b = Hill slope of the curve.

Kd for each of the sensor variants was calculated using the fit.

2.2.14.6 Determination of binding specificity

Normally distribution of acquired data was tested using the Shapiro-Wilk test. Significance of normally distributed measurements were determined using a two-tailed t-test. Non normally distributed measurements were analyzed using the Mann-Whitney U test. Measurements were compared to control measurements, where only the buffer without additional chemicals were applied.

3   Results

For the development of a genetically encoded serotonin sensor, the 5-HT$_{1A}$ receptor was chosen as the sensing domain for 5-HT because of its high specificity for 5-HT (Kd = 1,8nM ± 0,3, (Ho et al., 1992). To detect the binding of 5-HT we decided to substitute the third intracellular loop (ICL3) with the circular permuted form of GFP (cpGFP). The idea to substitute the third intracellular loop with a fluorescence protein to generate a genetically encoded biosensor was already shown to be successful for example for dopamine and the sensor dLight (Patriarchi et al., 2018).

One advantage of this approach is, that the substitution of the third intracellular loop of the GPCR, in our case the 5-HT$_{1A}$ receptor, could lead to an inhibition of intracellular signaling cascades triggered by the receptor upon activation. Because the sensor should be used as an *in vivo* tool for visualizing serotonin dynamics of different neuronal populations later on, expression of a protein which is able to trigger signaling cascades would be unusable as a genetically encoded sensor.

In the following, the generation of a genetically encoded serotonin sensor is presented.

The first results are showing the insertion of cpGFP inside the third intracellular loop of the 5-HT$_{1A}$ receptor. In these approaches, randomly chosen insertion sites were used and the cpGFP was either directly inserted, or flanked at the N- and C-terminus by two flexible (Gly)$_5$ linkers. In an approach later on, only one part of the cpGFP was inserted into the third intracellular loop of the 5-HT$_{1A}$ receptor, while the rest was fused to the C-terminus of the receptor.

After these approaches did not yield a protein sensitive to serotonin, an approach based on the dopamine sensor dLight (Patriarchi et al., 2018) was chosen. This led to a successful generation of different proteins which showed a measurable fluorescence change after application of serotonin.

Later on, the characterization and enhancement of one of these proteins, which seemed to be best suitable as a serotonin sensor, is shown.

3.1 Random Insertion

In first experiments done in this work, the circular permuted form of GFP, cpGFP was inserted into the third intracellular loop of the 5-HT$_{1A}$ receptor (Fig. 11). In theory, binding of 5-HT to the receptor and the conformational change involving the movement of the sixth transmembrane domain within the GPCRs could potentially be relayed to the inserted cpGFP, leading to a changes of its fluorescence (Fig. 9b).

All sensor protein candidates for this first approach were cloned into an pAAV-Vector under the control of the CMV promoter (see 6.2). The insertion of cpGFP was done at specific positions using either highly flexible (Gly)$_5$ linkers, or no linkers at all (Fig. 11). The resulting proteins were called S1A3lcG I-IV. They were expressed in HEK cells and measured with confocal microscopy. Serotonin was applied to the bath solution by switching the input of a peristaltic pump to a solution containing PBS and serotonin (100µM).

Overall, fluorescence was visible in all four constructs when expressed by HEK cells. Still there was no visible elevated fluorescence signal in the membrane of the HEK cells and the fluorescence signal of the proteins was seemingly located in the cytoplasm of the cells, sparing the cell nucleus (Fig. 12a, 13a, 14a).

Measurement of all four constructs led to no direct change in fluorescence intensity upon application of 5-HT to the bath solution (Fig. 12c, 13c, 14c). The fluorescence changes were happening gradually over time, within the magnitudes of - 10,89% ± 6,52% (SEM, n = 5) for 1AcpGFPS I, 10,69% ± 4,87% (SEM, n = 5) for 1AcpGFPS II, 0,08% ± 1,28% (SEM, n = 5) for 1AcpGFPS III and - 4,82% ± 2,08% (SEM, n = 5) for 1AcpGFPS IV after serotonin application at the 100s mark compared to the fluorescence before serotonin application.

Overview
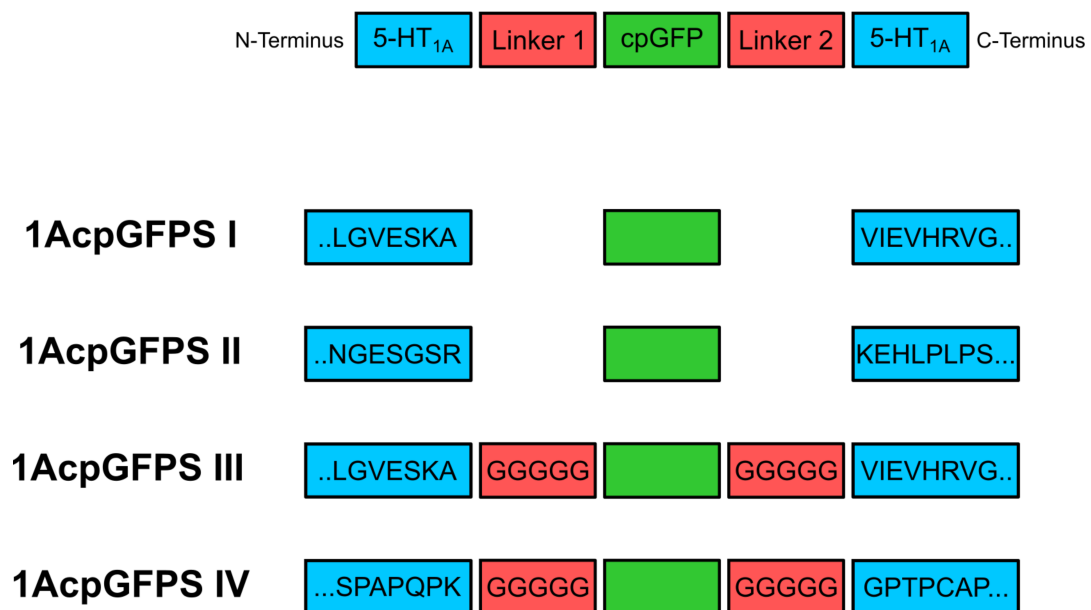
Figure 11: Sequences of random third loop substitution of 5-HT$_{1A}$ by cpGFP.

+5-HT
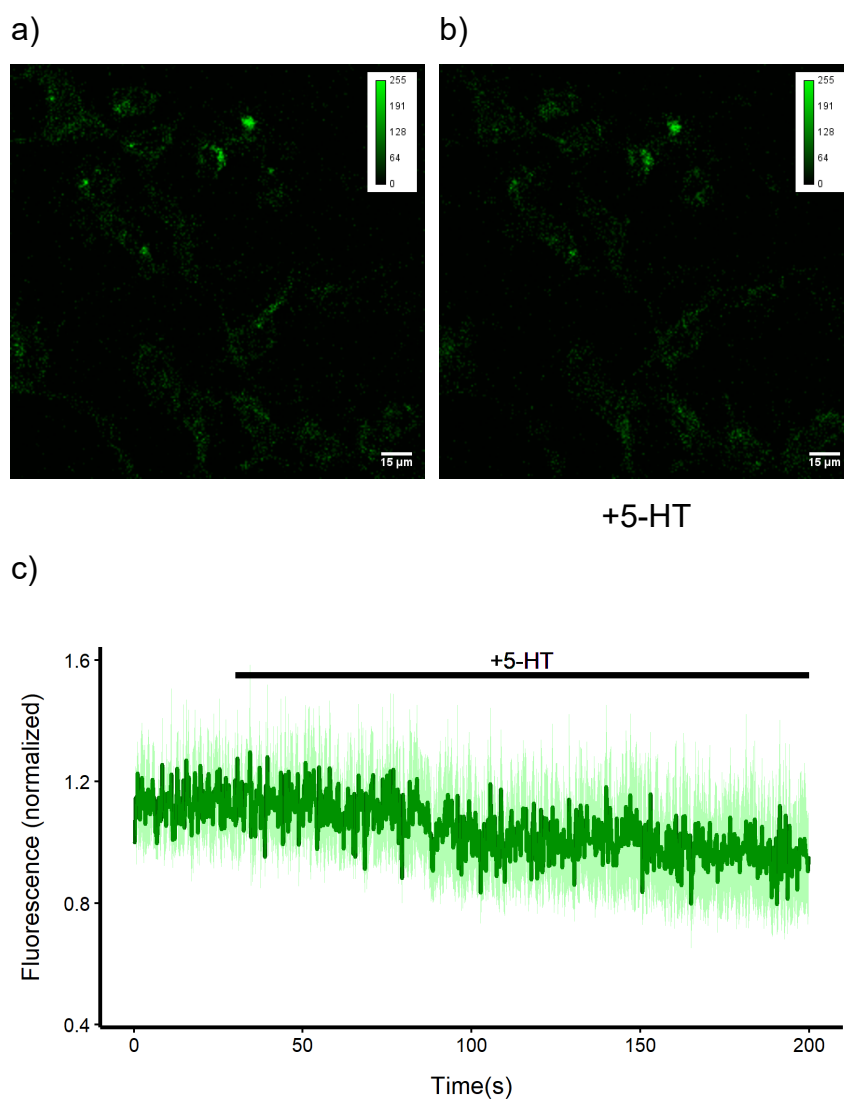
Figure 12: Measurement of S1A3LcG construct I

HEK cells expressing S1A3LcG I a) before application of serotonin and b) after application of serotonin; c)
fluorescence intensity of cells over time with application of 5-HT (100 µM), black bar represents 5-HT
application, green ribbon = SEM.

Figure 13: Measurement of S1A3LcG construct II

HEK cells expressing S1A3LcG II a) before application of serotonin and b) after application of serotonin; c)
fluorescence intensity of cells over time with application of 5-HT (100 µM), black bar represents 5-HT
application, green ribbon = SEM.

a)

b)

+5-HT

c)

Figure 14: Measurement of S1A3LcG construct III

HEK cells expressing S1A3LcG III a) before application of serotonin and b) after application of serotonin; c) fluorescence intensity of cells over time with application of 5-HT (100 µM), black bar represents 5-HT application, green ribbon = SEM.

a)

b)

+5-HT

c)

Figure 15: Measurement of S1A3LcG construct IV

HEK cells expressing S1A3LcG IV a) before application of serotonin and b) after application of serotonin; c)
fluorescence intensity of cells over time with application of 5-HT (100 µM), black bar represents 5-HT
application, green ribbon = SEM.

3.2 Split GFP Approach

Additionally, a GFP complementation approach was used to generate a functioning serotonin sensor.

In this, only a fraction of cpGFP was inserted into the third intracellular loop of the 5-HT$_{1A}$ receptor, while the rest of the protein was fused to the c-terminus of the 5-HT$_{1A}$ receptor. Through complementation of the cpGFP after expression of the full aminoacid chain, a full functioning fluorescence protein was thought to develop, linking the third intracellular loop to the c-terminus. This approach was thought to have a higher chance to create a protein which upon binding of 5-HT shows a visible fluorescence intensity change due to the fact, that the stability of the GFP could be larger effected by conformational changes within the 5-HT$_{1A}$ receptor backbone.

Two proteins were built containing a part of cpGFP without the "GGTGGS" linker, which was used in the initial circular permutation of GFP. Either Aminoacids Asn^{1}-Lys^{90} or Aminoacids Met^{97}-Asn^{241} of cpGFP were inserted in the third intracellular loop of the 5-HT$_{1A}$ receptor, while the remaining part was fused to the C-terminus of the receptor (Fig. 16).

A fluorescence signal was visible in both construct (Fig 17a, 18a) but it was not pronounced in the cell membrane and mostly visible in the cytosolic portions of the cell.

Measurements of both constructs did not show any fluorescence change upon application of 5-HT to the expressing HEK cells (Fig. 17c, 18c). The fluorescence change before and after serotonin application was - 17,73% ± 3,38% (SEM, n = 5) for the construct "splitG" and - 13,71% ± 5,48% (SEM, n = 5) for the construct "splitcG".

Overview
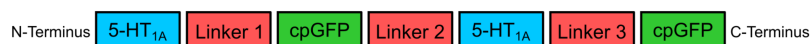
Figure 16: Substitutions of ICL3 of the 5-HT$_{1A}$ receptor and insertion and c-terminal fusing of parts of cpGFP.

a)

b)

+5-HT

c)
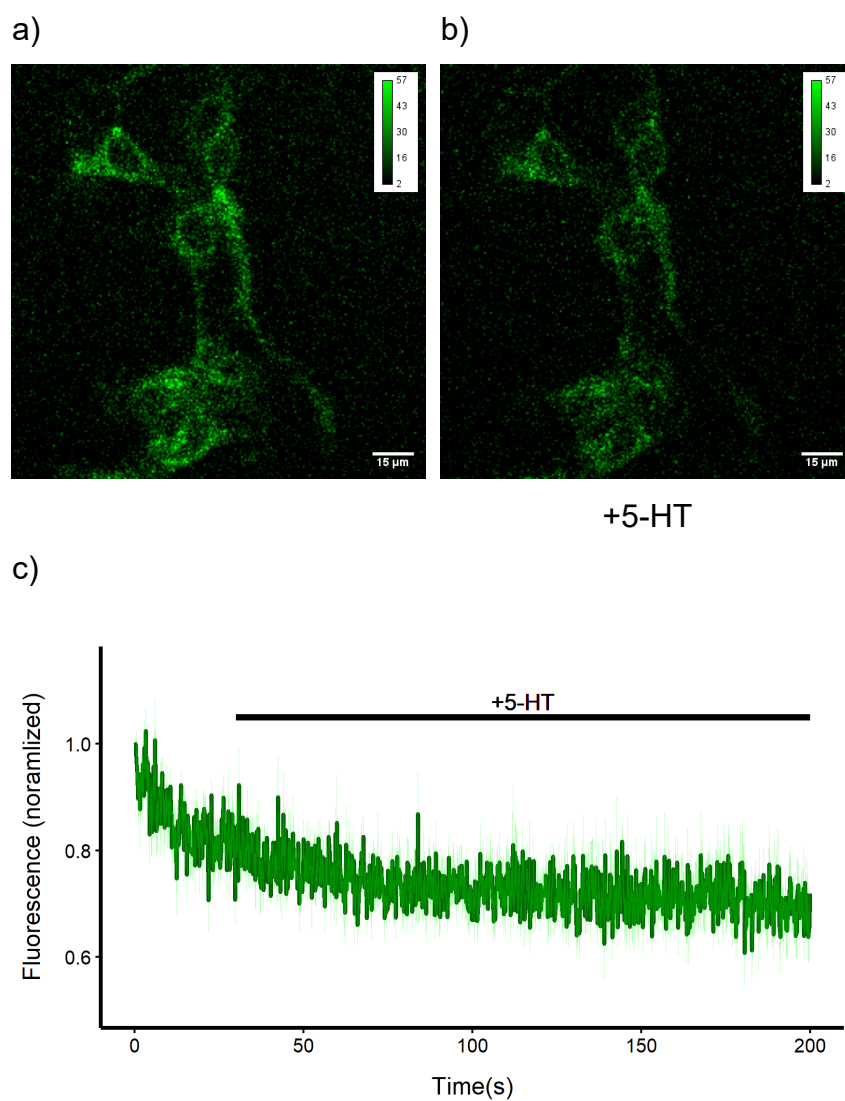
Figure 17: Measurement of S1A3LcG splitG I

HEK cells expressing S1A3LcG splitG a) before application of serotonin and b) after application of serotonin; c) fluorescence intensity of cells over time with application of 5-HT (100 µM), black bar represents 5-HT application, green ribbon = SEM.
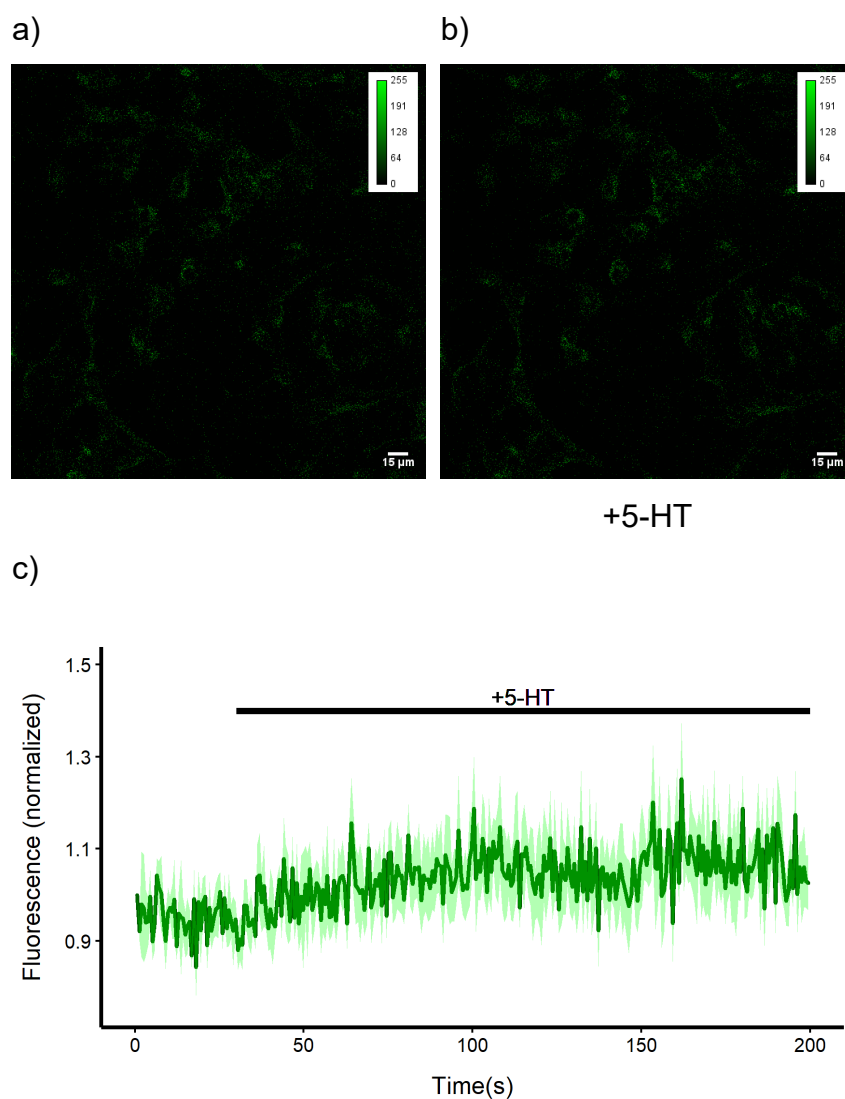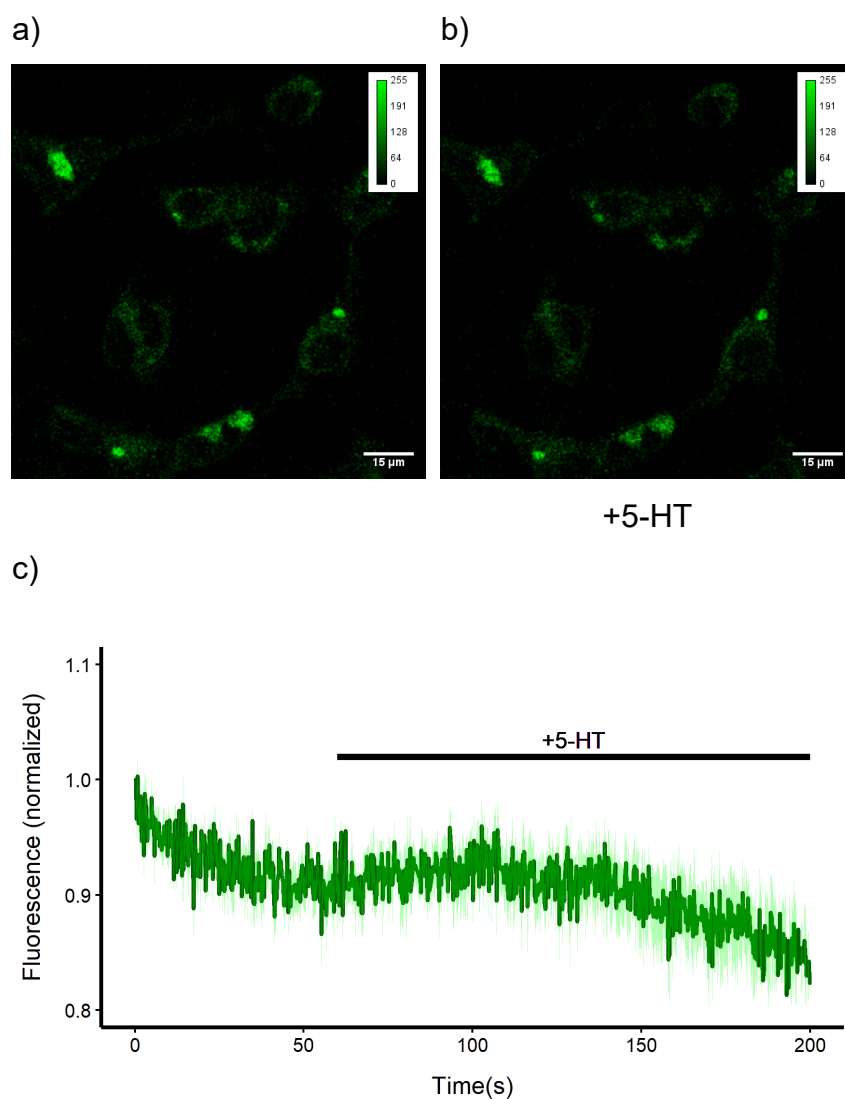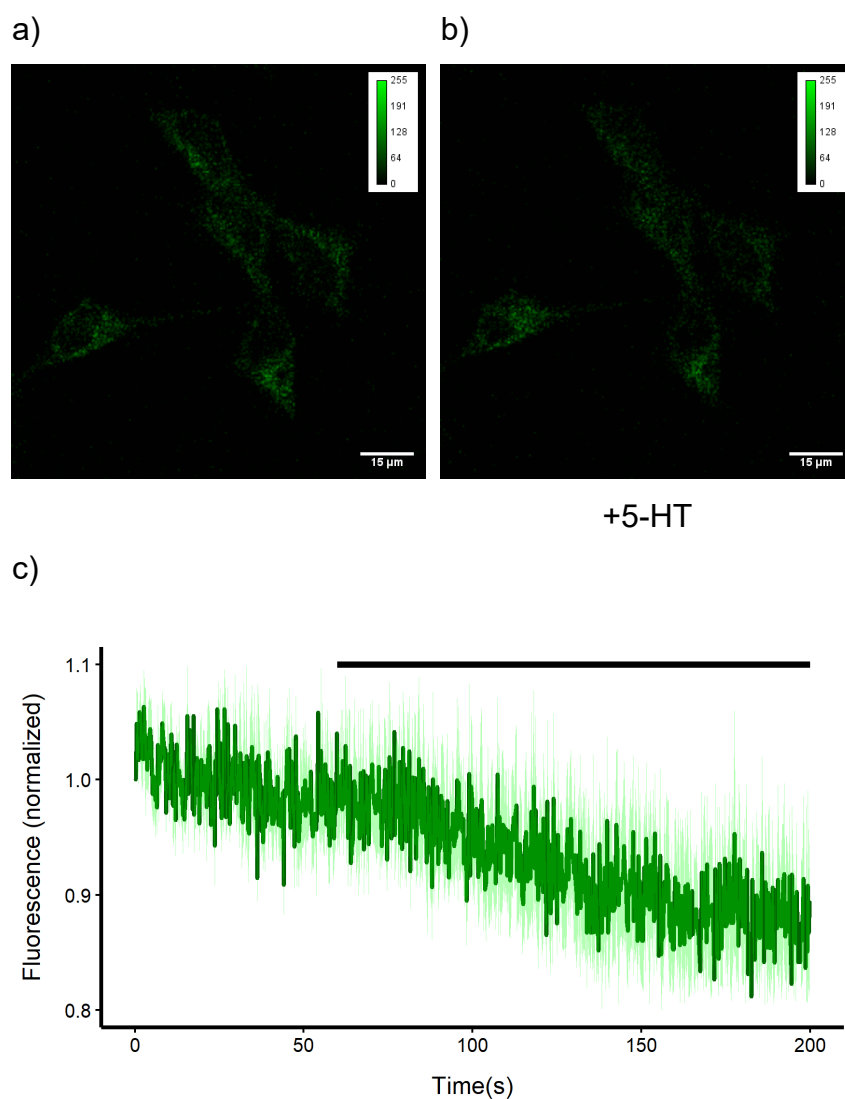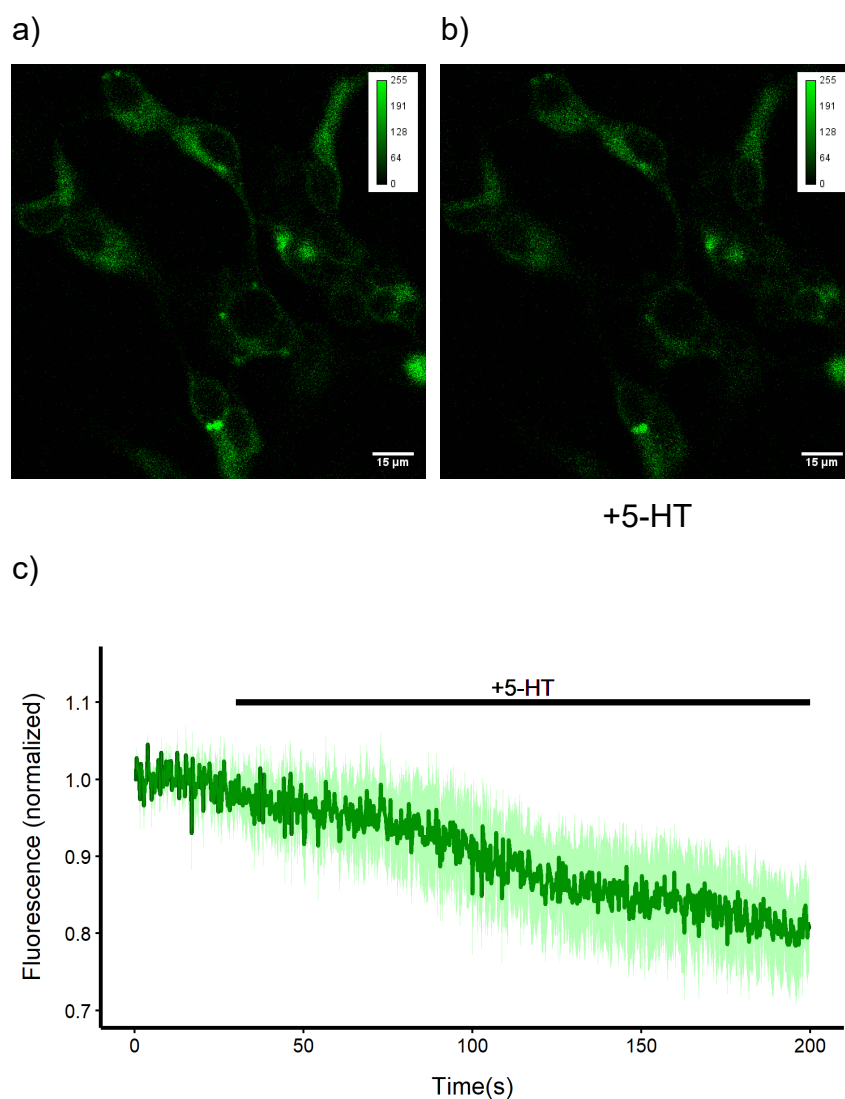
Figure 18: Measurement of S1A3LcG splitcG II

HEK cells expressing S1A3LcG splitcG a) before application of serotonin and b) after application of serotonin; c) fluorescence intensity of cells over time with application of 5-HT (100 µM), black bar represents 5-HT application, green ribbon = SEM.

3.3 After dLight

After random insertion of the circular permuted GFP into the third intracellular loop of the 5-HT$_{1A}$ receptor, substitutions based on alignments with the dopamine sensor dLight1 were carried out (Patriarchi et al., 2018).

Two substitution sites were chosen, based on alignments to the DRD1 receptor substitution and the 5-HT$_{2A}$ receptor substitution (Patriarchi et al., 2018) (Fig. 19, 20). The substitution of the third intracellular loop of the DRD1 receptor is corresponding to the substitution used to generate the dopamine sensor dLight1. The substitution of the 5HT$_{2A}$ receptor corresponds to the substitution used to show the general feasibility of the approach. The specific sites identified for substitution of the third intracellular loop of the 5HT$_{1A}$ receptor were located between aminoacids Arg^{223} and Ala^{338}, based on the substitution in dLight1 and between the 5-HT$_{1A}$ receptor aminoacids Phe^{224} and Arg^{337}, which were based on the 5-HT$_{2A}$ receptor substitution. Mutants of the dLight1 based insertion site were named "light" and mutants based on the 5-HT$_{2A}$ receptor insertion site were were called "2AS".

As the cpGFP flanking Linkers, cpGFP flanking sequences of the calcium sensor GCamp6 were used and randomly mutated (T.-W. Chen et al., 2013). In the initial step, four aminoacids were randomly mutated to generate a library of mutants which were screened for fluorescence change after application of serotonin. The mutated aminoacids were the two closest aminoacids to the cpGFP in both linkers.

The generation of random mutation was carried out using triplets of NNK bases in the primer synthesis.

Figure 19: Sequence alignment of dopamine sensor dLight1 with 5HT$_{1A}$ receptor substitution "light"

Blue: Sequence of GPCRs DRD1 receptor (top) or 5-HT$_{1A}$ receptor (bottom); Green: sequence of cpGFP; Red: Linker sequences.

Figure 20: Sequence alignment of 5-HT$_{2A}$ substitution site with 5HT$_{1A}$ receptor substitution "2AS"

Blue: Sequence of GPCRs 5-HT$_{2A}$ receptor (top) or 5-HT$_{1A}$ receptor (bottom); Green: sequence of cpGFP; Red: Linker sequences.

Screening of the mutants with a fluorescence microscope showed differences between each mutant. The fluorescence signal was either located within the cell membrane, in different intracellular locations within the cells or there was no fluorescence signal visible at all (examples under 6.3 Example fluorescence profiles). Ruling out mutants with no visible or low fluorescence signals, the fluorescence change of different mutants ("light" and "2AS") were measured by application of serotonin (100 µM) to the bath solution, via a gravity flow driven perfusion system (Fig. 21).

From the screening of mutants of the mutant library "light" (n = 12), corresponding to the insertion site of the genetically encoded dopamine sensor dLight1 within the DRD1 receptor, no candidate showed a visible change in fluorescence intensity after application of serotonin (Fig. 21, "light").

Screening of the mutant library of mutants "2AS" (n = 58), corresponding to the insertion site of the $5HT_{2A}$ receptor, multiple mutants showed changes in fluorescence upon application of serotonin. Of these mutants, one mutant, "2AS M24", showed an increase in fluorescence of 19,56% ± 0,03%, (SEM, n = 5) while another mutant, "2AS M34", showed a strong decrease of - 74,33% ± 0,05%, (SEM, n = 5) (Fig. 21, "2AS").

For further mutations, the DNA sequences of eight mutants from the mutant library "2AS" were determined by sanger sequencing (Tab. 5). Out of these eight sequenced mutants, five showed a fluorescence change in the magnitude over |10%| after 5-HT application, with one mutant reacting with an increase in fluorescence (Tab. 5, "2AS M24"). The two other mutants showed a small fluorescence change under |10%| and or no fluorescence change at all (Tab. 5, "2AS M20" and "2AS M44").
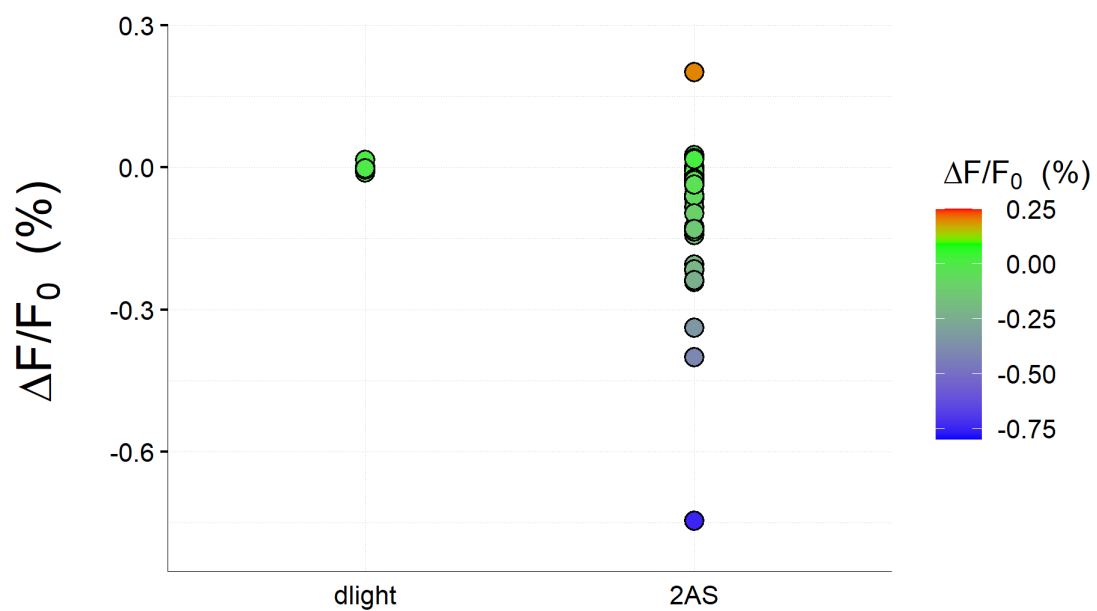
Figure 21: Fluorescence change of mutants from mutant libraries "light" and "2AS".

Table 5: Linker sequences of various 2AS Mutants

Sample	Linker1		Linker2		dF/F (%)
	Position 1	Position 2	Position 3	Position 4	
2AS M4	T	M	C	V	-33,9% ±2,01 (SEM)
2AS M8	L	D	C	F	-22,58% ±2,69% (SEM)
2AS M20	R	N	F	C	-8,82% ±1,41% (SEM)
2AS M24	T	C	R	R	18,4% ±5,81% (SEM)
2AS M34	Y	K	C	F	-74,33% ±0,05% (SEM)
2AS M40	H	R	V	Y	-24,7% ±3,5% (SEM)
2AS M44	S	N	D	S	0,64% ±1,17% (SEM)
2AS M45	H	C	C	W	-42,39% ±6,52% (SEM)

Identification of the aminoacid composition in the randomly mutated linkers showed, that the negative reacting mutants have a prevalence of specific aminoacids in the second c-terminally located linker (Tab. 5). In position three, cysteine was prevalent in samples, reacting with a decrease in fluorescence upon application of serotonin. In the fourth position, aromatic aminoacids (Phe, Trp, Tyr) seemed to be more prevalent (Tab. 5).

Based on this finding, more mutant libraries were generated containing the aminoacid Cys in the third linker position and the aminoacids Phe orTrp in fourth position. Generated mutant libraries were named "CF" and "CW".

For generating more mutants reacting with an increase in fluorescence upon application of serotonin, additional mutational libraries were cloned, containing either the aminoacids Thr and Cys named "TC" at position 1 and 2 of linker 1 or Arg and Arg at position 3 and 4 of linker 2 named "RR" based on the only mutant reacting with an increase in fluorescence "2AS M24".

Furthermore to check if a shift in the insertion site could lead to stronger reacting mutants, mutant libraries were generated containing the second linker with the aminoacids Cys and Phe of the "2AS" insertion site, which seemed beneficial to produce reacting mutants, while changing the insertion site of the first linker n-terminally in the 5-HT$_{1A}$ receptor to the insertion site of the "light" mutants. The first linker did undergo random mutations at position 1+2 while Cys and Phe in position three and four in the second linker were fixed. The generated mutants of this variant were called "L2".

In addition, mutant libraries were generated containing mutants in which the other three positions in both linker sequences were randomly mutated. Aminoacids located in the linker sequences which were not mutated, were based on the strongest reacting mutant "2AS M34". These libraries were either called "NGN", for mutants where the other three aminoacids in the first linker were mutated (XXXYK) or "NGC" where three aminoacids in the second linker were mutated (-CFXXX-).

A detailed overview of the different mutant libraries created is visualized in Fig. 22. Of all these mutant libraries the fluorescence change upon application of serotonin (100 µM) was measured for different mutants expressed in HEK cells.
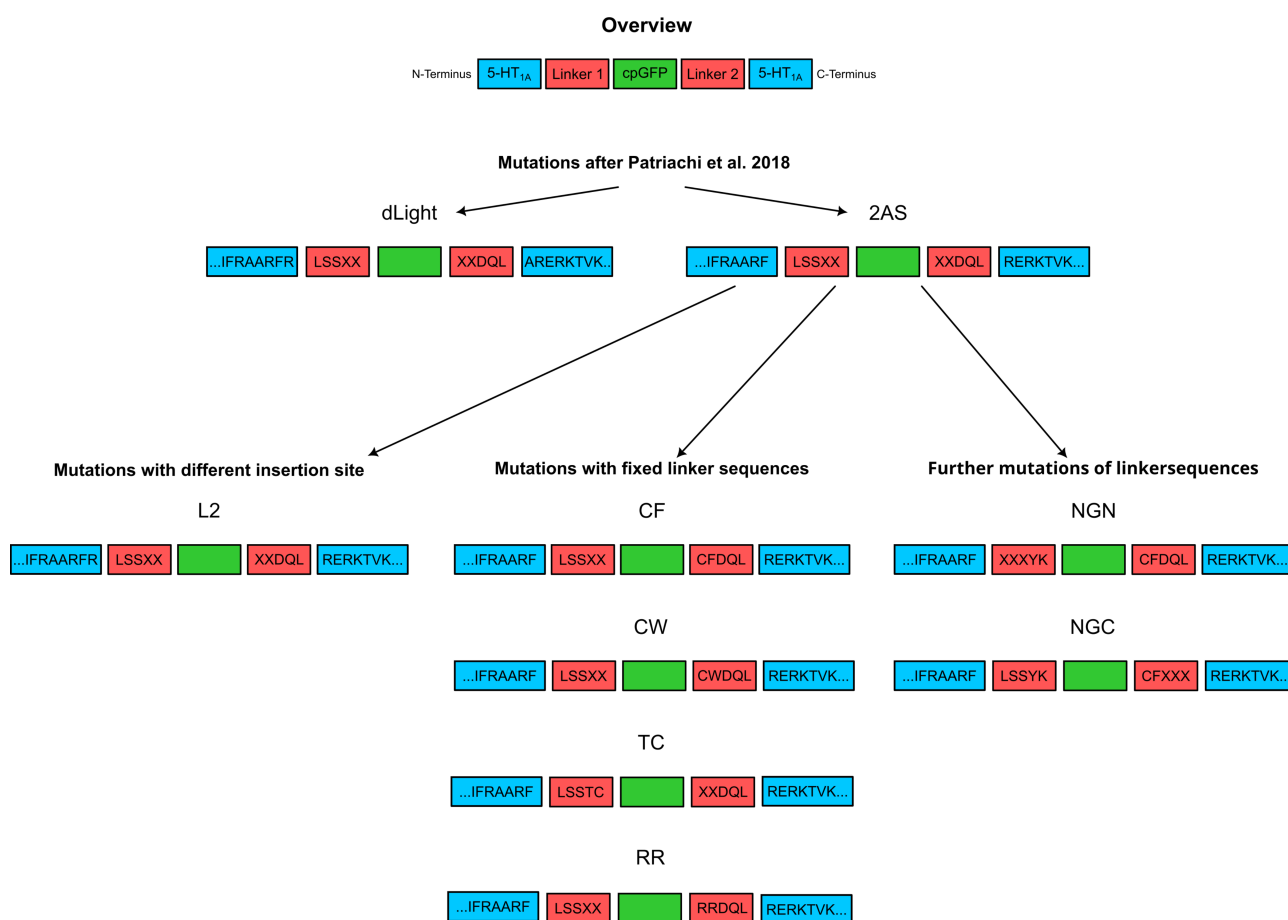
Figure 22: Sequences of mutant libraries generated and measured.

Measurements of the different mutants led to multiple candidates with different magnitudes in their fluorescence change after application of 5-HT (Fig. 23).

The screening of the mutant libraries "2AS CF" (n = 60) and "2AS CW" (n = 10) showed more candidates reacting with a stronger decrease in fluorescence after application of serotonin than the initial "2AS" mutants. The strongest decrease in fluorescence was shown by the mutant 2AS CF M1 which showed a decrease in fluorescence of - 78,73% ± 0,03% (SEM, n = 5) in comparison to the mutant 2AS M34 which showed a decrease of - 74,33% ± 0,05%, (SEM, n = 5) (Fig. 24).

Screening of the mutant library called "RR" (n = 24) showed small to no changes in different mutants. The mutant showing the highest reaction to serotonin "RR M8", reacted with a decrease of - 7,55% ± 0,02% (SEM, N = 5). The screening of mutant library "TC" (n = 20) yielded mutants, reacting with a decrease of fluorescence, with the strongest decrease of - 47,48% ± 0,04% (SEM, n = 5) measured in "TC M5". Still both libraries failed

to yield more mutants reacting with an increase in fluorescence upon application of serotonin (Fig. 24).

Screening of the mutant library "L2" (n = 20), did not yield a protein showing a greater fluorescence change than the initial mutant "2AS M34" which the library was based upon. The highest reacting mutant "L2 M11" showed a change of - 52,35% ± 0,03% (SEM, n = 5), in comparison to the mutant 2AS M34 which showed a decrease of - 74,33% ± 0,05%, (SEM, n = 5) (Fig. 24).

On top of that, mutants where other aminoacids of the linker regions of "2AS M34" were mutated, did not show fluorescence changes greater in magnitude than the initial mutant "2AS M34" upon serotonin application. The highest fluorescence change measured of the screened mutants of library "NGN" (n = 10) was shown by mutant "NGN M10" with a decrease of fluorescence of - 45,19% ± 0,02% (SEM, n = 5). The highest fluorescence change measured for mutants of mutant library "NGC" was - 50,7% ± 0,02% (SEM, n = 5) of the mutant "NGC M4". In comparison the inital mutant "2AS M34" showed a decrease of fluorescence by - 74,33% ± 0,05%, (SEM, n = 5) (Fig. 24).
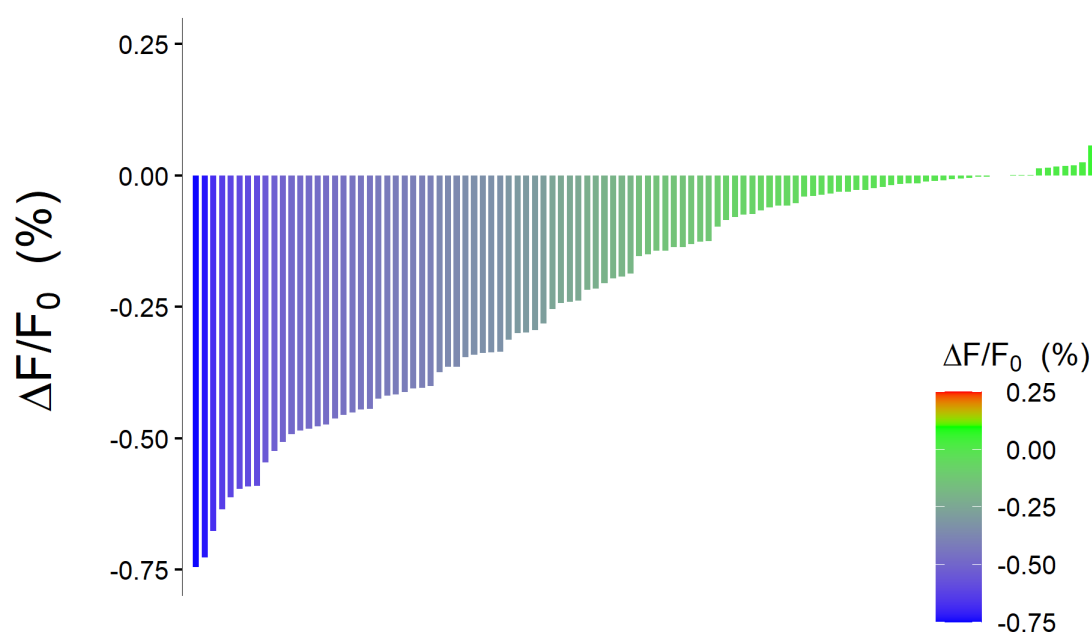
Figure 23: Overview of measured fluorescence change of different mutants.
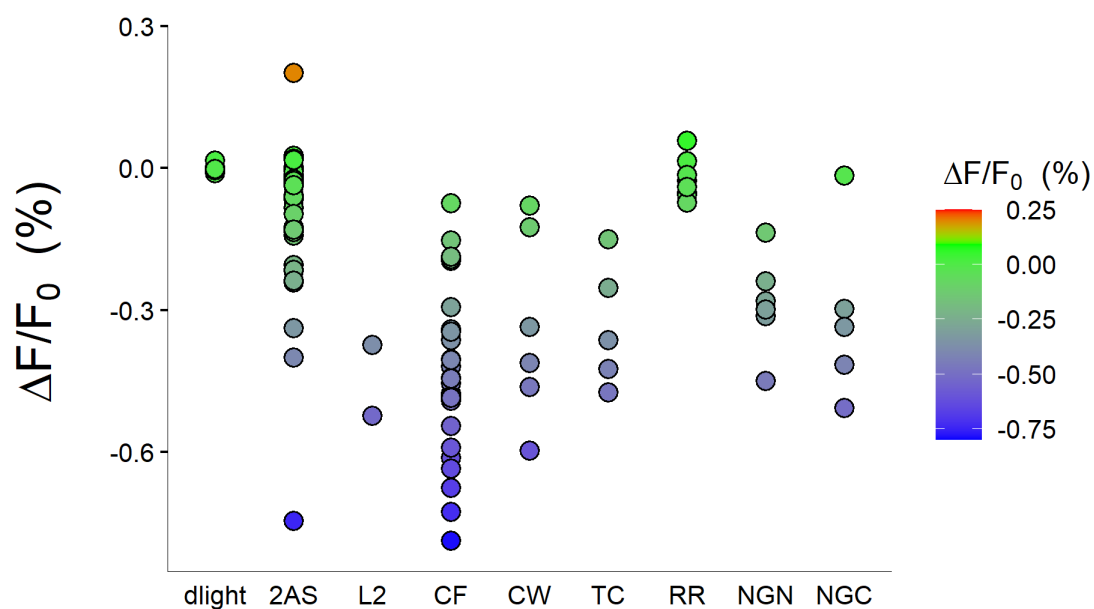
Figure 24: Fluorescence change of different mutants ordered by their respective mutant library.

To look for the viability of the mutants with the highest change (2AS M34 and CF M1) for their usage as a serotonin sensor, both mutants were expressed in HEK cells and their fluorescence evaluated. While the fluorescence change of "CF M1" upon application is higher compared to "2AS M34", ("CF M1" with - 78,73% ± 0,03% [SEM, n = 5] vs."2AS M34" with - 74,33% ± 0,05%, [SEM, n = 5]), the baseline fluorescence of "2AS M34" seemed to be much higher under the same conditions (Fig. 25). Therefore "2AS M34" was chosen as a candidate for a new serotonin sensor, with better baseline fluorescence and a comparable strong decrease in fluorescence upon binding of 5-HT in comparison to "CF M1". The mutant "2AS M34" was named "*sDarken*" because of its darkening of fluorescence after application of serotonin and is called *sDarken* (serotonin darkening 5-HT$_{1A}$ receptor-based sensor) from here onwards.

a)

b)
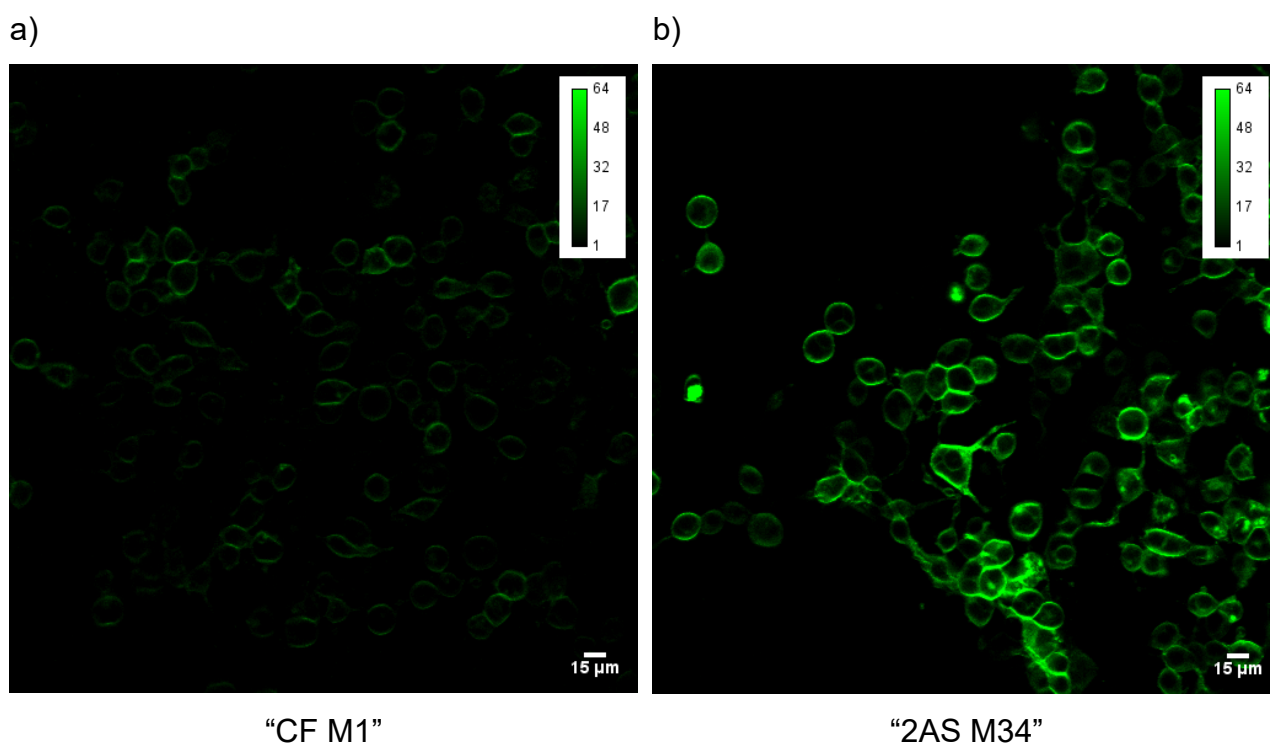
"CF M1"

"2AS M34"

Figure 25: Fluorescence picture of HEK cells expressing most promising mutants.
a) "CF M1" and b) "2AS M34"

sDarken showed a high fluorescence change of - 74,33% ± 0,05%% upon application of serotonin to HEK cells expressing it (Fig 26c). Furthermore the fluorescence signal was barely visible inside the cell and strongly located at the cell membrane when no serotonin was applied (Fig. 26a).

To check, that the decrease of the fluorescence signal triggered by 5-HT application is reversible, multiple applications of 5-HT (30µL 10µM 5-HT per application) to *sDarken* expressing HEK cells were performed. After each application, cells were washed with PBS for around three minutes to wash out the applied serotonin. Each time serotonin was applied to the cells via a short puff, a strong fluorescence decrease was observable (Fig. 27). The first application showed a decrease of fluorescence of - 65,1% ± 0,01%, the second serotonin application a decrease of - 65,6% ± 0,01%, the third serotonin application a decrease of - 65,99% ± 0,01% and the fourth serotonin application a decrease of - 64,12% ± 0,01% (SEM, n = 5). The fluorescence signal regained nearly base level, when serotonin was washed out in between the puffs (Fig. 27).

Different pH values within cells could have an effect on *sDarken*. To check if *sDarkens* fluorescence change is affected by different pH values, measurements were done incubating cells in different pH values (pH = 6,2, 6,6, 7,0, 7,4, 7,8) while serotonin was applied (Fig. 28). The fluorescence change triggered by 5-HT application was - 75,12% ± 1,57% (SEM, n = 14) for a pH of 6,2, - 75,72% ± 2,34% (SEM, n = 14) for a pH of 6,6, - 72,03% ± 2,21% (SEM, n = 13) for a pH value of 7,0, - 74,17% ± 2,20% (SEM, n =12) for a pH value of 7,4 and - 75,08% ± 1,67% (SEM, n = 14) for a pH value of 7,8. Using a one-way ANOVA, no significant difference between the measurements (P = 0,724) could be found.

Since *sDarken* was built on the basis of the 5-HT$_{1A}$ receptor, an antagonist (WAY-100635) of the 5-HT$_{1A}$ receptor was applied after triggering the fluorescence decrease by 5-HT application of *sDarken* to investigate if WAY-100635 is able to reverse the effect of 5-HT. Application of WAY-100635 after serotonin application led to a fluorescence increase back to the baseline fluorescence with a magnitude of 159% ± 11,9% (SEM, n = 5) after an initial fluorescence decrease triggered by serotonin application of - 55% ± 0,01% (SEM n = 5) (Fig. 29a-d). Interestingly, analyzing the intracellular portions of the fluorescence signal showed a small decrease of the fluorescence signal after serotonin application and a two fold strong increase in fluorescence after application of WAY-100635 (Fig. 29e).

While *sDarken* showed a strong fluorescence signal within the cell membrane, the expression of *sDarken* was evaluated further. To investigate the expression of *sDarken*, the red fluorescence protein mCherry was fused to the c-Terminus of *sDarken*. Measurements of *sDarken* with application of serotonin were carried out and pictures taken in two channels (Range of GFP channel 500-550nm, Range of RFP channel: 592,5 nm-667,5 nm). The fluorescence signal of mCherry was not congruent with the fluorescence signal measured in the GFP channel of *sDarken* (Fig. 30a, c, e) when no serotonin is applied. When serotonin is present, both fluorescence channels show similar fluorescence patterns (Fig. 30b, d, f)

To measure the 5-HT affinity of *sDarken*, the fluorescence change of *sDarken* was measured in dependence of the concentrations of applied 5-HT (Fig. 31). Measurements were carried out with fourteen different concentrations and the data was fitted using a four

parameter sigmoidal fit. Using the function of the calculated fit, the Kd value of 5-HT for *sDarken* determined to be in the magnitude of 126 nM.

To investigate if *sDarken* is specific for 5-HT, different chemicals were applied to HEK cells expressing *sDarken* and their contribution to possible fluorescence change was monitored over time (Fig 32a, b). The chemicals used were the 5-HT$_{1A}$ receptor agonist 8-OH-DPAT (7-[Dipropylamino]-5,6,7,8-tetrahydronaphthalen-1-ol), the precursor in serotonin synthesis tryptophan, the metabolite 5-HIAA (5-hydroxyindoleacetic acid), the monoaminergic neruotransmitters dopamine, histamine and norepinephrine and the neurotransmitters GABA (γ-aminobutric acid), glutamate and acetylcholine.

For application of different chemicals (10µM), fluorescence changes in the magnitude of - 39,7% ± 1,97% (SEM, n = 15) for 8-OH-DPAT, 1% ± 0,75% (SEM, n = 15) for tryptophan, 4,08% ± 0,8% (SEM, n = 15) for 5-HIAA, - 2,25% ± 0,5% (SEM, n = 15) for dopamine, 0,11% ± 0,8% (SEM, n = 15) for histamine, - 3,13% ± 0,95% (SEM, n = 15) for norepinephrine, - 1,77% ± 1,03% (SEM, n = 15) for GABA, - 1,53% ± 0,67% (SEM, n = 15) for glutamate, 2,42% ± 0,72% (SEM, n = 15) for acetylcholine, - 78,74% ± 1,3% (SEM, n = 15) for 5-HT were measured and - 0,5% ± 0,5% for the control (PBS) (SEM, n = 15) (Fig. 32b). Comparing the control to each chemical using a two-tailed t-test, revealed significant differences in fluorescence response for the chemicals 5-HIAA (P = 0,006), 5-HT (P = <0,001), 8-OH-DPAT (P = <0,001), Acetylcholine (P = 0,001) and Dopamine (P = 0,018).

Since the dynamic range of *sDarken* seem to be limited to a range of approximatly 10 nM and 1 µM (Fig. 31), different approaches were followed to generate a variety of sensors which showed different dynamic ranges, to cover a wider range of concentrations which could be detected using specific forms of *sDarken*.

In an attempt to increase the affinity of *sDarken* for serotonin, the circular permuted GFP was substituted for the circular permuted form of superfolder GFP or sfGFP.

The protein generated in this approach was called high affinity *sDarken* or *H-sDarken*. *H-sDarken* showed a comparable change in fluorescence upon application of serotonin with a fluorescence decrease of *sDarken* in the magnitude of - 78,74% ± 1,3% (SEM, n = 15) and *H-sDarken* with a decrease of - 66,83% ± 1,28% (SEM, n = 15) (Fig. 33a-c).

To measure the affinity of *H-sDarken*, the fluorescence change was measured in dependence of different applied 5-HT concentrations (Fig. 34). The data was fitted using a four parameter sigmoidal fit. The Kd of *H-sDarken* was calculated using the function of the graph and resulted in a concentration of 70 nM.

To elucidate, if *H-sDarken* shows specificity for serotonin the fluorescence signals with application of different chemicals (10µM) were measured. The fluorescence changes measured for different chemicals were - 26,32% ± 2,03% (SEM, n = 15) for 8-OHDPAT, - 5,6% ± 0,94% (SEM, n = 15) for 5-HIAA, - 5,95% ± 0,62% (SEM, n = 15) for tryptophan, - 5,51% ± 0,61% (SEM, n = 15) for dopamine, - 6,9% ± 0,74% (SEM, n = 15) for Norepinephrine, - 5,19% ± 0,51% (SEM, n = 15) for histamin, - 5,42% ± 0,69% (SEM, n = 15) for glutamate, - 7,62% ± 0,68% (SEM, n = 15) for GABA, - 6,43% ± 0,67% (SEM, n = 15) for acetylcholine, - 66,83% ± 1,28% (SEM, n = 15) for 5-HT and - 4,09% ± 0,66% for the control (PBS) (SEM, n =15) (Fig. 35a, b). Comparing the control to each chemical using a two-tailed t-test, showed significant differences in fluorescence response for the chemicals 5-HT (P = <0,001), 8-OH-DPAT (P = <0,001), Acetylcholine (P = 0,001), GABA (P = <0,001), tryptophan (P = 0,049) and Norepinephrine (P = 0,009).

In another attempt, specific mutations within the sequence of the 5-HT_{1A} receptor were carried out, to generate *sDarken* variants with lower affinity to 5-HT. The mutations were based on mutational experiments done with the 5-HT_{1A} receptor (Ho et al., 1992).
One mutation, D116N proved to be a promising candidate and was called low affinity *sDarken* or *L-sDarken*.
L-sDarken showed a comparable fluorescence decrease upon application of 5-HT as *sDarken,* with a decrease of - 67,77% ± 1,82% (SEM, n = 15) of *L-sDarken* in comparison to a decrease of - 78,74% ± 1,3% (SEM, n = 15) of *sDarken* (Fig. 36a-c).
Measurements of fluorescence change in dependence of applied 5-HT concentrations were carried out. The acquired data was fitted using a four parameter sigmoidal fit. The Kd was determined using the calculated function of the fit.The Kd of *L-sDarken* is 37 µM (Fig. 37).

As done with *sDarken* and *H-sDarken*, the specificity of *L-sDarken* was measured by application of different chemicals (3mM) while monitoring the fluorescence signal over time. Fluorescence changes for the chemicals were in the magnitude of - 61,4% ± 1,05% (SEM, n = 15) for 8-OH-DPAT, - 12,59% ± 1,20% (SEM, n = 15) for 5-HIAA, - 7,8% ± 1,05% (SEM, n = 15) for tryptophan, - 6,05% ± 0,74% (SEM, n = 15) for Norepinephrine, - 6,54% ± 0,89% (SEM, n = 15) for dopamine, - 6,28% ± 0,9% (SEM, n = 15) for histamin, - 5,64% ± 1% (SEM, n = 15) for GABA, - 8,94% ± 1,38% (SEM, n = 15) for glutamate, - 7,77% ± 1% (SEM, n = 15) for acetylcholine, - 67,77% ± 1,82% (SEM, n = 15) for 5-HT and - 3,05% ± 0,46% (SEM, n = 15) for the control (PBS) (Fig. 38a, b). Comparing the control to each chemical using a two-tailed t-test, showed significant differences in fluorescence response for the chemicals 5HIAA (P = <0,001), 5-HT (P = <0,001), 8-OH-DPAT (P = <0,001), Acetylcholine (P = 0,038), Dopamine (P = 0,009), tryptophan (P = 0,004) and Norepinephrine (P = 0,004).

a)

b)

+5-HT

c)
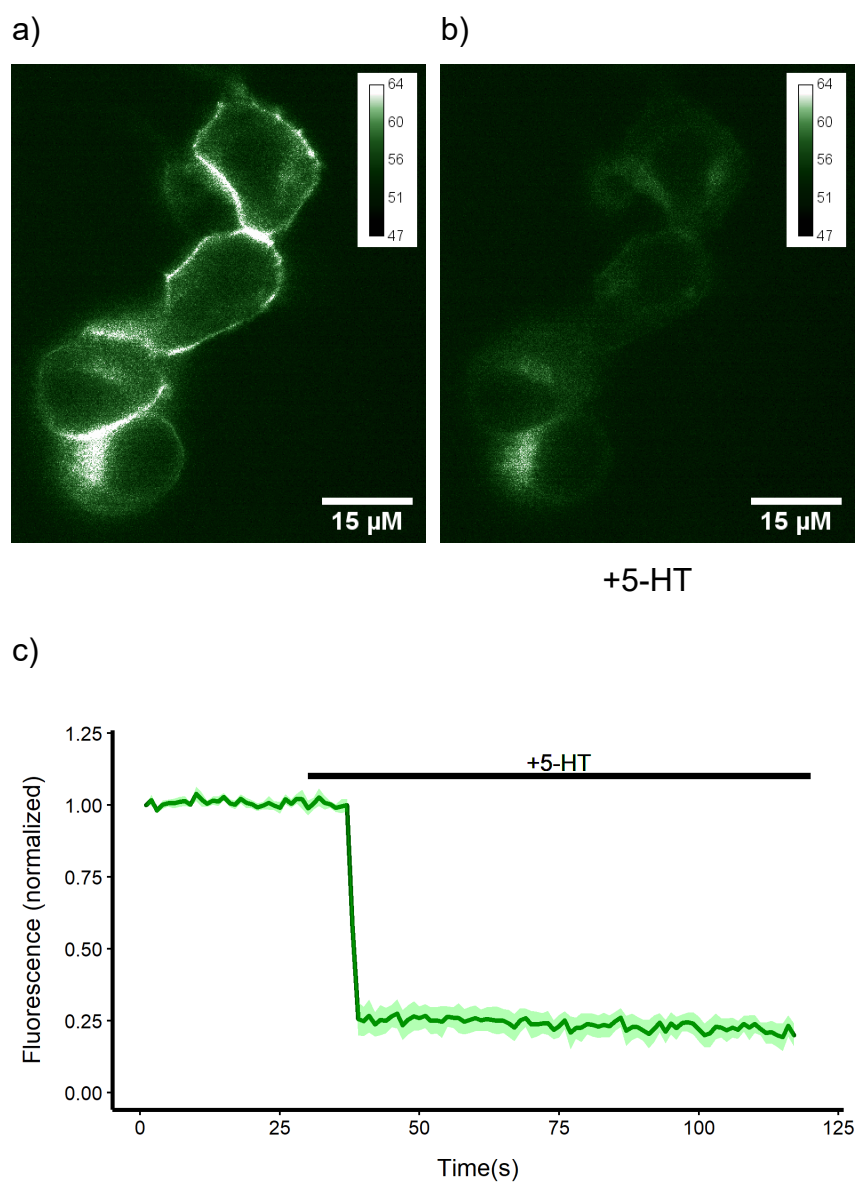
Figure 26: Fluorescence change of M34

Fluorescence pictures of cells expressing sDarken a) without and b) with 100 µM 5-HT present, c) Mean Fluorescence change of Darken after application of 100 µM 5-HT, black bar indicates application of 5-HT, Ribbon shows SEM.
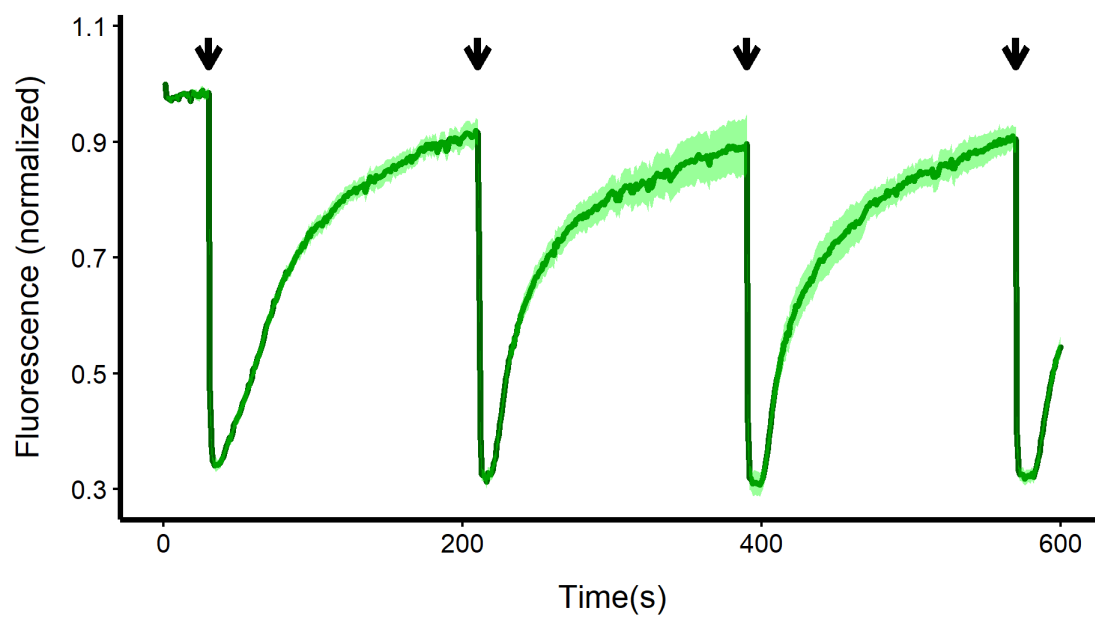
Figure 27: Repetitive stimulation of sDarken

Mean fluorescence signal of sDarken with repetitive application of 5-HT; arrows indicating time points of applications, ribbon shows SEM.
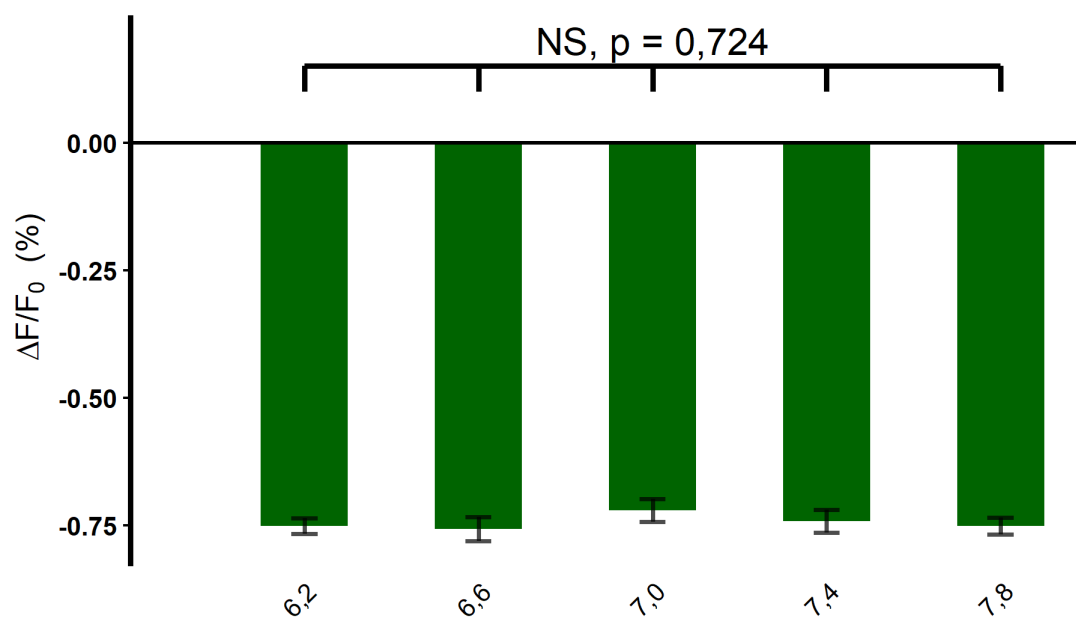
Figure 28: Influence of different pH values to sDarkens fluorescence change

Measurement of the fluorescence change after serotonin application of sDarken expressing HEK cells when incubated in PBS buffer with different pH values, error bars depict SEM, n = 12-14.

a)

b)

c)

+5-HT

+5-HT
+WAY-100635

d)
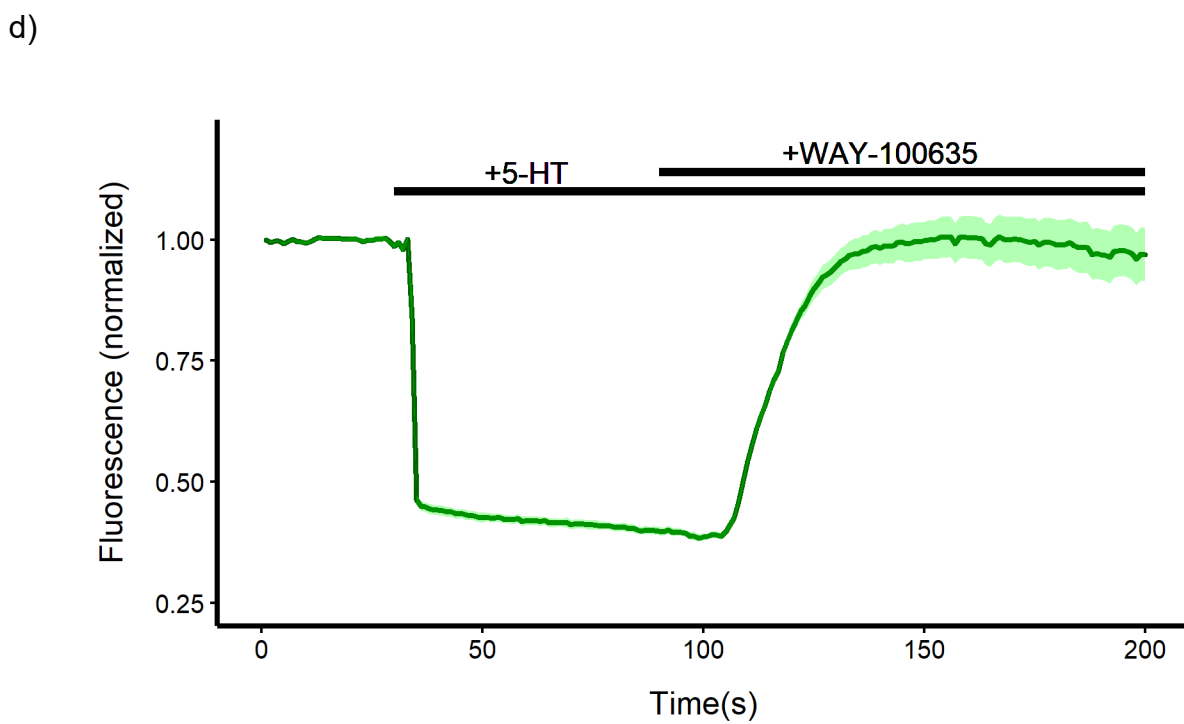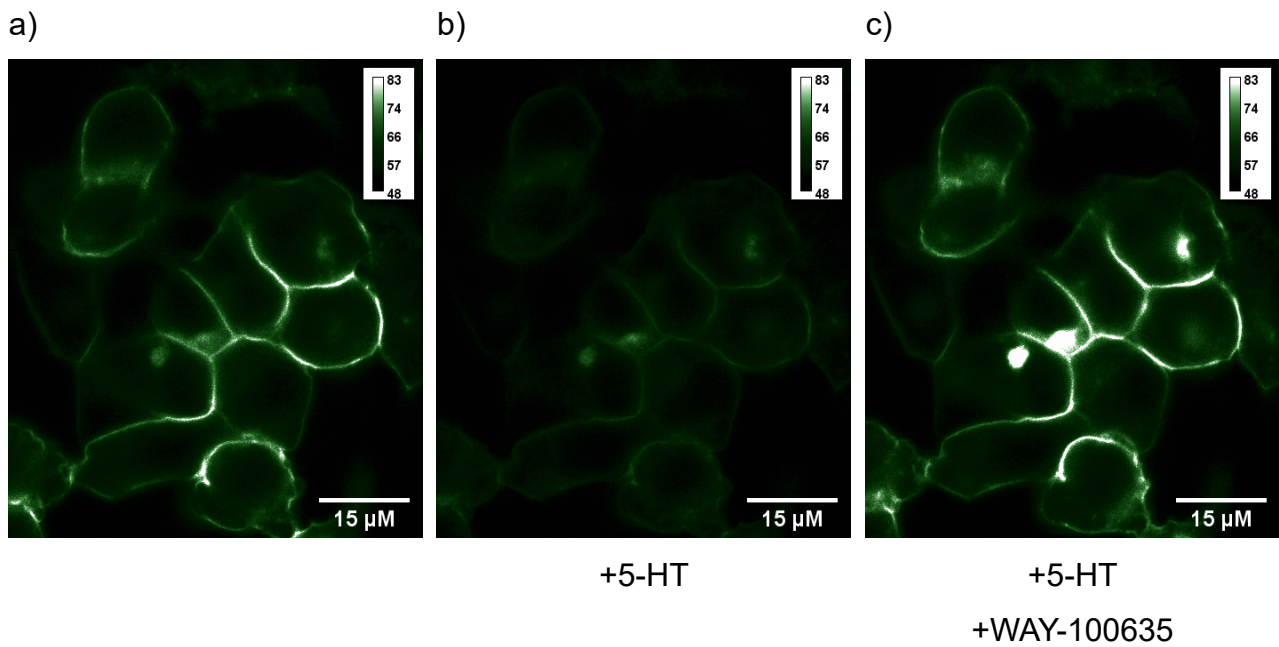
e)
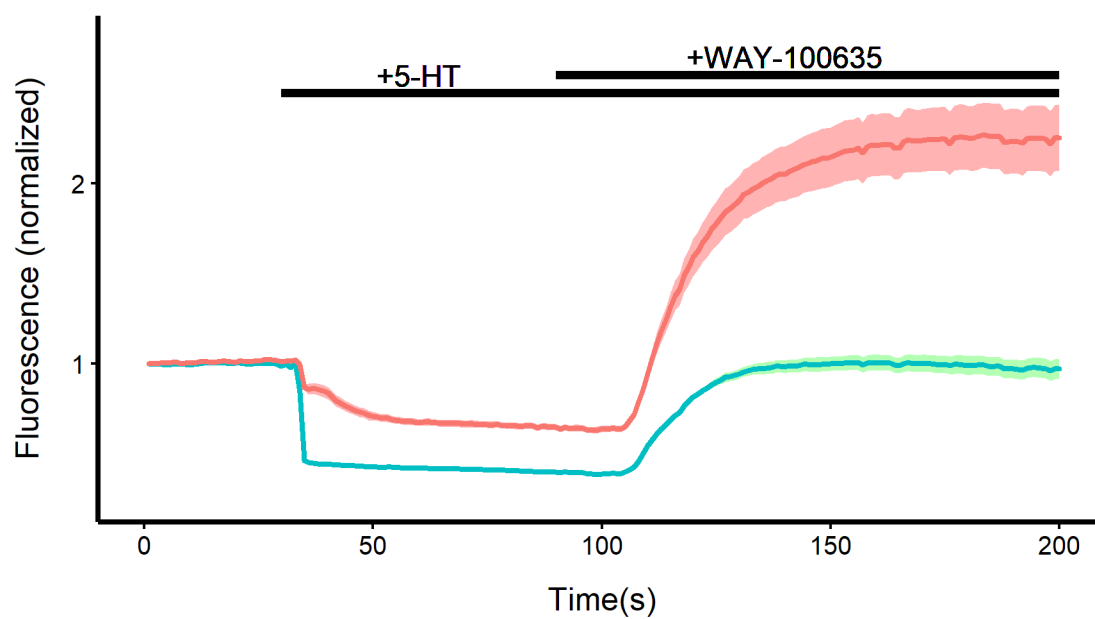
Figure 29: Inhibition of sDarken;

HEK cells expressing sDarken a) before application of chemicals, b) after application of 5-HT and c) after application of 5-HT and WAY-100635; d) Mean Fluorescence intensity of membrane portion of the cells over time, black bars indicating times of chemical application, Ribbon depicts SEM, e) Mean Fluorescence intensity of membrane portion (green) and inner cell fluorescence (red) over time, black bars indicating times of chemical application, Ribbon depicts SEM.
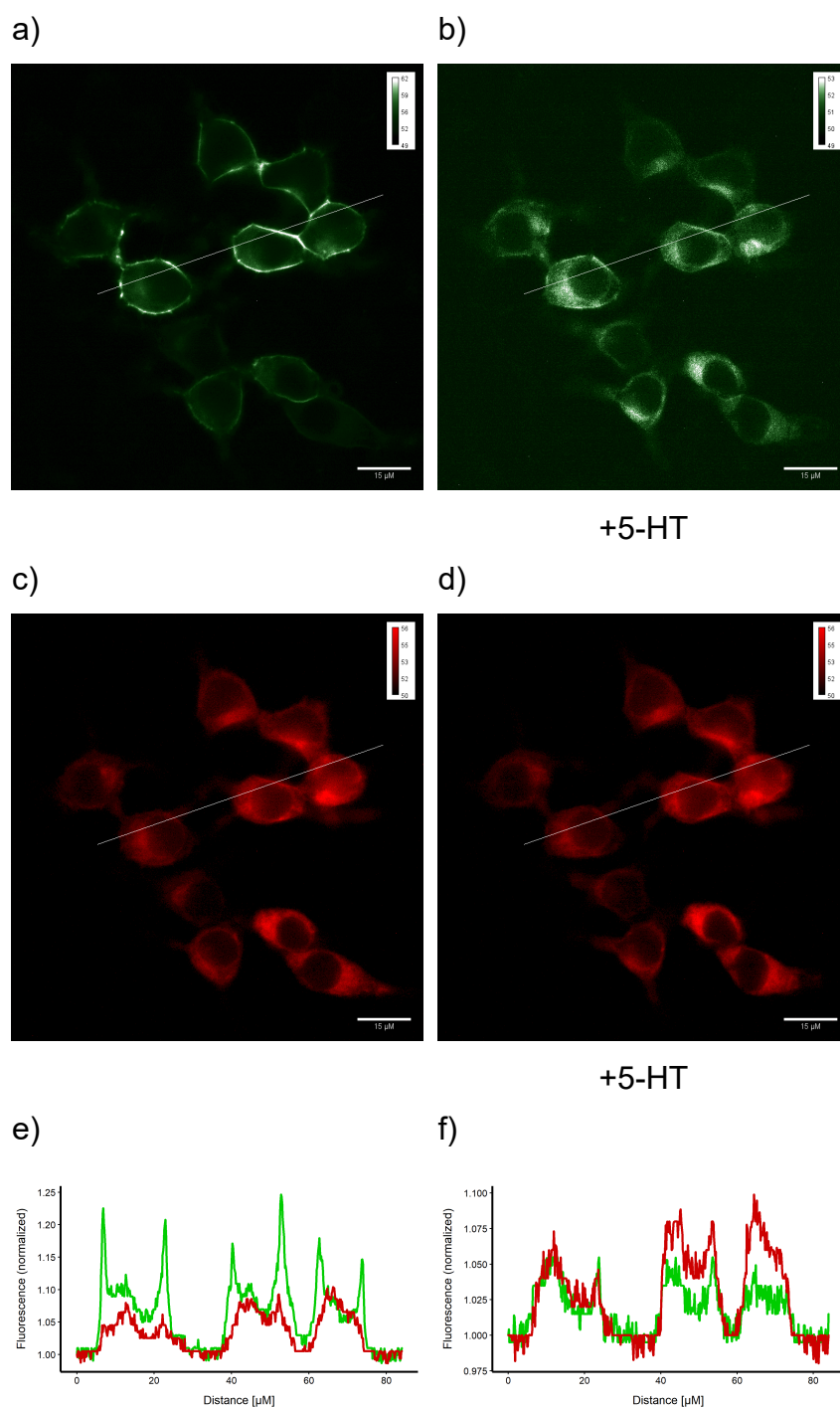
Figure 30: sDarken-mCherry Expression in HEK Cells;

Fluorescence of sDarken-mCherry expressing HEK cells a), c) without and b), d) with 5-HT (100 µM), Plot profiles of Green channel and Red channel from line scans (white lines) before d) and after e) 5-HT application; Green channel emission: 500 nm - 550 nm, Red channel emission: 592,5 nm - 667,5 nm.
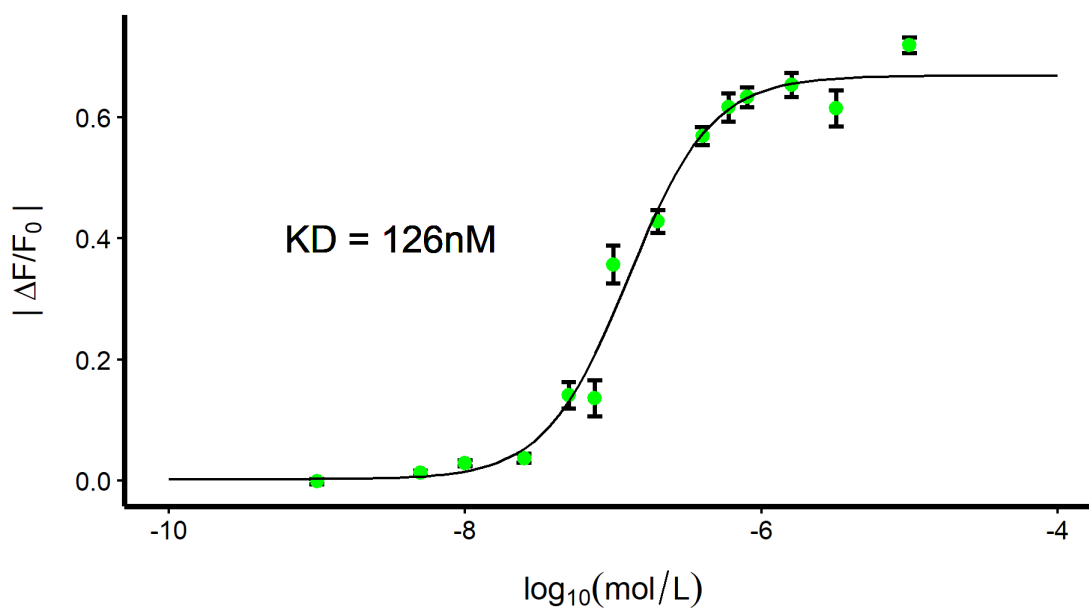
Figure 31: Affinity measurement of sDarken;

Absolute values of $\Delta F/F_0$ from multiple measurements of sDarkens fluorescence change in relation to the concentration of 5-HT applied; Data was fitted using a sigmoid four parameter fit, Kd was calculated from the fit, error bars show SEM, n = 10-20 cells per measurement.

a)

b)
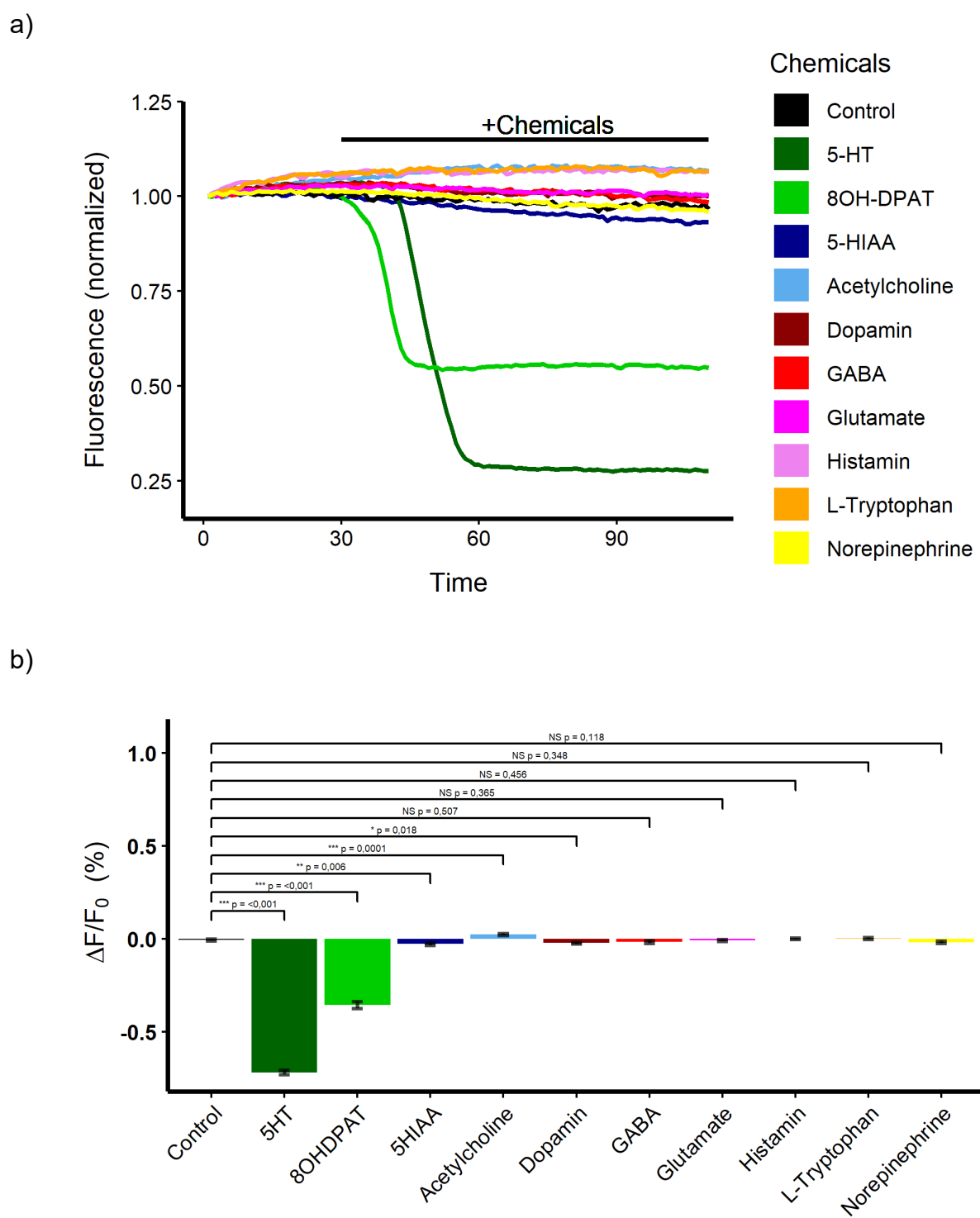
Figure 32: Specificity of sDarken to Serotonin;

a) Mean fluorescence signals of sDarken expressed in HEK cells with application of different chemicals, black bar indicates point of chemical application (100 µM), n = 15.

b) Comparison of the fluorescence change of sDarken triggered by different chemicals (100 µM) to the control application of PBS, n = 15, error bars indicating SEM.

a)

b)

+5-HT

c)
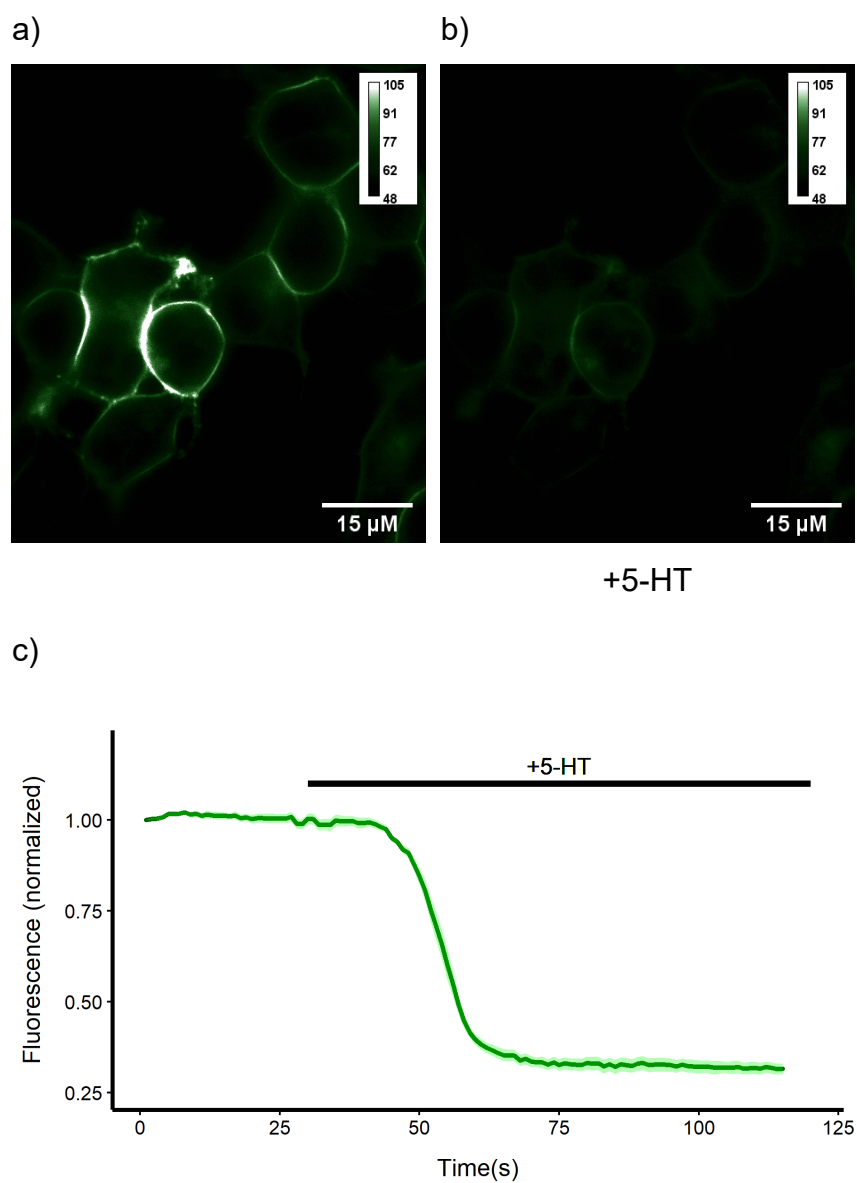
Figure 33: The higher sensitive Darken: H-sDarken;

Fluorescence of HEK cells expressing H-sDarken a) before and b) after application of 100 µM 5-HT; c)
Fluorescence intensity over time of cells expressing H-sDarken with application of 5-HT, black bar indicates
time of 5-HT application, Ribbon shows SEM, n = 5.
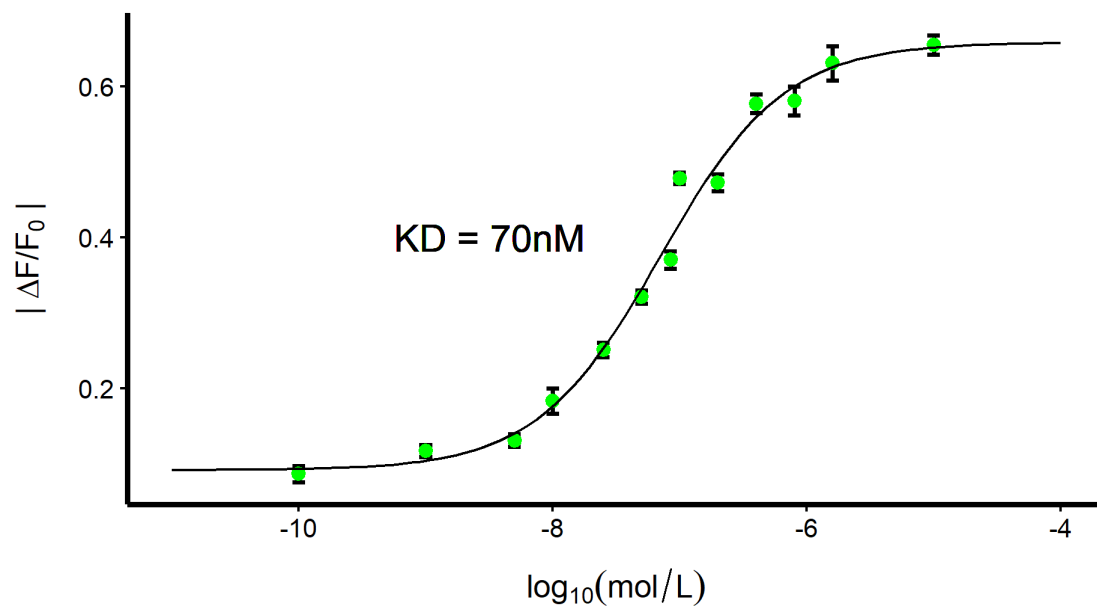
Figure 34: Affinity measurement of H-sDarken;

Absolute values of $\Delta F/F_0$ from multiple measurements of H-sDarkens fluorescence change in relation to the concentration of 5-HT applied; Data was fitted using a sigmoid four parameter fit, Kd was calculated from the fit, error bars show SEM, n = 5-20 cells per measurement.

a)

b)
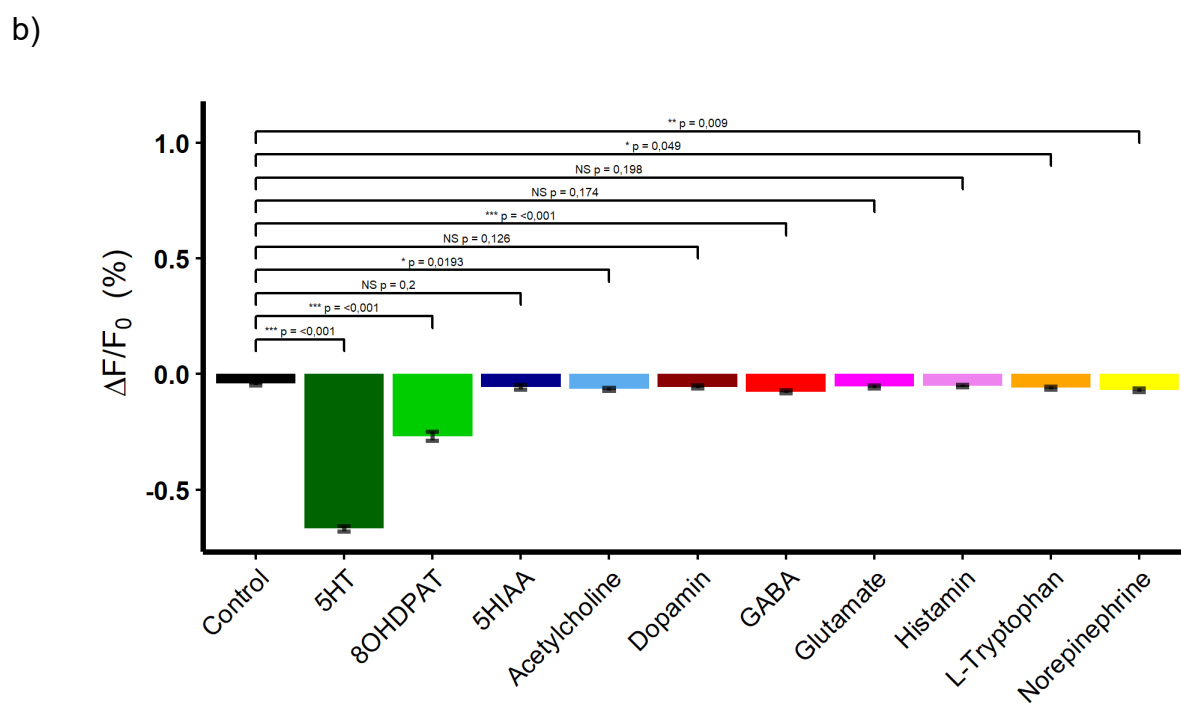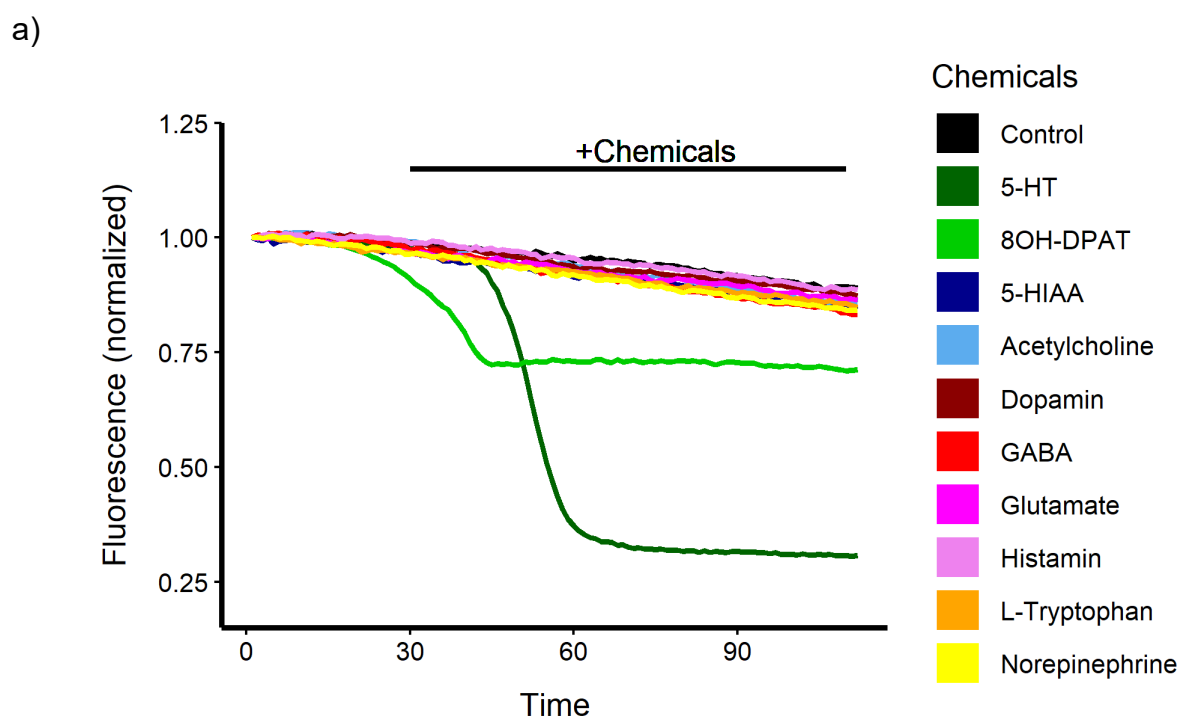
Figure 35: Specificity of H-sDarken to Serotonin;

a) Mean fluorescence signals of H-sDarken expressed in HEK cells with application of different chemicals, black bar indicates point of chemical application (100 µM), n = 15.

b) Comparison of the fluorescence change of H-sDarken triggered by different chemicals (100µM) to the control application of PBS, n = 15, error bars indicating SEM.

a)

b)

+5-HT

c)
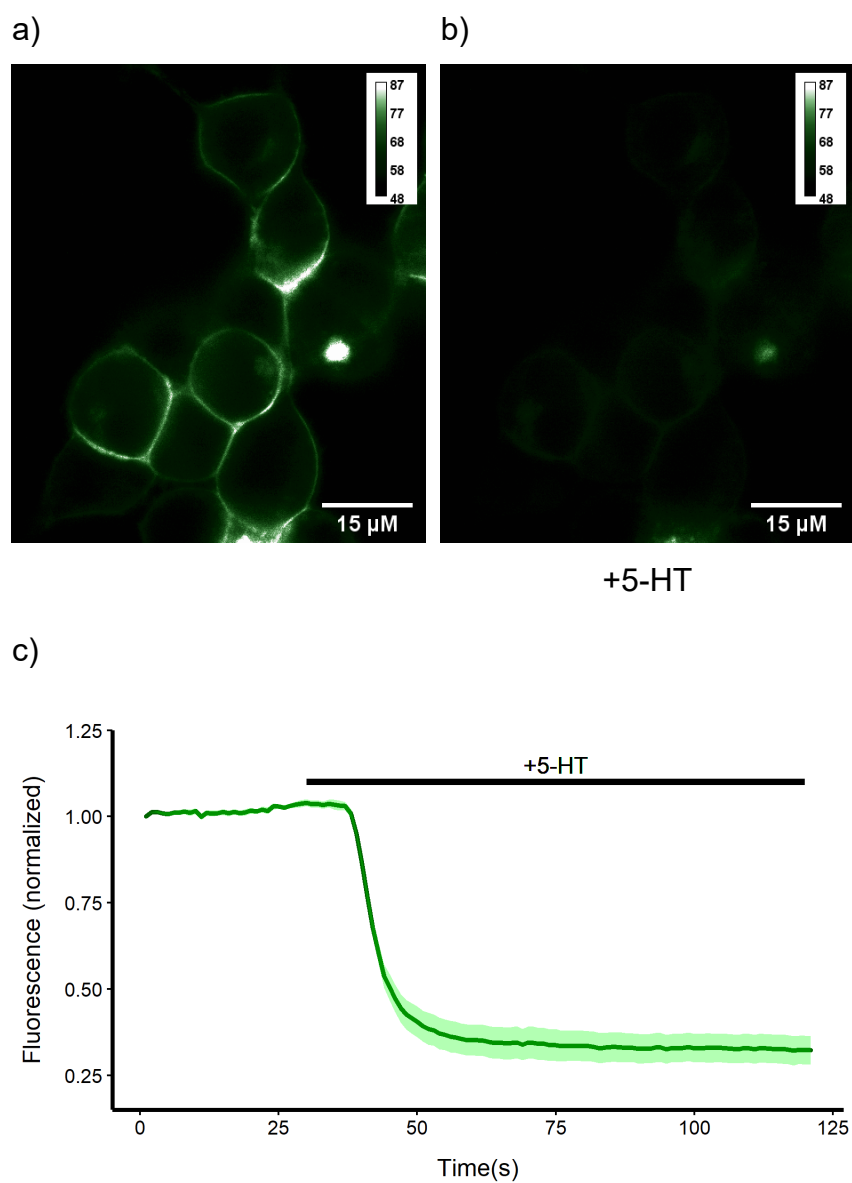
Figure 36: The lower sensitive L-sDarken;

a) Fluorescence picture of HEK cells expressing L-sDarken before and b) after application of 100 µM 5-HT;

c) Fluorescence intensity of L-sDarken expressing HEK cells over time with application of 5-HT, black bar indicates time of 5-HT application, ribbon shows SEM, n = 5.
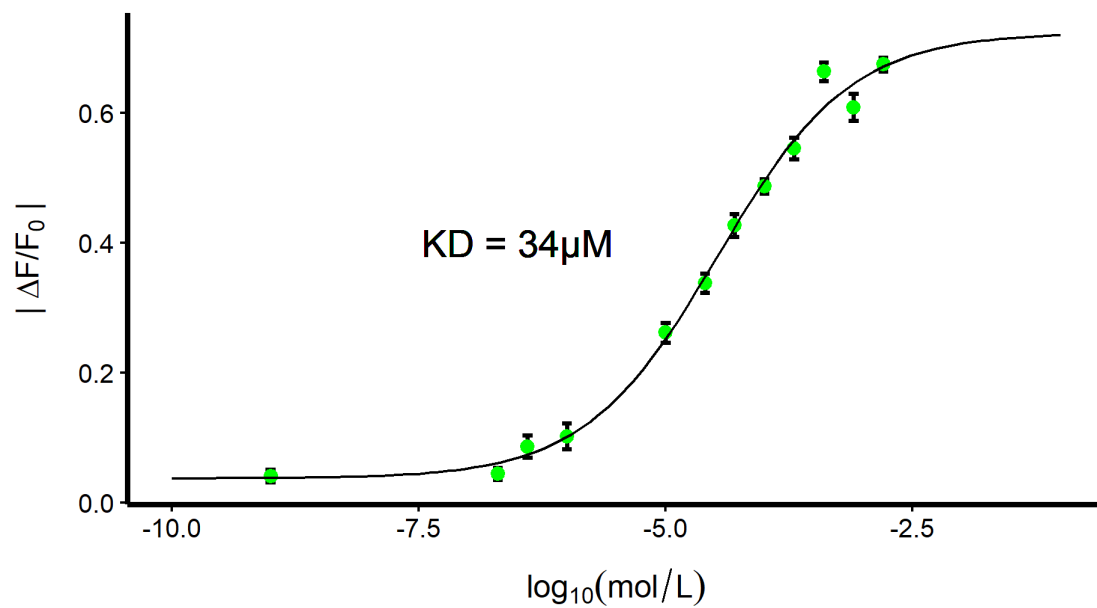
Figure 37: Affinity measurement of L-sDarken;

Absolute values of ΔF/F$_0$ from multiple measurements of L-sDarkens fluorescence change in relation to the concentration of 5-HT applied; Data was fitted using a sigmoid four parameter fit, Kd was calculated from the fit, error bars show SEM, n = 5-20 cells per measurement.

a)

b)
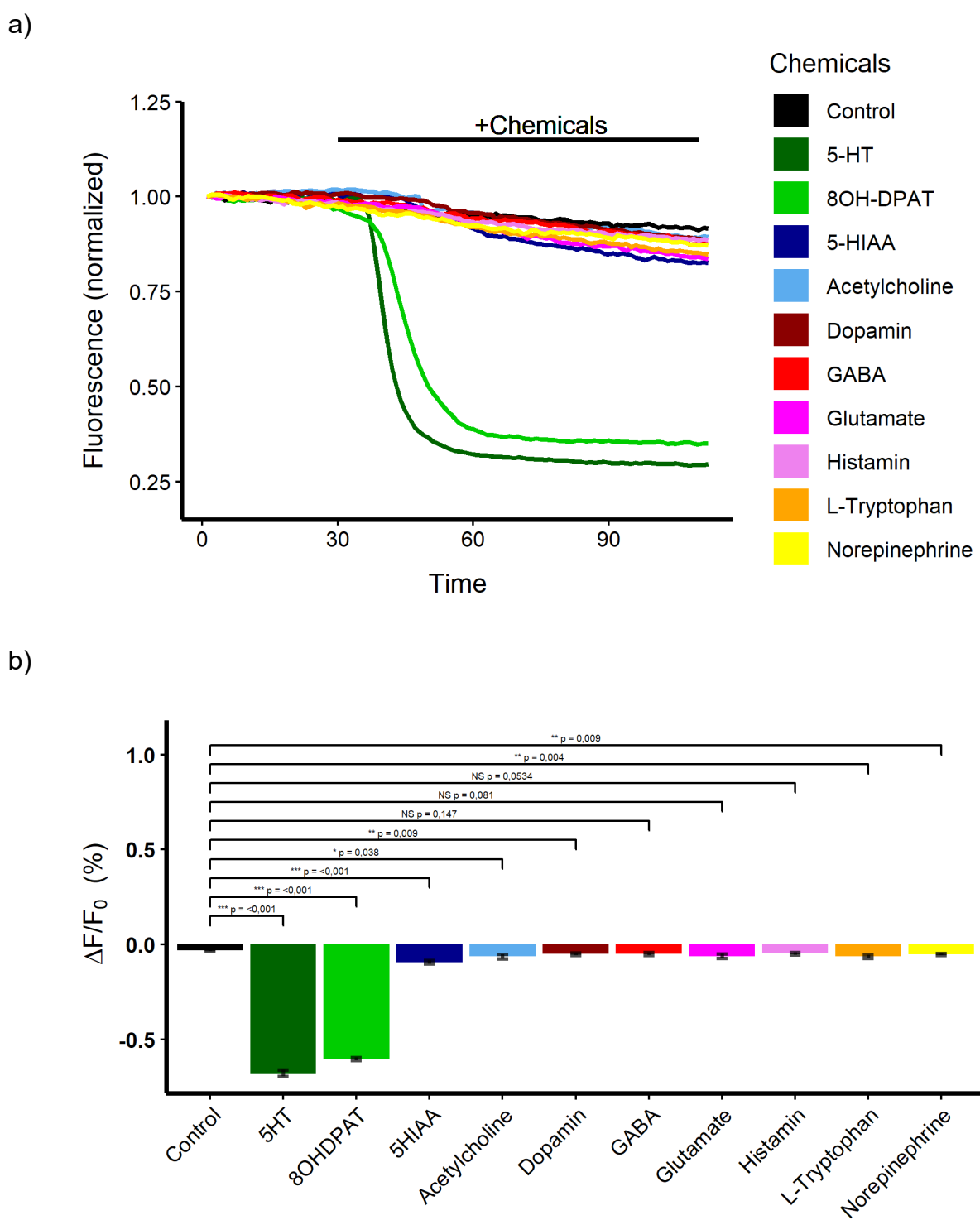
Figure 38: Specificity of L-sDarken to Serotonin;

a) Mean fluorescence signals of L-sDarken expressed in HEK cells with application of different chemicals, black bar indicates point of chemical application (100 µM), n = 15.

b) Comparison of the fluorescence change of L-sDarken triggered by different chemicals (100µM) to the control application of PBS, n = 15, error bars indicating SEM.

4   Discussion

The serotonergic system is a complex neuromodulatory system controlling a variety of physiological and behavioral functions. Disruptions in this system are linked to different mental illnesses, making it crucial to have different tools at hand to study serotonergic signaling and changes occurring within this system in the course of these illnesses.

In this regard, genetically encoded biosensors capable of measuring neurotransmitter dynamics are extremely promising tools, enabling measurements of molecular events in high spacial and temporal resolution. In this thesis *sDarken*, a genetically encoded biosensor capable of detecting serotonin was developed. *SDarken* is based on the 5-HT$_{1A}$ receptor and the circular permuted form of the green fluorescent protein cpGFP.

4.1   Random Insertion

First experiments where the insertion sites within the 5-HT$_{1A}$ receptor were chosen randomly, while the inserted circular permuted cpGFP was flanked with or without a flexible "GGGGS" linker, did not yield proteins capable of detecting serotonin. The expression of the sensors did not seem to be enriched within the plasmamembrane and when expressed in HEK cells, application of serotonin did not yield a measurable response within the different constructs (Fig. 11-Fig. 15). Furthermore, using only part of the cpGFP, so the protein is not directly synthesized and has to be build after full protein synthesis via complementation, did yield mutants which showed fluorescence, but no apparent fluorescence change was visible upon serotonin application (Fig. 16-Fig. 18).

4.2   Mutant generation

Generation of mutant libraries with different insertion sites homologous to dLight, a dopamine genetically encoded sensor (Patriarchi et al., 2018), led to different mutants reacting to serotonin application when expressed in HEK cells (Fig. 21). The insertion site

showing responsive mutants was derived of a sequence alignment of the 5-HT$_{2A}$ receptor insertion site (Patriarchi et al., 2018) ("2AS", Fig. 20). The insertion site derived of the sequence alignment with dLight1 (Fig. 19) did not yield reacting mutants when used with the 5-HT$_{1A}$ receptor base ("light" n = 12, Fig. 21). Still, since there are four mutations, two in each linker, the possible combinations of different linker combinations are 4^{20}, therefore there is still a chance that reacting mutants can be generated using this insertion site. But because already a small number of reacting mutants were generated with the other insertion site "2AS", this insertion site was used for further mutations.

Sequencing of nine mutants with or without a response to serotonin showed a prevalence for cystein in position three of the second linker (Table 5, "M4", "M8", "M34", "M45") for negatively reacting mutants. Furthermore, aromatic aminoacids (C, F and W) were dominating in the fourth position of the second linker (Table 5, M8, M34, M40, M45). The only mutant showing an increase in fluorescence with serotonin application contained two arginine in position three and four of the second linker (Tab. 5, "2AS M24").

For the N-terminal linker 1, within the positions 1 and 2, there was not a prevalence identifiable, therefore the aminoacids in linker 2 containing cystein phenylalanine/trypthophan were fixed in that position for further rounds of mutations to generate a sensor reacting with a fluorescence decrease upon serotonin binding.

To generate more mutants reacting positive to serotonin, the n- or c-terminal linker of the only mutant reacting with a fluorescence increase were further separately mutated while the other linker was conserved. But measuring mutants with the conserved N-terminal linker ("TC") as well as measuring mutants with the conserved c-terminal linker ("RR") did not yield additional positive reacting mutants (Fig. 24).

For the generation of mutants reacting with a stronger decrease further mutations were carried out, which contained a change in the insertion site of cpGFP within the n-terminal region of the 5-HT$_{1A}$ receptor ("L2"). But out of these mutants, only two out of twenty mutants measured reacted to serotonin with a fluorescence decrease (Fig. 24). Compared to "2AS M34" the fluorescence change of the mutants was smaller and while there are 2^{20} possible aminoacid combinations, further mutations were not carried out.

For the generation of more promising mutants, further mutation were carried out, conserving the aminoacids in the second c-terminal linker ("CF/W") while mutating the

aminoacids of the n-terminal linker. Out of these two, the aminoacid composition "CF" yielded multiple mutants reacting with a strong fluorescence decrease (Fig. 24).

The two strongest reacting mutants until then, "2AS M34" and "CF M1" were both expressed in HEK cells and their fluorescence measured under the same conditions. While "CF M1" showed a greater response to serotonin ("CF M1" with - 78,73% vs."2AS M34" with - 74,33%), "2AS M34" seemed to show a higher baseline fluorescence (Fig. 25a, b). While HEK cells were both transfected with the same amount of DNA it has to be noted, that this effect could be caused by different expression levels of the two proteins.

Still, as 2AS M34 showed a robust fluorescence change upon serotonin application and additionally also showing a high baseline fluorescence it was chosen for two last rounds of mutations. In them, the other three aminoacids in each linker were mutated. Screening of both mutant libraries "NGN" and "NGC" did not yield mutants reacting stronger to serotonin application (Fig. 24, "NGC", "NGN") than the initial mutant "2AS M34". Still the n number of the mutants measured is too low (n = 10 per mutant library) to reach a valid conclusion if further mutations could lead to stronger reacting mutants, it could be one path for future approaches to generate stronger reacting mutants. Going further, "2AS M34" was named *sDarken* (serotonin darkening 5-HT$_{1A}$ receptor-based sensor) and was investigated in terms of different properties to determine its use as a serotonin sensor.

4.3   sDarken

4.3.1 Fluorescence response and reversibility

When *sDarken* is expressed in HEK cells, it shows a strong decrease in fluorescence upon application of serotonin in the magnitude of - 74,33% (Fig. 26a-c). This reaction is reversible as shown by washing out serotonin in between applications, although it seems that the washing steps were not carried out long enough to regain baseline fluorescence. Still it is observable, that sequential activations of *sDarken* are possible (Fig. 27).

4.3.2 pH-Sensivity

The circular permutation of GFP leads to a stronger sensitivity to acidic pH values. An effect which could drastically change the fluorescence emission (Baird et al., 1999). While the overall fluorescence was not evaluated within this thesis, the fluorescence decrease of *sDarken* triggered by serotonin was measured within different pH-values to check if the sensor behaves differently in terms of maximal fluorescence response between measurements. The measurements showed, that the fluorescence decrease triggered by 5-HT does not seem to be influenced by different pH values (Fig. 28). Still the overall brightness within different pH values has to be evaluated in further experiments. But in *in vivo* experiments the pH sensitivity of *sDarken* should not strongly be influencing sDarkens fluorescence, since the cytosolic pH, where the cpGFP of sDarken resides is strictly regulated between pH 7-7,4 (Madshus, 1988).

4.3.3 Way-100635 application

The fluorescence decrease of *sDarken* triggered by the application of 5-HT is reversible using the 5-HT$_{1A}$ receptor antagonist WAY-100635 (Fig. 29d). Way-100635 which is an antagonist of the 5-HT$_{1A}$ receptor seems to be able to bind to *sDarken* and subsequently inhibiting the binding of 5-HT to *sDarken.* Inhibition of the 5-HT binding leads to an increase of fluorescence if serotonin is bound to *sDarken* before. Interestingly, *sDarken* also shows a fluorescence decrease and increase within the intracellular portions of the cells when exposed to 5-HT and the 5-HT$_{1A}$ receptor antagonist WAY-100635 (Fig. 29a-c, e). The initial intracellular fluorescence decrease triggered by 5-HT seems to be smaller (- 33,87%) compared to the decrease shown by the membrane portions of the cell (- 55%). The subsequent fluorescence increase after WAY-100635 application is higher (252,62%) compared to the observed increase of fluorescence in the membrane portions (159%). The decrease and subsequent increase in the membrane portions of the cells do elevate the fluorescence signal back to the fluorescence baseline which was observable before application of both chemicals (Fig. 29d). This is not visible within the intracellular regions. Here, application of both chemicals, led to a smaller decrease, and around two fold increase of fluorescence, compared to the initial baseline fluorescence (Fig. 29e). There are different possibilities as to why this behavior is occurring. On the premise, that the cell

membrane is impermeable for 5-HT and WAY-100635, the measured fluorescence changes could be signals from out of focus cellular parts, since the measurement was done without using a confocal microscope. On the other hand, the observation, that the fluorescence reaches above baseline levels, an effect which was not visible within the membrane portions, does speak against the idea that this is caused by out of focus changes because they should react equally in that instance.

Another possible explanation could be, that the fluorescence changes within the cells are triggered by the activation of intracellular pathways, which are triggered through *sDarken.* This could lead to subsequently activity changes of *sDarken* proteins residing in intracellular portions of the cells. In other measurements made, the activation of G-protein pathways by *sDarken* were examined and no activation was observed (Kubitschke et al., 2022). Therefore, in light of these findings, the activation of G-protein independent pathways have to be investigated to rule out possible intracellular interactions of *sDarken* which could have led to the observed intracellualr changes.

A third possible explanation is, that the cell membranes are, to some extent, permeable for 5-HT and WAY-100635. For 5-HT the possibility is given by endogenous expressed receptors. With experiments which looked for the expression of endogenous transporting proteins in different cell lines it was found out, that the transporter OCT1 is in low levels expressed in HEK cells (Ahlin et al., 2009). The OCTs (Organic Cation Transporter) OCT1 and OCT2 have been shown to be able to transport serotonin (Busch et al., 1996; Gebauer et al., 2021). Therefore it is possible for serotonin to activate *sDarken* inside the cell lumen leading to the detected decrease of fluorescence after serotonin application.

For WAY-100635, it has been reported that it is possible to be transported through the blood brain barrier by measuring its permeability within a MDR-MDCK cell monolayer (Zheng et al., 2015). But evidence for the permeability or impermeability of WAY-100635 for the plasma membrane of HEK cells specifically was not found in a literature search. Still it is a possible explanation for the intracellular increase of fluorescence after WAY-100635 application. It could bind to *sDarken* located on intracellular organelles and stabilizing its "inactive" highly fluorescent conformation. This idea is strengthened by findings which are discussed in the next paragraph, discussing the expression of *sDarken*. To note, the idea that 5-HT and WAY-100635 are leading to internalization and recycling processes of *sDarken* from and to the membrane, which trigger the observed decrease

and increase of fluorescence, does not seem to fit to the data. The decrease of fluorescence in the membrane is not accompanied with an increase of fluorescence in the intracellular parts of the cells as well as there is no increase in membrane fluorescence while there is a decrease in intracellular fluorescence.

4.3.4 Expression

While the first images of *sDarken* showed predominantly expression within the plasma membrane (Fig. 26a), linking the fluorescence protein mCherry to *sDarkens* c-terminus did reveal a different expression pattern. Fusing mCherry to the c-terminus of *sDarken* did seemingly not impair or change the functionality or the fluorescence signal distribution, as there was no visible change in the expression pattern (Fig. 26a, Fig. 30a) and there was still a reaction to serotonin application (Fig. 30a, b). However the fluorescence signal distribution of mCherry is different to *sDarkens* expression pattern in the serotonin unbound state and does not show the high fluorescence signal within the plasma membrane which is visible in *sDarken* (Fig. 30a, c). Interestingly, the expression patterns of *sDarken* and the linked mCherry seems to be more in line, when mCherry is compared to the 5-HT bound form of *sDarken* (Fig. 30b, d). The fluorescence protein mCherry shows high pH stability and as a monomer it should not influence the expression of *sDarken*. Furthermore, its fluorescence does not seem to be influenced by the application of 5-HT to *sDarken*, compared to the fluorescence of cpGFP in the third intracellular loop. In case of the cpGFP, the fluorescence signal is strongly influenced by the conformation of the 5-HT$_{1A}$ receptor base it is incorporated in. Therefore the high fluorescence signal visible in the plasma membrane of HEK cells expressing *sDarken* could be explained by an inactive GPCR conformation which influences the fluorescence signal of cpGFP to reach a maximum. Within the cell intracellular organelles, *sDarken* could show other conformational states, which differ from the conformation of the receptors located in the plasma membrane. This could lead to the lower fluorescence signals of cpGFP within intracellular organelles.

The different conformations, leading to the different measured fluorescent signals, may be explained by the heterogeneity of cellular membranes in terms of their lipid composition.

The catalyzed oligonucleotide exchange of the 5-HT$_{1A}$ receptor was shown to be effected by lipid bilayer compositions when using varying compositions of POPC (1-palmitoyl-2-oleoyl-sn-glycero-3-phosphocholine), BSM (brain sphingomyelin) and CHOL (Cholesterol) (Gutierrez et al., 2016). CHOL depletion was also shown to enhance 5-HT$_{1A}$ receptor ligand binding in isolated membranes of cholesterol-depleted cells (Prasad et al., 2009). An effect which was also shown for 5-HT$_{1A}$ receptors expressed in CHO (chinese hamster ovary) cells treated with an enzyme catalyzing the hydrolysis of the phospholipid sphingomyelin (Jafurulla et al., 2008).

Interestingly, the compositions of cell membranes differ in terms of their lipid contents. The ratio of CHOL to phospholipids is highest in the plasma membrane while being 2 to 10-fold lower in intracellular organelles like the late endosome, endoplasmatic reticulum, golgi apparatus and mitochondria (van Meer et al., 2008).

The functionality of the 5-HT$_{1A}$ receptor is influenced by different lipid compositions within the membrane its expressed in, so it is plausible that the function of *sDarken* could also be affected. Therefore it is possible, that the different fluorescent intensities within the cell observed for *sDarken* could be a direct result of different lipid contents within the different membranes. Interestingly, the earlier discussed results of the application of WAY-100635 seem to be in line with that idea. Application of 5-HT and of WAY-100635 did lead to fluorescence changes within the intracellular portions in the cell. While the changes triggered by 5-HT are smaller compared to the changes in the cellular membranes, this behavior could be explained if there were less receptors in the "inactive conformation" residing in intracellular organelles due to different lipid compositions of these organelles. Stabilization of the inactive, highly fluorescent state by the 5-HT$_{1A}$ receptor antagonist WAY-100635 would effect the receptors which were not present to a great extend in this state before. Therefore the high fluorescence increase which showed a fluorescence signal exceeding the baseline fluorescence by two fold might be explained.

For future experiments, controls could be done showing in which organelles *sDarken* is enriched inside the expressing cells. Furthermore, the depletion of CHOL or sphingomyelin could be used to monitor possible effects of theses lipids on *sDarkens* fluorescence. The fluorescence intensity effect within the cell was not reported for other GPCR based sensors so far. Therefore it could be interesting if this effect is specific for *sDarken*, or if this is observable when using other GPCR based genetically encoded sensors and their

antagonists or agonists. Also different antagonists of the 5-HT_{1A} receptor could be applied to *sDarken* expressing HEK cells, to investigate if the effect of WAY-100635 is specific for this antagonists.

4.3.5 5-HT affinity

Compared to the native 5-HT_{1A} receptor, which has a Kd for Serotonin of 1,8 nM ± 0,3 (Ho et al., 1992), *sDarken* shows a nearly 70-fold decrease in serotonin affinity with a Kd for serotonin of 126 nM (Fig. 31). Concentrations of synaptic transmission of serotonin are estimated by extrapolation of voltammetrical measurements of serotonin in the Snr (substentia nigra) to reach concentrations in the magnitude of 6 mM (Bunin & Wightman, 1999). This should trigger the full response of *sDarken*, which shows full activation above 1 µM serotonin (Fig. 31). In terms of sertonin affinity, *sDarken* should therefore be suitable for the use as a serotonin sensor to visualize synaptic transmission *in vivo*. Nevertheless it has to be kept in mind that these are just estimations and synaptical release might differ in different regions, making a direct measurement and analysis of *sDarken* in *in vivo* experiments necessary.

The concentrations which are reached by volume transmission are reported within different ranges. They reach a low to mid nM range for the dorsal raphe (between 1,3 nM to 5,4 nM, calculated from different studies (Adell et al., 2002) up to 100 ± 20 nM (Bunin & Wightman, 1998). The detectable concentration of *sDarken* seems to be in the range between 10 nM and 1 µM. The fluorescence decrease of *sDarken* in the upper limit of the reported volume transmission concentration of 100 nM is - 35,7%. Therefore, *sDarken*s viability in measuring serotonergic volume transmission is probably limited, since the triggered fluorescence change within even the highest reported concentrations is less than half of the full response.

In comparison the affinity of serotonin to the other two versions of *sDarken* was determined to be 70 nM for *H-sDarken* (Fig. 34) and 34 µM for *L-sDarken* (Fig. 37).

Interestingly, the substitution of cpGFP for sfcpGFP in *H-sDarken* led to an increased affinity for serotonin (70 nM vs 126 nM; Fig. 34, Fig. 31) as well as a change in its detectable concentration range. While there is no direct explanation for this behavior, there are different cases where the same behavior occurred. For example, introducing some of

the superfolder GFP mutations into GCamp2 led to an increased affinity to Ca^{2+} in comparison to the initial Gcamp2 variant (Muto et al., 2011). Also, using a circular permuted variant of superfolder GFP instead of cpGFP led to an improved brightness and dynamic range in the generation of the voltage sensor ASAP1 (St-Pierre et al., 2014). Lastly, using a specific mutant of superfolder GFP K99V, led to an increased dynamic range in the development of a genetically encoded Zn^{2+} sensor, still to note here, that this may be caused by a decrease of the baseline fluorescence (Qin et al., 2016).

While the affinity of *H-sDarken* is lower compared to *sDarken* it does not seem to be very much of an improvement in terms of its range of concentrations it is able to detect. Still the chance to measure the volume transmission of serotonin effectively would be higher using the sensor *H-sDarken*.

For *L-sDarken*, the difference of its dynamic range which spans around 100 nM and 3 μM does unfold new possibility's for the monitoring of serotonin. Its usage would be more interesting within synaptic transmission, as it seems to be unaffected by the concentrations which theoretically are reached due to volume transmission. This could be interesting in scientific questions where only the synaptic release of serotonin is of interest and a sensor is needed, that is unaffected by volume transmission.

4.3.6 Specificity

To evaluate the specificity of *sDarken* to 5-HT, different chemicals were applied to HEK cells expressing *sDarken* and their effect on the fluorescence signal was measured (Fig. 32a, b). In comparison to the control, 5-HT, 8-OH-DPAT, 5-HIAA, acetylcholine and dopamine had a significant effect on the fluorescence signal of *sDarken*. Still the highest measured fluorescence change of the chemicals 5-HIAA, Acetylcholine and Dopamine was 4,08% (5-HIAA). This effect could be explained by the binding of the chemicals to *sDarken* when applied in high concentrations. It was already shown in the first successful cloning of the 5-HT_{1A} receptor, that the receptor has an affinity for dopamine and histamine in the range of >1000 nM for dopamine and >5000 nM for histamine respectively (Kobilka et al., 1987). While for the other compounds, affinity values were not found, it is possible that with high concentrations non specific receptor binding is occurring. These effects are also visible in the other two *sDarken* versions *H-sDarken* and *L-sDarken* (Fig. 35 Fig. 38).

In both of these construct, significant differences were observable compared to the control in terms of their effect on the fluorescence. The strongest effect was triggered by 5-HIAA with a fluorescence change of - 12,59%. The control showed a fluorescence change of - 3,05%, which could be due to bleaching or cellular movement. The effect of 5-HIAA was much stronger, but this could be due to the fact that in the case of *L-sDarken*, the chemicals applied were used in much higher concentrations to trigger *L-sDarkens* full response, since *L-sDarken* showed lower affinitys for 5-HT (3 mM for *L-sDarken* with the exception of 300 µM for 8-OH-DPAT vs. 10 µM for *H-sDarken* and *sDarken* in all measurements). If binding of other chemicals occurs to some extend, the high concentrations used in this experiments would favor these effects.

The fluorescence decrease triggered by 8-OH-DPAT did not seem to show a comparable response to 5-HT in the constructs *sDarken* (8-OH-DPAT - 39,7% vs. 5-HT - 78,74% for 5-HT) and *H-sDarken* (- 26,32% for 8-OH-DPAT vs. - 66,83% for 5-HT). In *L-sDarken* the response to 8-OH-DPAT (- 61,4%) is close to the response to 5-HT (- 67,77%). It is possible, that the concentrations used in the measurements of *sDarken* and *H-sDarken* are too low to trigger the full response of the sensor by 8-OH-DPAT. The Kd of *sDarken* for serotonin was decreased 70-fold compared to the Kd of the endogenous 5-HT$_{1A}$ receptor. The published Kd of the 5-HT$_{1A}$ receptor for 8-OH-DPAT is 1,3 ± 0,07 nM (SE) (Watson et al., 2000). It is possible, that due to the substitution of the third intracellular loop, the affinity to 8-OH-DPAT is stronger effected than for 5-HT leading to the observed differences. This effect could be investigated measuring the affinity of 8-OH-DPAT for all three of the sensor versions.

4.4 Comparison to other genetical encoded 5-HT sensors

Three other serotonin sensors were developed simultaneously by different groups, which include the PBP based iSeroSNFR (Unger et al., 2020), the GPCR based sensors GRAB5-HT1.0 (Wan et al., 2021) and the GPCR based sensor Psychlight (C. Dong et al., 2021) which are based on the 5-HT$_{2C}$ receptor and the 5-HT$_{2A}$ receptor respectively.

These published serotonin sensors expressed in HEK cells showed fluorescence increase of 1700% with a Kd of 390 µM for iSeroSNFR, a 250% increase in fluorescence with an EC50 of 22 nM for GRAB5-HT1.0 and 79,6% fluorescence increase with an EC50 of

26,3 nM for Psychlight. While iSeroSNFR shows the highest fluorescence increase, the Kd is in a high µM range, which may be problematic for the detection of serotonin events with a lower serotonin concentration. Apart from their Kd and their measurable fluorescence change, the sensors will each differ in brightness, expression, photostability, folding efficiency and cellular toxicity. Now, that there are a bundle of serotonin sensors described, a comparison between each should clarify which performs best in different scenarios and is suited best in specific measurements.

4.5 Potential drawbacks

4.5.1 Overexpression

For imaging of genetically encoded biosensors a sufficient signal is necessary. For dLight, at least a 10-fold overexpression compared to the endogenous GPCR is estimated to reach the sufficient signal to noise ratio needed for imaging (Sabatini & Tian, 2020).

To reach a sufficient signal to noise ratio, overexpression of *sDarken* is probably mandatory. But overexpression of *sDarken* could lead to changes within the expression of the endogenous 5-HT$_{1A}$ receptor in neuronal populations. For the somato-dendritic targeting of the 5-HT$_{1A}$ receptor the c-terminal part of the receptor is important. It was found that mutation of I^{414} and I^{415} to alanine led to low expression in the plasma membrane and co-localization of the receptor with regions marked for the endoplasmatic reticulum (Carrel et al., 2006). Furthermore the 5-HT$_{1A}$ receptor seems to interact with Yif1B, which is involved in the somatodendric targeting (Carrel et al., 2008). For the interaction with Yif1B, the 5-HT$_{1A}$ receptor contains a tribasic motif in the c-terminus (K^{405}/R^{421}/R^{422}), which, when mutated to alanine, leads to an abolishment of the binding between the two proteins. In the case of *sDarken*, the involved motifs are still present in the protein. Therefore expression of *sDarken*, which may interact with the same proteins as the 5-HT$_{1A}$ receptor, could lead to less available protein transport complexes for endogenous proteins like the 5-HT$_{1A}$ receptor in neurons.

Furthermore, overexpression of a genetically encoded biosensor able to bind serotonin could specifically affect serotonergic signaling of the different 5-HT receptors by buffering

serotonin. Since *sDarken* shows a high affinity for serotonin, *sDarken* could diminish released serotonin concentrations within a synapse or lower serotonin concentrations released extrasynaptically intended for endogenous 5-HT receptors.

Therefore the expression of *sDarken* could effect neuronal populations and ultimately behavioral outcomes of *sDarken* expressing animals and for this reason each behavioral test has to be controlled.

4.5.2 Dimerisation

Another obstacle that has to be addressed in the future is the dimerisation of GPCRs, with themselves (homo-oligomeres) or with other proteins (hetero-oligomeres). This effect can regulate the binding of ligands (George et al., 2000; Hilairet et al., 2003; Levoye et al., 2006), coupling to G-proteins (George et al., 2000; Lee et al., 2004; Levoye et al., 2006; Łukasiewicz et al., 2016) or receptor trafficking (Zhou et al., 2006).

Receptor dimerisatizon could essentially effect *sDarken* as well as other GPCR based sensors. For the backbone of *sDarken*, the 5-HT_{1A} receptor, different GPCR oligomeres are already identified. The 5-HT_{1A} receptor was shown to form homo-oligomeres (Kobe et al., 2008). Additionally, the 5-HT_{1A} receptor can form hetero-oligomeres with the 5-HT_7 receptor (Renner et al., 2012), FGFR1 receptor (Borroto-Escuela et al., 2012), GalR1-Gal2-5-HT_{1A} receptor (Millón et al., 2016), the 5-HT_{2A} (Borroto-Escuela et al., 2017), dopaminergic D2 receptors (Kolasa et al., 2018; Szlachta et al., 2018), opioid receptors (Cussac et al., 2012) and GPR39 receptors (Tena-Campos et al., 2015).

In the case of rhodopsin, W^{175} and Y^{206} are potentially involved aminoacids to form the dimer interface (Kota et al., 2006). Evidence suggests, that the motifs regulating the dimerisation of the 5-HT_{1A} receptor are within TMD4/TMD5 (Gorinski et al., 2012). Aminoacids involved in the dimerisation were Trp^{175}, Tyr^{198}, Arg^{151} and Arg^{152}. All of which are present in *sDarken* and were not in the substituted region. Therefore dimeristation of *sDarken* with endogenous GPCR might be possible due to the fact, that the dimerisation motif may not be disrupted and fully functional. This could effect *sDarken*s fluorescence responses upon 5-HT application or might lead to fluorescence changes without 5-HT present if *sDarken* conformation is effected by interacting GPCRs. Therefore, it is

necessary to carry out experiments checking dimerisation effects of known 5-HT$_{1A}$ dimerisation partners to exclude their effects on *sDarken*.

The activation of intracellular pathways by *sDarken*, G-protein activation and beta arrestin signaling, were not measured within this thesis. But using *sDarken in vivo,* possible effects onto expressing cells by activation of intracellular pathways would be highly unbeneficial. Dependent on the substitution of the third intracellular loop, GPCR based sensors "may not completely suppress downstream signaling as evidenced by weak activation of the Gq dependent calcium signaling pathway observed in GRABACh" (Sabatini & Tian, 2020). The GPCR based sensor GACH2.0 showed a seven-fold smaller coupling efficiency compared to the wild type receptor for the Gq pathway, while there was no detectable coupling to the Gs pathway. (Jing et al., 2018). The insertion of cpGFP into the third intracellular loop of M3R in GACh2.0 was within a modified third intracellular loop of the beta-2 adrenergic receptor (β$_2$AR), that was used as a substitute for the native M3R third intracellular loop. In comparison to GACh2.0, the substitution carried out in *sDarken* based on the sensor dLight1 used less aminoacids of the n- and c-terminal part of the third intracellular loop which introduced the third intracellular loop of β$_2$AR into the sensor (Fig. 39).

Figure 39 Multiple Sequence Alignment GACH2.0 and sDarken

Orange: M$_3$R, Yellow: β$_2$AR, Red: Linker sequences, Green: cpGFP, Blue: 5-HT$_{1A}$ receptor

G-proteins interacting to intracellular parts of GPCRs, that consists of the "bottom halves of TMD3, TMD5, TMD6, ICL2 along with ICL3" (Glukhova et al., 2018). Therefore, dependent on the substitution carried out it is probably possible to disrupt binding of G-proteins, when interaction sites of G-proteins within the GPCR are removed.

However, the G-protein dependent as well as the G-protein independent pathways have to be fully examined. While there was already a full screening of G-protein dependent activation (Kubitschke et al., 2022), the G-protein independent pathway still has to be investigated. There might be a disruption of β-arrestin signaling, as the binding of β-arrestin was examined in the similar sensor GRAB5-HT1.0 where no signaling of the sensor could be detected (Wan et al., 2021).

4.6 Outlook

The genetically encoded serotonin sensor *sDarken* seems to be a useful tool for future experiments. Still more optimization, for example enhancing the brightness, the measurable fluorescence change and the dynamic range, should be accomplished.

A better brightness as well as an increased fluorescence change would be benefical to *sDarken* as an *in vivo* tool, as it would decrease the need of high overexpression. These would mitigate some of the addressed effects like serotonin buffering or the effects on endogenous serotonin receptors or other proteins which are transported by the same protein complexes.

Therefore more mutants have to be generated. There are different approaches which can be followed to obtain improved mutants.

First, more mutational experiments within the linker domains of *sDarken* can be carried out, generating more mutants containing the cysteine and phenylalanine in the second linker. This specific linker combination yielded more mutants showing greater fluorescence responses and is more likely to generate mutants with a higher fluorescence change.

In another approach, random mutations by error prone PCR within the cpGFP sequence could lead to new viable mutants. This was already successfully used in the generation of the serotonin sensor GRAB5-HT1.0 (Wan et al., 2021).

Further, mutations in other parts of the 5-HT$_{1A}$ receptor backbone could lead to sensors with a better dynamic range or better brightness. Mutations in the second intracellular loop were used in the development of genetically encoded fluorescent sensors of orexin neuropeptides, which did improve the dynamic range of the receptor (Duffet et al., 2022).

In a different approach, using other variations of GFP or other fluorescence proteins could be utilized to generate a new genetically encoded biosensor. An interesting candidate would be Staygold, which shows great photostability and brightness (Hirano et al., 2022) Still, this approach is risky since there is no monomeric version of the protein available yet as well as there is no circular permuted form of the protein described. Besides possible beneficial increases of the parameters of *sDarken*, using other fluorescence proteins could potentially widen the field of use of *sDarken*. Using red shifted versions of the sensor, utilizing red or even far red fluorescence proteins would allow measurement of serotonin dynamics while simultaneously activate or inactivate neuronal populations with optogenetics. In case of far red shifted sensors serotonin measurements could be done while applying optogenetics and additionally measuring calcium signals simultaneously within cells.

In terms of the sensors dynamic range, there are great possibilities to generate different *sDarken* versions capable of detecting a wide variety of concentrations. To measure serotonin within higher concentrations, some possibilities are already shown within this thesis based on the mutants D82N, D116N and S198A (Ho et al., 1992). Still there are other possible mutations described in the literature which can be used to achieve different binding affinities of *sDarken* for serotonin. For example the pharmacology of different polymorphic variants of the 5-HT$_{1A}$ receptor were described showing multiple possible mutation sites which could increase or decrease the affinity of *sDarken* for serotonin (Del Tredici et al., 2004). These could be used as a great starting point for future experiments tuning the affinity of *sDarken* to the needs of specific experiments, since the levels of endogenous serotonin concentrations are varying among synaptic transmission or extrasynaptical release within different regions in the brain.

As for future applications, GPCR based fluorescence biosensors could be used in a variety of different tasks. They could be used as a powerful tool to monitor dynamics of various neurotransmitters *in vivo*, which was already done by monitoring dopamine levels in the

dorsal striatum of mice during the spontanous sleep-wake cycle and different stimuli (H. Dong et al., 2019), serotonin release in the anterior cingulate cortex of mice to study consolation behavior (L. Li et al., 2021) or the acetylcholine release in the basolateral amygdala of mice during the cue reward learning task (Crouse et al., 2020).

Furthermore, genetically encoded biosensors, specifically based on G-Protein coupled receptors, could be used to screen for ligands of the specific GPCR it is based upon, therefore being used to find new receptor specific drugs. For example Psychlight a genetically encoded 5-HT sensor based on the 5-HT$_{2A}$ receptor that was used to identify a non-hallucinogenic psychedelic analog, which showed antidepressant action (C. Dong et al., 2021). For *sDarken* it is shown here that the 5-HT$_{1A}$ receptor agonist 8-OH-DPAT as well as the 5-HT$_{1A}$ receptor inhibitor WAY-100635 both are able to effect the fluorescence of the sensor (Fig. 29, Fig. 32).

With GPCR based genetically biosensors it is probably not possible to study the effects of ligands of the receptors in terms of specific pathways triggered, but it could be possible to detect different ligands of the used receptor. In the case of *sDarken*, it would be really interesting to investigate if there is a difference in the fluorescence change triggered in biased ligands of the 5-HT$_{1A}$ receptor. For the 5-HT$_{1A}$ receptor some biased agonists are identified, for example F15599 or F13714 (Maurel et al., 2007). A comparison of their possible triggered fluorescence change to the change triggered by the agonists 5-HT or 8-OH-DPAT would indicate if there is a potential of using *sDarken* to screen for ligands of the 5-HT$_{1A}$ receptor while already indicating if the agonists are biased or non biased.

5 References

Adell, A., Celada, P., Abellán, M. T., & Artigas, F. (2002). Origin and functional role of the extracellular serotonin in the midbrain raphe nuclei. *Brain Research Reviews*, *39*(2–3), 154–180. https://doi.org/10.1016/S0165-0173(02)00182-0

Ahlin, G., Hilgendorf, C., Karlsson, J., Szigyarto, C. A.-K., Uhlén, M., & Artursson, P. (2009). Endogenous Gene and Protein Expression of Drug-Transporting Proteins in Cell Lines Routinely Used in Drug Discovery Programs. *Drug Metabolism and Disposition*, *37*(12), 2275–2283. https://doi.org/10.1124/dmd.109.028654

Albert, P. R. (2012). Transcriptional regulation of the 5-HT1A receptor: Implications for mental illness. *Philosophical Transactions of the Royal Society of London. Series B, Biological Sciences*, *367*(1601), 2402–2415. https://doi.org/10.1098/rstb.2011.0376

Albert, P. R., Sajedi, N., Lemonde, S., & Ghahremani, M. H. (1999). Constitutive Gi2-dependent Activation of Adenylyl Cyclase Type II by the 5-HT1A Receptor: INHIBITION BY ANXIOLYTIC PARTIAL AGONISTS *. *Journal of Biological Chemistry*, *274*(50), Article 50. https://doi.org/10.1074/jbc.274.50.35469

Altieri, S. C., Garcia-Garcia, A. L., Leonardo, E. D., & Andrews, A. M. (2013). Rethinking 5-HT1A receptors: Emerging modes of inhibitory feedback of relevance to emotion-related behavior. *ACS Chemical Neuroscience*, *4*(1), 72–83. https://doi.org/10.1021/cn3002174

Alvarez, C. E. (2008). On the origins of arrestin and rhodopsin. *BMC Evolutionary Biology*, *8*(1), 222. https://doi.org/10.1186/1471-2148-8-222

Amato, D. (2015). Serotonin in antipsychotic drugs action. *Behavioural Brain Research*, *277*, 125–135. https://doi.org/10.1016/j.bbr.2014.07.025

Ambrose, C., James, M., Barnes, G., Lin, C., Bates, G., Altherr, M., Duyao, M., Groot, N., Church, D., Wasmuth, J. J., Lehrach, H., Housman, D., Buckler, A., Gusella, J. F., & MacDonald, M. E. (1992). A novel G protein-coupled receptor kinase gene cloned

from 4p16.3. *Human Molecular Genetics*, *1*(9), 697–703. https://doi.org/10.1093/hmg/1.9.697

Andrade, R., Malenka, R. C., & Nicoll, R. A. (1986). A G protein couples serotonin and GABAB receptors to the same channels in hippocampus. *Science (New York, N.Y.)*, *234*(4781), Article 4781. https://doi.org/10.1126/science.2430334

Ansorge, M. S., Zhou, M., Lira, A., Hen, R., & Gingrich, J. A. (2004). Early-Life Blockade of the 5-HT Transporter Alters Emotional Behavior in Adult Mice. *Science*, *306*(5697), 879–881. https://doi.org/10.1126/science.1101678

Asberg, M. (1997). Neurotransmitters and suicidal behavior. The evidence from cerebrospinal fluid studies. *Annals of the New York Academy of Sciences*, *836*, 158–181. https://doi.org/10.1111/j.1749-6632.1997.tb52359.x

Attramadal, H., Arriza, J. L., Aoki, C., Dawson, T. M., Codina, J., Kwatra, M. M., Snyder, S. H., Caron, M. G., & Lefkowitz, R. J. (1992). Beta-arrestin2, a novel member of the arrestin/beta-arrestin gene family. *Journal of Biological Chemistry*, *267*(25), 17882–17890. https://doi.org/10.1016/S0021-9258(19)37125-X

Awaji, T., Hirasawa, A., Shirakawa, H., Tsujimoto, G., & Miyazaki, S. (2001). Novel Green Fluorescent Protein-Based Ratiometric Indicators for Monitoring pH in Defined Intracellular Microdomains. *Biochemical and Biophysical Research Communications*, *289*(2), 457–462. https://doi.org/10.1006/bbrc.2001.6004

Azmitia, E. C. (2020). Chapter 1 - Evolution of serotonin: Sunlight to suicide. In C. P. Müller & K. A. Cunningham (Eds.), *Handbook of Behavioral Neuroscience* (Vol. 31, pp. 3–22). Elsevier. https://doi.org/10.1016/B978-0-444-64125-0.00001-3

Baird, G. S., Zacharias, D. A., & Tsien, R. Y. (1999). Circular permutation and receptor insertion within green fluorescent proteins. *Proceedings of the National Academy of Sciences*, *96*(20), 11241–11246. https://doi.org/10.1073/pnas.96.20.11241

Bajar, B. T., Lam, A. J., Badiee, R. K., Oh, Y.-H., Chu, J., Zhou, X. X., Kim, N., Kim, B. B., Chung, M., Yablonovitch, A. L., Cruz, B. F., Kulalert, K., Tao, J. J., Meyer, T., Su, X.-

D., & Lin, M. Z. (2016). Fluorescent indicators for simultaneous reporting of all four cell cycle phases. *Nature Methods*, *13*(12), Article 12. https://doi.org/10.1038/nmeth.4045

Baker, K. G., Halliday, G. M., Hornung, J.-P., Geffen, L. B., Cotton, R. G. H., & To¨rk, I. (1991). Distribution, morphology and number of monoamine-synthesizing and substance P-containing neurons in the human dorsal raphe nucleus. *Neuroscience*, *42*(3), 757–775. https://doi.org/10.1016/0306-4522(91)90043-N

Barlic, J., Andrews, J. D., Kelvin, A. A., Bosinger, S. E., DeVries, M. E., Xu, L., Dobransky, T., Feldman, R. D., Ferguson, S. S. G., & Kelvin, D. J. (2000). Regulation of tyrosine kinase activation and granule release through β-arrestin by CXCR1. *Nature Immunology*, *1*(3), 227–233. https://doi.org/10.1038/79767

Beaulieu, J.-M., Sotnikova, T. D., Marion, S., Lefkowitz, R. J., Gainetdinov, R. R., & Caron, M. G. (2005). An Akt/β-Arrestin 2/PP2A Signaling Complex Mediates Dopaminergic Neurotransmission and Behavior. *Cell*, *122*(2), 261–273. https://doi.org/10.1016/j.cell.2005.05.012

Belousov, V. V., Fradkov, A. F., Lukyanov, K. A., Staroverov, D. B., Shakhbazov, K. S., Terskikh, A. V., & Lukyanov, S. (2006). Genetically encoded fluorescent indicator for intracellular hydrogen peroxide. *Nature Methods*, *3*(4), 281–286. https://doi.org/10.1038/nmeth866

Benovic, J. L., & Gomez, J. (1993). Molecular cloning and expression of GRK6. A new member of the G protein-coupled receptor kinase family. *Journal of Biological Chemistry*, *268*(26), 19521–19527. https://doi.org/10.1016/S0021-9258(19)36546-9

Benovic, J. L., Mayor, F., Somers, R. L., Caron, M. G., & Lefkowitz, R. J. (1986). Light-dependent phosphorylation of rhodopsin by beta-adrenergic receptor kinase. *Nature*, *321*(6073), 869–872. https://doi.org/10.1038/321869a0

Benovic, J. L., Onorato, J. J., Arriza, J. L., Stone, W. C., Lohse, M., Jenkins, N. A., Gilbert, D. J., Copeland, N. G., Caron, M. G., & Lefkowitz, R. J. (1991). Cloning, expression,

and chromosomal localization of beta-adrenergic receptor kinase 2. A new member of the receptor kinase family. *Journal of Biological Chemistry*, *266*(23), 14939–14946. https://doi.org/10.1016/S0021-9258(18)98568-6

Berman, R. M., Cappiello, A., Anand, A., Oren, D. A., Heninger, G. R., Charney, D. S., & Krystal, J. H. (2000). Antidepressant effects of ketamine in depressed patients. *Biological Psychiatry*, *47*(4), 351–354. https://doi.org/10.1016/S0006-3223(99)00230-9

Bhargava, Y., Hampden-Smith, K., Chachlaki, K., Wood, K. C., Vernon, J., Allerston, C. K., Batchelor, A. M., & Garthwaite, J. (2013). Improved genetically-encoded, FlincG-type fluorescent biosensors for neural cGMP imaging. *Frontiers in Molecular Neuroscience*, *6*. https://doi.org/10.3389/fnmol.2013.00026

Bhattacharya, M., Anborgh, P. H., Babwah, A. V., Dale, L. B., Dobransky, T., Benovic, J. L., Feldman, R. D., Verdi, J. M., Rylett, R. J., & Ferguson, S. S. G. (2002). β-Arrestins regulate a Ral-GDS–Ral effector pathway that mediates cytoskeletal reorganization. *Nature Cell Biology*, *4*(8), 547–555. https://doi.org/10.1038/ncb821

Blier, P., Pineyro, G., El Mansari, M., Bergeron, R., & Montigny, C. (1998). Role of Somatodendritic 5-HT Autoreceptors in Modulating 5-HT Neurotransmissiona. *Annals of the New York Academy of Sciences*, *861*(1 ADVANCES IN S), 204–216. https://doi.org/10.1111/j.1749-6632.1998.tb10192.x

Boersma, A. J., Zuhorn, I. S., & Poolman, B. (2015). A sensor for quantification of macromolecular crowding in living cells. *Nature Methods*, *12*(3), Article 3. https://doi.org/10.1038/nmeth.3257

Borden, P. M., Zhang, P., Shivange, A. V., Marvin, J. S., Cichon, J., Dan, C., Podgorski, K., Figueiredo, A., Novak, O., Tanimoto, M., Shigetomi, E., Lobas, M. A., Kim, H., Zhu, P. K., Zhang, Y., Zheng, W. S., Fan, C., Wang, G., Xiang, B., … Looger, L. L. (2020). *A fast genetically encoded fluorescent sensor for faithful* in vivo *acetylcholine*

detection in mice, fish, worms and flies [Preprint]. Neuroscience. https://doi.org/10.1101/2020.02.07.939504

Borroto-Escuela, D. O., Carlsson, J., Ambrogini, P., Narváez, M., Wydra, K., Tarakanov, A. O., Li, X., Millón, C., Ferraro, L., Cuppini, R., Tanganelli, S., Liu, F., Filip, M., Diaz-Cabiale, Z., & Fuxe, K. (2017). Understanding the Role of GPCR Heteroreceptor Complexes in Modulating the Brain Networks in Health and Disease. *Frontiers in Cellular Neuroscience*, *11*. https://doi.org/10.3389/fncel.2017.00037

Borroto-Escuela, D. O., Romero-Fernandez, W., Mudó, G., Pérez-Alea, M., Ciruela, F., Tarakanov, A. O., Narvaez, M., Di Liberto, V., Agnati, L. F., Belluardo, N., & Fuxe, K. (2012). Fibroblast Growth Factor Receptor 1– 5-Hydroxytryptamine 1A Heteroreceptor Complexes and Their Enhancement of Hippocampal Plasticity. *Biological Psychiatry*, *71*(1), 84–91. https://doi.org/10.1016/j.biopsych.2011.09.012

Brejc, K., Sixma, T. K., Kitts, P. A., Kain, S. R., Tsien, R. Y., Ormö, M., & Remington, S. J. (1997). Structural basis for dual excitation and photoisomerization of the *Aequorea victoria* green fluorescent protein. *Proceedings of the National Academy of Sciences*, *94*(6), 2306–2311. https://doi.org/10.1073/pnas.94.6.2306

Bunin, M. A., & Wightman, R. M. (1998). Quantitative Evaluation of 5-Hydroxytryptamine (Serotonin) Neuronal Release and Uptake: An Investigation of Extrasynaptic Transmission. *The Journal of Neuroscience*, *18*(13), 4854–4860. https://doi.org/10.1523/JNEUROSCI.18-13-04854.1998

Bunin, M. A., & Wightman, R. M. (1999). Paracrine neurotransmission in the CNS: Involvement of 5-HT. *Trends in Neurosciences*, *22*(9), 377–382. https://doi.org/10.1016/S0166-2236(99)01410-1

Busch, A. E., Quester, S., Ulzheimer, J. C., Gorboulev, V., Akhoundova, A., Waldegger, S., Lang, F., & Koepsell, H. (1996). Monoamine neurotransmitter transport mediated by the polyspecific cation transporter rOCT1. *FEBS Letters*, *395*(2–3), 153–156. https://doi.org/10.1016/0014-5793(96)01030-7

Calizo, L. H., Akanwa, A., Ma, X., Pan, Y., Lemos, J. C., Craige, C., Heemstra, L. A., & Beck, S. G. (2011). Raphe serotonin neurons are not homogenous: Electrophysiological, morphological and neurochemical evidence. *Neuropharmacology*, *61*(3), 524–543. https://doi.org/10.1016/j.neuropharm.2011.04.008

Carrel, D., Hamon, M., & Darmon, M. (2006). Role of the C-terminal di-leucine motif of 5-HT1A and 5-HT1B serotonin receptors in plasma membrane targeting. *Journal of Cell Science*, *119*(20), 4276–4284. https://doi.org/10.1242/jcs.03189

Carrel, D., Masson, J., Al Awabdh, S., Capra, C. B., Lenkei, Z., Hamon, M., Emerit, M. B., & Darmon, M. (2008). Targeting of the 5-HT1A Serotonin Receptor to Neuronal Dendrites Is Mediated by Yif1B. *Journal of Neuroscience*, *28*(32), 8063–8073. https://doi.org/10.1523/JNEUROSCI.4487-07.2008

Chalfie, M., Tu, Y., Euskirchen, G., Ward, W. W., & Prasher, D. C. (1994). Green Fluorescent Protein as a Marker for Gene Expression. *Science*, *263*(5148), Article 5148. https://doi.org/10.1126/science.8303295

Chauveau, J., Fert, V., Morel, A. M., & Delaage, M. A. (1991). Rapid and specific enzyme immunoassay of serotonin. *Clinical Chemistry*, *37*(7), 1178–1184. https://doi.org/10.1093/clinchem/37.7.1178

Chen, C. A., & Manning, D. R. (2001). Regulation of G proteins by covalent modification. *Oncogene*, *20*(13), 1643–1652. https://doi.org/10.1038/sj.onc.1204185

Chen, S., Chen, Z., Ren, W., & Ai, H. (2012). Reaction-Based Genetically Encoded Fluorescent Hydrogen Sulfide Sensors. *Journal of the American Chemical Society*, *134*(23), 9589–9592. https://doi.org/10.1021/ja303261d

Chen, T.-W., Wardill, T. J., Sun, Y., Pulver, S. R., Renninger, S. L., Baohan, A., Schreiter, E. R., Kerr, R. A., Orger, M. B., Jayaraman, V., Looger, L. L., Svoboda, K., & Kim, D. S. (2013). Ultrasensitive fluorescent proteins for imaging neuronal activity. *Nature*, *499*(7458), 295–300. https://doi.org/10.1038/nature12354

Claing, A., Chen, W., Miller, W. E., Vitale, N., Moss, J., Premont, R. T., & Lefkowitz, R. J. (2001). β-Arrestin-mediated ADP-ribosylation Factor 6 Activation and β2-Adrenergic Receptor Endocytosis. *Journal of Biological Chemistry*, *276*(45), 42509–42513. https://doi.org/10.1074/jbc.M108399200

Clapham, D. E., & Neer, E. J. (1997). G PROTEIN βγ SUBUNITS. *Annual Review of Pharmacology and Toxicology*, *37*(1), 167–203. https://doi.org/10.1146/annurev.pharmtox.37.1.167

Claustre, Y., Bénavidès, J., & Scatton, B. (1988). 5-HT1A receptor agonists inhibit carbachol-induced stimulation of phosphoinositide turnover in the rat hippocampus. *European Journal of Pharmacology*, *149*(1), Article 1. https://doi.org/10.1016/0014-2999(88)90054-4

Colino, A., & Halliwell, J. V. (1987). Differential modulation of three separate K-conductances in hippocampal CA1 neurons by serotonin. *Nature*, *328*(6125), Article 6125. https://doi.org/10.1038/328073a0

Colombo, M. L., Sweedler, J. V., & Shen, M. (2015). Nanopipet-Based Liquid-Liquid Interface Probes for the Electrochemical Detection of Acetylcholine, Tryptamine, and Serotonin via Ionic Transfer. *Analytical Chemistry*, *87*(10), 5095–5100. https://doi.org/10.1021/ac504151e

Coppen, A. (1967). The Biochemistry of Affective Disorders. *British Journal of Psychiatry*, *113*(504), 1237–1264. https://doi.org/10.1192/bjp.113.504.1237

Cormack, B. P., Valdivia, R. H., & Falkow, S. (1996). FACS-optimized mutants of the green fluorescent protein (GFP). *Gene*, *173*(1), 33–38. https://doi.org/10.1016/0378-1119(95)00685-0

Crawford, L. K., Rahman, S. F., & Beck, S. G. (2013). Social Stress Alters Inhibitory Synaptic Input to Distinct Subpopulations of Raphe Serotonin Neurons. *ACS Chemical Neuroscience*, *4*(1), 200–209. https://doi.org/10.1021/cn300238j

Crouse, R. B., Kim, K., Batchelor, H. M., Girardi, E. M., Kamaletdinova, R., Chan, J., Rajebhosale, P., Pittenger, S. T., Role, L. W., Talmage, D. A., Jing, M., Li, Y., Gao, X.-B., Mineur, Y. S., & Picciotto, M. R. (2020). Acetylcholine is released in the basolateral amygdala in response to predictors of reward and enhances the learning of cue-reward contingency. *ELife*, *9*, e57335. https://doi.org/10.7554/eLife.57335

Cubitt, A. B., Heim, R., Adams, S. R., Boyd, A. E., Gross, L. A., & Tsien, R. Y. (1995). Understanding, improving and using green fluorescent proteins. *Trends in Biochemical Sciences*, *20*(11), Article 11. https://doi.org/10.1016/S0968-0004(00)89099-4

Curzon, G., & Green, A. R. (1970). Rapid method for the determination of 5-hydroxytryptamine and 5-hydroxyindoleacetic acid in small regions of rat brain. *British Journal of Pharmacology*, *39*(3), 653–655. https://doi.org/10.1111/j.1476-5381.1970.tb10373.x

Cussac, D., Rauly-Lestienne, I., Heusler, P., Finana, F., Cathala, C., Bernois, S., & De Vries, L. (2012). μ-opioid and 5-HT1A receptors heterodimerize and show signalling crosstalk via G protein and MAP-kinase pathways. *Cellular Signalling*, *24*(8), 1648–1657. https://doi.org/10.1016/j.cellsig.2012.04.010

Dahlström, A., & Fuxe, K. (1964). Localization of monoamines in the lower brain stem. *Experientia*, *20*(7), 398–399. https://doi.org/10.1007/BF02147990

De Lean, A., Stadel, J. M., & Lefkowitz, R. J. (1980). A ternary complex model explains the agonist-specific binding properties of the adenylate cyclase-coupled beta-adrenergic receptor. *Journal of Biological Chemistry*, *255*(15), 7108–7117. https://doi.org/10.1016/S0021-9258(20)79672-9

De Vivo, M., & Maayani, S. (1986). Characterization of the 5-hydroxytryptamine1a receptor-mediated inhibition of forskolin-stimulated adenylate cyclase activity in

guinea pig and rat hippocampal membranes. *The Journal of Pharmacology and Experimental Therapeutics*, *238*(1), Article 1.

DeFea, K. A., Zalevsky, J., Thoma, M. S., Déry, O., Mullins, R. D., & Bunnett, N. W. (2000). ɴʟ-Arrestin–dependent Endocytosis of Proteinase-activated Receptor 2 Is. *The Journal of Cell Biology*, *148*, 15.

Del Tredici, A. L., Schiffer, H. H., Burstein, E. S., Lameh, J., Mohell, N., Hacksell, U., Brann, M. R., & Weiner, D. M. (2004). Pharmacology of polymorphic variants of the human 5-HT1A receptor. *Biochemical Pharmacology*, *67*(3), 479–490. https://doi.org/10.1016/j.bcp.2003.09.030

Delagrave, S., Hawtin, R. E., Silva, C. M., Yang, M. M., & Youvan, D. C. (1995). Red-shifted excitation mutants of the green fluorescent protein. *Bio/Technology (Nature Publishing Company)*, *13*(2), Article 2. https://doi.org/10.1038/nbt0295-151

Delgado, P. L., Miller, H. L., Salomon, R. M., Licinio, J., Krystal, J. H., Moreno, F. A., Heninger, G. R., & Charney, D. S. (1999). Tryptophan-depletion challenge in depressed patients treated with desipramine or fluoxetine: Implications for the role of serotonin in the mechanism of antidepressant action. *Biological Psychiatry*, *46*(2), 212–220. https://doi.org/10.1016/S0006-3223(99)00014-1

Descarries, L., Riad, M., & Parent, M. (2010). Ultrastructure of the Serotonin Innervation in the Mammalian Central Nervous System. In *Handbook of Behavioral Neuroscience* (Vol. 21, pp. 65–101). Elsevier. https://doi.org/10.1016/S1569-7339(10)70072-2

Descarries, L., Watkins, K. C., Garcia, S., & Beaudet, A. (1982). The serotonin neurons in nucleus raphe dorsalis of adult rat: A light and electron microscope radioautographic study. *The Journal of Comparative Neurology*, *207*(3), 239–254. https://doi.org/10.1002/cne.902070305

Deupi, X., & Standfuss, J. (2011). Structural insights into agonist-induced activation of G-protein-coupled receptors. *Current Opinion in Structural Biology*, *21*(4), 541–551. https://doi.org/10.1016/j.sbi.2011.06.002

Deuschle, K., Okumoto, S., Fehr, M., Looger, L. L., Kozhukh, L., & Frommer, W. B. (2005). Construction and optimization of a family of genetically encoded metabolite sensors by semirational protein engineering. *Protein Science: A Publication of the Protein Society*, *14*(9), Article 9. https://doi.org/10.1110/ps.051508105

Dong, C., Ly, C., Dunlap, L. E., Vargas, M. V., Sun, J., Hwang, I.-W., Azinfar, A., Oh, W. C., Wetsel, W. C., Olson, D. E., & Tian, L. (2021). Psychedelic-inspired drug discovery using an engineered biosensor. *Cell*, *184*(10), 2779-2792.e18. https://doi.org/10.1016/j.cell.2021.03.043

Dong, H., Wang, J., Yang, Y.-F., Shen, Y., Qu, W.-M., & Huang, Z.-L. (2019). Dorsal Striatum Dopamine Levels Fluctuate Across the Sleep–Wake Cycle and Respond to Salient Stimuli in Mice. *Frontiers in Neuroscience*, *13*, 242. https://doi.org/10.3389/fnins.2019.00242

Downes, G. B., & Gautam, N. (1999). The G Protein Subunit Gene Families. *Genomics*, *62*(3), 544–552. https://doi.org/10.1006/geno.1999.5992

Duffet, L., Kosar, S., Panniello, M., Viberti, B., Bracey, E., Zych, A. D., Radoux-Mergault, A., Zhou, X., Dernic, J., Ravotto, L., Tsai, Y.-C., Figueiredo, M., Tyagarajan, S. K., Weber, B., Stoeber, M., Gogolla, N., Schmidt, M. H., Adamantidis, A. R., Fellin, T., … Patriarchi, T. (2022). A genetically encoded sensor for in vivo imaging of orexin neuropeptides. *Nature Methods*, *19*(2), 231–241. https://doi.org/10.1038/s41592-021-01390-2

Edagawa, Y., Saito, H., & Abe, K. (1998). 5-HT1A receptor-mediated inhibition of long-term potentiation in rat visual cortex. *European Journal of Pharmacology*, *349*(2–3), 221–224. https://doi.org/10.1016/S0014-2999(98)00286-6

Ehrig, T., O'Kane, D. J., & Prendergast, F. G. (1995). Green-fluorescent protein mutants with altered fluorescence excitation spectra. *FEBS Letters*, *367*(2), Article 2. https://doi.org/10.1016/0014-5793(95)00557-P

Erapaneedi, R., Belousov, V. V., Schäfers, M., & Kiefer, F. (2016). A novel family of fluorescent hypoxia sensors reveal strong heterogeneity in tumor hypoxia at the cellular level. *The EMBO Journal*, *35*(1), Article 1. https://doi.org/10.15252/embj.201592775

Erspamer, V., & Asero, B. (1952). Identification of enteramine, the specific hormone of the enterochromaffin cell system, as 5-hydroxytryptamine. *Nature*, *169*(4306), Article 4306. https://doi.org/10.1038/169800b0

Evers, T. H., Appelhof, M. A. M., de Graaf-Heuvelmans, P. T. H. M., Meijer, E. W., & Merkx, M. (2007). Ratiometric Detection of Zn(II) Using Chelating Fluorescent Protein Chimeras. *Journal of Molecular Biology*, *374*(2), 411–425. https://doi.org/10.1016/j.jmb.2007.09.021

Fargin, A., Raymond, J. R., Regan, J. W., Cotecchia, S., Lefkowitz, R. J., & Caron, M. G. (1989). Effector coupling mechanisms of the cloned 5-HT1A receptor. *The Journal of Biological Chemistry*, *264*(25), Article 25.

Farrelly, L. A., Thompson, R. E., Zhao, S., Lepack, A. E., Lyu, Y., Bhanu, N. V., Zhang, B., Loh, Y.-H. E., Ramakrishnan, A., Vadodaria, K. C., Heard, K. J., Erikson, G., Nakadai, T., Bastle, R. M., Lukasak, B. J., Zebroski, H., Alenina, N., Bader, M., Berton, O., … Maze, I. (2019). Histone serotonylation is a permissive modification that enhances TFIID binding to H3K4me3. *Nature*, *567*(7749), Article 7749. https://doi.org/10.1038/s41586-019-1024-7

Fehr, M., Lalonde, S., Lager, I., Wolff, M. W., & Frommer, W. B. (2003). Imaging of the Dynamics of Glucose Uptake in the Cytosol of COS-7 Cells by Fluorescent Nanosensors. *Journal of Biological Chemistry*, *278*(21), 19127–19133. https://doi.org/10.1074/jbc.M301333200

Feng, J., Zhang, C., Lischinsky, J. E., Jing, M., Zhou, J., Wang, H., Zhang, Y., Dong, A., Wu, Z., Wu, H., Chen, W., Zhang, P., Zou, J., Hires, S. A., Zhu, J. J., Cui, G., Lin, D., Du, J., & Li, Y. (2019). A Genetically Encoded Fluorescent Sensor for Rapid and

Specific In Vivo Detection of Norepinephrine. *Neuron*, *102*(4), 745-761.e8. https://doi.org/10.1016/j.neuron.2019.02.037

Ferguson, S. S. (2001). Evolving concepts in G protein-coupled receptor endocytosis: The role in receptor desensitization and signaling. *Pharmacological Reviews*, *53*(1), Article 1.

Fernandez, S. P., Cauli, B., Cabezas, C., Muzerelle, A., Poncer, J.-C., & Gaspar, P. (2016). Multiscale single-cell analysis reveals unique phenotypes of raphe 5-HT neurons projecting to the forebrain. *Brain Structure and Function*, *221*(8), 4007–4025. https://doi.org/10.1007/s00429-015-1142-4

Forster, E. A., Cliffe, I. A., Bill, D. J., Dover, G. M., Jones, D., Reilly, Y., & Fletcher, A. (1995). A pharmacological profile of the selective silent 5-HT1A receptor antagonist, WAY-100635. *European Journal of Pharmacology*, *281*(1), Article 1. https://doi.org/10.1016/0014-2999(95)00234-c

Fosbrink, M., Aye-Han, N.-N., Cheong, R., Levchenko, A., & Zhang, J. (2010). Visualization of JNK activity dynamics with a genetically encoded fluorescent biosensor. *Proceedings of the National Academy of Sciences*, *107*(12), 5459–5464. https://doi.org/10.1073/pnas.0909671107

Fredriksson, R., Lagerström, M. C., Lundin, L.-G., & Schiöth, H. B. (2003). The G-protein-coupled receptors in the human genome form five main families. Phylogenetic analysis, paralogon groups, and fingerprints. *Molecular Pharmacology*, *63*(6), Article 6. https://doi.org/10.1124/mol.63.6.1256

Freis, E. D. (1954). Mental Depression in Hypertensive Patients Treated for Long Periods with Large Doses of Reserpine. *New England Journal of Medicine*, *251*(25), 1006–1008. https://doi.org/10.1056/NEJM195412162512504

Fuxe, K., Dahlström, A. B., Jonsson, G., Marcellino, D., Guescini, M., Dam, M., Manger, P., & Agnati, L. (2010). The discovery of central monoamine neurons gave volume

transmission to the wired brain. *Progress in Neurobiology*, *90*(2), 82–100. https://doi.org/10.1016/j.pneurobio.2009.10.012

Ganesan, S., Ameer-beg, S. M., Ng, T. T. C., Vojnovic, B., & Wouters, F. S. (2006). A dark yellow fluorescent protein (YFP)-based Resonance Energy-Accepting Chromoprotein (REACh) for Förster resonance energy transfer with GFP. *Proceedings of the National Academy of Sciences*, *103*(11), 4089–4094. https://doi.org/10.1073/pnas.0509922103

Ganguly, S., Coon, S. L., & Klein, D. C. (2002). Control of melatonin synthesis in the mammalian pineal gland: The critical role of serotonin acetylation. *Cell and Tissue Research*, *309*(1), Article 1. https://doi.org/10.1007/s00441-002-0579-y

Gebauer, L., Jensen, O., Neif, M., Brockmöller, J., & Dücker, C. (2021). Overlap and Specificity in the Substrate Spectra of Human Monoamine Transporters and Organic Cation Transporters 1, 2, and 3. *International Journal of Molecular Sciences*, *22*(23), 12816. https://doi.org/10.3390/ijms222312816

Geldenhuys, W. J., & Van der Schyf, C. J. (2011). Role of serotonin in Alzheimer's disease: A new therapeutic target? *CNS Drugs*, *25*(9), Article 9. https://doi.org/10.2165/11590190-000000000-00000

George, S. R., Fan, T., Xie, Z., Tse, R., Tam, V., Varghese, G., & O'Dowd, B. F. (2000). Oligomerization of μ- and δ-Opioid Receptors. *Journal of Biological Chemistry*, *275*(34), 26128–26135. https://doi.org/10.1074/jbc.M000345200

Gershon, M. D. (2013). 5-Hydroxytryptamine (serotonin) in the gastrointestinal tract. *Current Opinion in Endocrinology, Diabetes, and Obesity*, *20*(1), Article 1. https://doi.org/10.1097/MED.0b013e32835bc703

Gilbert, F., Dourish, C. T., Brazell, C., McClue, S., & Stahl, S. M. (1988). Relationship of increased food intake and plasma ACTH levels to 5-HT1A receptor activation in rats. *Psychoneuroendocrinology*, *13*(6), 471–478. https://doi.org/10.1016/0306-4530(88)90032-7

Gloriam, D. E., Fredriksson, R., & Schiöth, H. B. (2007). The G protein-coupled receptor subset of the rat genome. *BMC Genomics*, *8*(1), 338. https://doi.org/10.1186/1471-2164-8-338

Glukhova, A., Draper-Joyce, C. J., Sunahara, R. K., Christopoulos, A., Wootten, D., & Sexton, P. M. (2018). Rules of Engagement: GPCRs and G Proteins. *ACS Pharmacology & Translational Science*, *1*(2), 73–83. https://doi.org/10.1021/acsptsci.8b00026

Goodman, O. B., Krupnick, J. G., Santini, F., Gurevich, V. V., Penn, R. B., Gagnon, A. W., Keen, J. H., & Benovic, J. L. (1996). β-Arrestin acts as a clathrin adaptor in endocytosis of the β2-adrenergic receptor. *Nature*, *383*(6599), 447–450. https://doi.org/10.1038/383447a0

Gorinski, N., Kowalsman, N., Renner, U., Wirth, A., Reinartz, M. T., Seifert, R., Zeug, A., Ponimaskin, E., & Niv, M. Y. (2012). Computational and Experimental Analysis of the Transmembrane Domain 4/5 Dimerization Interface of the Serotonin 5-HT $_{1A}$ Receptor. *Molecular Pharmacology*, *82*(3), 448–463. https://doi.org/10.1124/mol.112.079137

Griesbeck, O., Baird, G. S., Campbell, R. E., Zacharias, D. A., & Tsien, R. Y. (2001). Reducing the Environmental Sensitivity of Yellow Fluorescent Protein. *Journal of Biological Chemistry*, *276*(31), Article 31. https://doi.org/10.1074/jbc.M102815200

Gurevich, E. V., Tesmer, J. J. G., Mushegian, A., & Gurevich, V. V. (2012). G protein-coupled receptor kinases: More than just kinases and not only for GPCRs. *Pharmacology & Therapeutics*, *133*(1), 40–69. https://doi.org/10.1016/j.pharmthera.2011.08.001

Gurevich, V. V., & Benovic, J. L. (1997). Mechanism of Phosphorylation-Recognition by Visual Arrestin and the Transition of Arrestin into a High Affinity Binding State. *Molecular Pharmacology*, *51*(1), 161–169. https://doi.org/10.1124/mol.51.1.161

Gurevich, V. V., & Gurevich, E. V. (2019). GPCR Signaling Regulation: The Role of GRKs and Arrestins. *Frontiers in Pharmacology*, *10*, 125. https://doi.org/10.3389/fphar.2019.00125

Gutierrez, M. G., Mansfield, K. S., & Malmstadt, N. (2016). The Functional Activity of the Human Serotonin 5-HT 1A Receptor Is Controlled by Lipid Bilayer Composition. *Biophysical Journal*, *110*(11), 2486–2495. https://doi.org/10.1016/j.bpj.2016.04.042

Hahn, A. T., Jones, J. T., & Meyer, T. (2009). Quantitative analysis of cell cycle phase durations and PC12 differentiation using fluorescent biosensors. *Cell Cycle*, *8*(7), 1044–1052. https://doi.org/10.4161/cc.8.7.8042

Han, Z., Jin, L., Platisa, J., Cohen, L. B., Baker, B. J., & Pieribone, V. A. (2013). Fluorescent Protein Voltage Probes Derived from ArcLight that Respond to Membrane Voltage Changes with Fast Kinetics. *PLoS ONE*, *8*(11), e81295. https://doi.org/10.1371/journal.pone.0081295

Harvey, C. D., Ehrhardt, A. G., Cellurale, C., Zhong, H., Yasuda, R., Davis, R. J., & Svoboda, K. (2008). A genetically encoded fluorescent sensor of ERK activity. *Proceedings of the National Academy of Sciences of the United States of America*, *105*(49), Article 49. https://doi.org/10.1073/pnas.0804598105

Hashemi, P., Dankoski, E. C., Wood, K. M., Ambrose, R. E., & Wightman, R. M. (2011). In vivo electrochemical evidence for simultaneous 5-HT and histamine release in the rat substantia nigra pars reticulata following medial forebrain bundle stimulation: In vivo electrochemical characterization of 5-HT. *Journal of Neurochemistry*, *118*(5), 749–759. https://doi.org/10.1111/j.1471-4159.2011.07352.x

Heim, R., Cubitt, A. B., & Tsien, R. Y. (1995). Improved green fluorescence. *Nature*, *373*(6516), Article 6516. https://doi.org/10.1038/373663b0

Heim, R., Prasher, D. C., & Tsien, R. Y. (1994). Wavelength mutations and posttranslational autoxidation of green fluorescent protein. *Proceedings of the*

National Academy of Sciences of the United States of America, *91*(26), Article 26. https://doi.org/10.1073/pnas.91.26.12501

Helassa, N., Dürst, C. D., Coates, C., Kerruth, S., Arif, U., Schulze, C., Wiegert, J. S., Geeves, M., Oertner, T. G., & Török, K. (2018). Ultrafast glutamate sensors resolve high-frequency release at Schaffer collateral synapses. *Proceedings of the National Academy of Sciences of the United States of America*, *115*(21), Article 21. https://doi.org/10.1073/pnas.1720648115

Henke, A., Kovalyova, Y., Dunn, M., Dreier, D., Gubernator, N. G., Dincheva, I., Hwu, C., Šebej, P., Ansorge, M. S., Sulzer, D., & Sames, D. (2018). Toward Serotonin Fluorescent False Neurotransmitters: Development of Fluorescent Dual Serotonin and Vesicular Monoamine Transporter Substrates for Visualizing Serotonin Neurons. *ACS Chemical Neuroscience*, *9*(5), 925–934. https://doi.org/10.1021/acschemneuro.7b00320

Hennessy, M. L., Corcoran, A. E., Brust, R. D., Chang, Y., Nattie, E. E., & Dymecki, S. M. (2017). Activity of *Tachykinin1* -Expressing *Pet1* Raphe Neurons Modulates the Respiratory Chemoreflex. *The Journal of Neuroscience*, *37*(7), 1807–1819. https://doi.org/10.1523/JNEUROSCI.2316-16.2016

Henzler-Wildman, K., & Kern, D. (2007). Dynamic personalities of proteins. *Nature*, *450*(7172), 964–972. https://doi.org/10.1038/nature06522

Hilairet, S., Bouaboula, M., Carrière, D., Le Fur, G., & Casellas, P. (2003). Hypersensitization of the Orexin 1 Receptor by the CB1 Receptor. *Journal of Biological Chemistry*, *278*(26), 23731–23737. https://doi.org/10.1074/jbc.M212369200

Hirano, M., Ando, R., Shimozono, S., Sugiyama, M., Takeda, N., Kurokawa, H., Deguchi, R., Endo, K., Haga, K., Takai-Todaka, R., Inaura, S., Matsumura, Y., Hama, H., Okada, Y., Fujiwara, T., Morimoto, T., Katayama, K., & Miyawaki, A. (2022). A highly

photostable and bright green fluorescent protein. *Nature Biotechnology*, *40*(7), 1132–1142. https://doi.org/10.1038/s41587-022-01278-2

Hires, S. A., Zhu, Y., & Tsien, R. Y. (2008). Optical measurement of synaptic glutamate spillover and reuptake by linker optimized glutamate-sensitive fluorescent reporters. *Proceedings of the National Academy of Sciences*, *105*(11), 4411–4416. https://doi.org/10.1073/pnas.0712008105

Hisatomi, O., Matsuda, S., Satoh, T., Kotaka, S., Imanishi, Y., & Tokunaga, F. (1998). A novel subtype of G-protein-coupled receptor kinase, GRK7, in teleost cone photoreceptors. *FEBS Letters*, *424*(3), 159–164. https://doi.org/10.1016/S0014-5793(98)00162-8

Ho, B. Y., Karschin, A., Branchek, T., Davidson, N., & Lester, H. A. (1992). The role of conserved aspartate and serine residues in ligand binding and in function of the 5-HT1A receptor: A site-directed mutation study. *FEBS Letters*, *312*(2–3), Article 2–3. https://doi.org/10.1016/0014-5793(92)80948-G

Hochbaum, D. R., Zhao, Y., Farhi, S. L., Klapoetke, N., Werley, C. A., Kapoor, V., Zou, P., Kralj, J. M., Maclaurin, D., Smedemark-Margulies, N., Saulnier, J. L., Boulting, G. L., Straub, C., Cho, Y. K., Melkonian, M., Wong, G. K.-S., Harrison, D. J., Murthy, V. N., Sabatini, B. L., … Cohen, A. E. (2014). All-optical electrophysiology in mammalian neurons using engineered microbial rhodopsins. *Nature Methods*, *11*(8), 825–833. https://doi.org/10.1038/nmeth.3000

Hoyer, D., Engel, G., & Kalkman, H. O. (1985). Molecular pharmacology of 5-HT1 and 5-HT2 recognition sites in rat and pig brain membranes: Radioligand binding studies with [3H]5-HT, [3H]8-OH-DPAT, (-)[125I]iodocyanopindolol, [3H]mesulergine and [3H]ketanserin. *European Journal of Pharmacology*, *118*(1–2), Article 1–2. https://doi.org/10.1016/0014-2999(85)90658-2

Huang, C., Duncan, J. A., Gilman, A. G., & Mumby, S. M. (1999). Persistent membrane association of activated and depalmitoylated G protein α subunits. *Proceedings of*

the National Academy of Sciences, *96*(2), 412–417. https://doi.org/10.1073/pnas.96.2.412

Iken, K., Chheng, S., Fargin, A., Goulet, A. C., & Kouassi, E. (1995). Serotonin upregulates mitogen-stimulated B lymphocyte proliferation through 5-HT1A receptors. *Cellular Immunology*, *163*(1), 1–9. https://doi.org/10.1006/cimm.1995.1092

Innis, R. B., & Aghajanian, G. K. (1987). Pertussis toxin blocks 5-HT1A and GABAB receptor-mediated inhibition of serotonergic neurons. *European Journal of Pharmacology*, *143*(2), 195–204. https://doi.org/10.1016/0014-2999(87)90533-4

Inouye, S., & Tsuji, F. I. (1994). *Aequorea* green fluorescent protein: Expression of the gene and fluorescence characteristics of the recombinant protein. *FEBS Letters*, *341*(2–3), Article 2–3. https://doi.org/10.1016/0014-5793(94)80472-9

International Human Genome Sequencing Consortium, Whitehead Institute for Biomedical Research, Center for Genome Research:, Lander, E. S., Linton, L. M., Birren, B., Nusbaum, C., Zody, M. C., Baldwin, J., Devon, K., Dewar, K., Doyle, M., FitzHugh, W., Funke, R., Gage, D., Harris, K., Heaford, A., Howland, J., Kann, L., Lehoczky, J., … Morgan, M. J. (2001). Initial sequencing and analysis of the human genome. *Nature*, *409*(6822), 860–921. https://doi.org/10.1038/35057062

Irwin, C. R., Farmer, A., Willer, D. O., & Evans, D. H. (2012). In-fusion® cloning with vaccinia virus DNA polymerase. *Methods in Molecular Biology (Clifton, N.J.)*, *890*, 23–35. https://doi.org/10.1007/978-1-61779-876-4_2

Jackson, B. P., Dietz, S. M., & Wightman, R. Mark. (1995). Fast-scan cyclic voltammetry of 5-hydroxytryptamine. *Analytical Chemistry*, *67*(6), 1115–1120. https://doi.org/10.1021/ac00102a015

Jafurulla, Md., Pucadyil, T. J., & Chattopadhyay, A. (2008). Effect of sphingomyelinase treatment on ligand binding activity of human serotonin1A receptors. *Biochimica et Biophysica Acta (BBA) - Biomembranes*, *1778*(10), 2022–2025. https://doi.org/10.1016/j.bbamem.2008.07.007

Jensen, A. A., & Spalding, T. A. (2004). Allosteric modulation of G-protein coupled receptors. *European Journal of Pharmaceutical Sciences*, *21*(4), 407–420. https://doi.org/10.1016/j.ejps.2003.11.007

Jing, M., Zhang, P., Wang, G., Feng, J., Mesik, L., Zeng, J., Jiang, H., Wang, S., Looby, J. C., Guagliardo, N. A., Langma, L. W., Lu, J., Zuo, Y., Talmage, D. A., Role, L. W., Barrett, P. Q., Zhang, L. I., Luo, M., Song, Y., … Li, Y. (2018). A genetically encoded fluorescent acetylcholine indicator for in vitro and in vivo studies. *Nature Biotechnology*, *36*(8), Article 8. https://doi.org/10.1038/nbt.4184

Joh, T. H., Shikimi, T., Pickel, V. M., & Reis, D. J. (1975). Brain tryptophan hydroxylase: Purification of, production of antibodies to, and cellular and ultrastructural localization in serotonergic neurons of rat midbrain. *Proceedings of the National Academy of Sciences of the United States of America*, *72*(9), Article 9. https://doi.org/10.1073/pnas.72.9.3575

Kahsai, A. W., Pani, B., & Lefkowitz, R. J. (2018). GPCR signaling: Conformational activation of arrestins. *Cell Research*, *28*(8), Article 8. https://doi.org/10.1038/s41422-018-0067-x

Karschin, A., Ho, B. Y., Labarca, C., Elroy-Stein, O., Moss, B., Davidson, N., & Lester, H. A. (1991). Heterologously expressed serotonin 1A receptors couple to muscarinic K+ channels in heart. *Proceedings of the National Academy of Sciences*, *88*(13), 5694–5698. https://doi.org/10.1073/pnas.88.13.5694

Kaushalya, S. K., Desai, R., Arumugam, S., Ghosh, H., Balaji, J., & Maiti, S. (2008). Three-photon microscopy shows that somatic release can be a quantitatively significant component of serotonergic neurotransmission in the mammalian brain. *Journal of Neuroscience Research*, *86*(15), 3469–3480. https://doi.org/10.1002/jnr.21794

Khan, S. M., Sleno, R., Gora, S., Zylbergold, P., Laverdure, J.-P., Labbé, J.-C., Miller, G. J., & Hébert, T. E. (2013). The Expanding Roles of G *βγ* Subunits in G Protein–

Coupled Receptor Signaling and Drug Action. *Pharmacological Reviews*, *65*(2), 545–577. https://doi.org/10.1124/pr.111.005603

Kim, T.-J., Lei, L., Seong, J., Suh, J.-S., Jang, Y.-K., Jung, S. H., Sun, J., Kim, D.-H., & Wang, Y. (2019). Matrix Rigidity-Dependent Regulation of Ca $^{2+}$ at Plasma Membrane Microdomains by FAK Visualized by Fluorescence Resonance Energy Transfer. *Advanced Science*, *6*(4), 1801290. https://doi.org/10.1002/advs.201801290

Kimple, A. J., Bosch, D. E., Giguère, P. M., & Siderovski, D. P. (2011). Regulators of G-Protein Signaling and Their Gα Substrates: Promises and Challenges in Their Use as Drug Discovery Targets. *Pharmacological Reviews*, *63*(3), 728–749. https://doi.org/10.1124/pr.110.003038

Kobe, F., Renner, U., Woehler, A., Wlodarczyk, J., Papusheva, E., Bao, G., Zeug, A., Richter, D. W., Neher, E., & Ponimaskin, E. (2008). Stimulation- and palmitoylation-dependent changes in oligomeric conformation of serotonin 5-HT1A receptorsi. *Biochimica et Biophysica Acta (BBA) - Molecular Cell Research*, *1783*(8), 1503–1516. https://doi.org/10.1016/j.bbamcr.2008.02.021

Kobilka, B. K., Frielle, T., Collins, S., Yang-Feng, T., Kobilka, T. S., Francke, U., Lefkowitz, R. J., & Caron, M. G. (1987). An intronless gene encoding a potential member of the family of receptors coupled to guanine nucleotide regulatory proteins. *Nature*, *329*(6134), Article 6134. https://doi.org/10.1038/329075a0

Kolasa, M., Solich, J., Faron-Górecka, A., Żurawek, D., Pabian, P., Łukasiewicz, S., Kuśmider, M., Szafran-Pilch, K., Szlachta, M., & Dziedzicka-Wasylewska, M. (2018). Paroxetine and Low-dose Risperidone Induce Serotonin 5-HT1A and Dopamine D2 Receptor Heteromerization in the Mouse Prefrontal Cortex. *Neuroscience*, *377*, 184–196. https://doi.org/10.1016/j.neuroscience.2018.03.004

Kota, P., Reeves, P. J., RajBhandary, U. L., & Khorana, H. G. (2006). Opsin is present as dimers in COS1 cells: Identification of amino acids at the dimeric interface.

Proceedings of the National Academy of Sciences, *103*(9), 3054–3059. https://doi.org/10.1073/pnas.0510982103

Kristiansen, K. (2004). Molecular mechanisms of ligand binding, signaling, and regulation within the superfamily of G-protein-coupled receptors: Molecular modeling and mutagenesis approaches to receptor structure and function. *Pharmacology & Therapeutics*, *103*(1), 21–80. https://doi.org/10.1016/j.pharmthera.2004.05.002

Krupnick, J. G., Goodman, O. B., Keen, J. H., & Benovic, J. L. (1997). Arrestin/Clathrin Interaction. *Journal of Biological Chemistry*, *272*(23), 15011–15016. https://doi.org/10.1074/jbc.272.23.15011

Kubitschke, M., Müller, M., Wallhorn, L., Pulin, M., Mittag, M., Pollok, S., Ziebarth, T., Bremshey, S., Gerdey, J., Claussen, K. C., Renken, K., Groß, J., Gneiße, P., Meyer, N., Wiegert, J. S., Reiner, A., Fuhrmann, M., & Masseck, O. A. (2022). Next generation genetically encoded fluorescent sensors for serotonin. *Nature Communications*, *13*(1), 7525. https://doi.org/10.1038/s41467-022-35200-w

Kunapuli, P., & Benovic, J. L. (1993). Cloning and expression of GRK5: A member of the G protein-coupled receptor kinase family. *Proceedings of the National Academy of Sciences*, *90*(12), 5588–5592. https://doi.org/10.1073/pnas.90.12.5588

Kuner, T., & Augustine, G. J. (2000). A genetically encoded ratiometric indicator for chloride: Capturing chloride transients in cultured hippocampal neurons. *Neuron*, *27*(3), 447–459. https://doi.org/10.1016/s0896-6273(00)00056-8

Laporte, S. A., Oakley, R. H., Holt, J. A., Barak, L. S., & Caron, M. G. (2000). The Interaction of β-Arrestin with the AP-2 Adaptor Is Required for the Clustering of β2-Adrenergic Receptor into Clathrin-coated Pits. *Journal of Biological Chemistry*, *275*(30), 23120–23126. https://doi.org/10.1074/jbc.M002581200

Laporte, S. A., Oakley, R. H., Zhang, J., Holt, J. A., Ferguson, S. S. G., Caron, M. G., & Barak, L. S. (1999). The NL2-adrenergic receptor‾NLarrestin complex recruits the clathrin adaptor AP-2 during endocytosis. *Cell Biology*, 6.

Latorraca, N. R., Venkatakrishnan, A. J., & Dror, R. O. (2017). GPCR Dynamics: Structures in Motion. *Chemical Reviews*, *117*(1), 139–155. https://doi.org/10.1021/acs.chemrev.6b00177

Lee, S. P., So, C. H., Rashid, A. J., Varghese, G., Cheng, R., Lança, A. J., O'Dowd, B. F., & George, S. R. (2004). Dopamine D1 and D2 Receptor Co-activation Generates a Novel Phospholipase C-mediated Calcium Signal. *Journal of Biological Chemistry*, *279*(34), 35671–35678. https://doi.org/10.1074/jbc.M401923200

Lesch, K.-P., & Waider, J. (2012). Serotonin in the Modulation of Neural Plasticity and Networks: Implications for Neurodevelopmental Disorders. *Neuron*, *76*(1), 175–191. https://doi.org/10.1016/j.neuron.2012.09.013

Levoye, A., Dam, J., Ayoub, M. A., Guillaume, J.-L., Couturier, C., Delagrange, P., & Jockers, R. (2006). The orphan GPR50 receptor specifically inhibits MT1 melatonin receptor function through heterodimerization. *The EMBO Journal*, *25*(13), 3012–3023. https://doi.org/10.1038/sj.emboj.7601193

Li, L., Zhang, L.-Z., He, Z.-X., Ma, H., Zhang, Y.-T., Xun, Y.-F., Yuan, W., Hou, W.-J., Li, Y.-T., Lv, Z.-J., Jia, R., & Tai, F.-D. (2021). Dorsal raphe nucleus to anterior cingulate cortex 5-HTergic neural circuit modulates consolation and sociability. *ELife*, *10*, e67638. https://doi.org/10.7554/eLife.67638

Li, Y.-T., Zhang, S.-H., Wang, L., Xiao, R.-R., Liu, W., Zhang, X.-W., Zhou, Z., Amatore, C., & Huang, W.-H. (2014). Nanoelectrode for Amperometric Monitoring of Individual Vesicular Exocytosis Inside Single Synapses. *Angewandte Chemie International Edition*, n/a-n/a. https://doi.org/10.1002/anie.201404744

Lin, S.-H., Lee, L.-T., & Yang, Y. K. (2014). Serotonin and Mental Disorders: A Concise Review on Molecular Neuroimaging Evidence. *Clinical Psychopharmacology and Neuroscience*, *12*(3), Article 3. https://doi.org/10.9758/cpn.2014.12.3.196

Lindenburg, L. H., Vinkenborg, J. L., Oortwijn, J., Aper, S. J. A., & Merkx, M. (2013). MagFRET: The First Genetically Encoded Fluorescent Mg2+ Sensor. *PLoS ONE*, *8*(12), e82009. https://doi.org/10.1371/journal.pone.0082009

Liu, R.-J., Lambe, E. K., & Aghajanian, G. K. (2005). Somatodendritic autoreceptor regulation of serotonergic neurons: Dependence on l-tryptophan and tryptophan hydroxylase-activating kinases: Autoreceptor regulation of serotonergic neurons. *European Journal of Neuroscience*, *21*(4), 945–958. https://doi.org/10.1111/j.1460-9568.2005.03930.x

Lohse, M. J., Andexinger, S., Pitcher, J., Trukawinski, S., Codina, J., Faure, J. P., Caron, M. G., & Lefkowitz, R. J. (1992). Receptor-specific desensitization with purified proteins. Kinase dependence and receptor specificity of beta-arrestin and arrestin in the beta 2-adrenergic receptor and rhodopsin systems. *Journal of Biological Chemistry*, *267*(12), 8558–8564. https://doi.org/10.1016/S0021-9258(18)42479-9

López-Gil, X., Jiménez-Sánchez, L., Campa, L., Castro, E., Frago, C., & Adell, A. (2019). Role of Serotonin and Noradrenaline in the Rapid Antidepressant Action of Ketamine. *ACS Chemical Neuroscience*, *10*(7), 3318–3326. https://doi.org/10.1021/acschemneuro.9b00288

Lovenberg, T. W., Baron, B. M., de Lecea, L., Miller, J. D., Prosser, R. A., Rea, M. A., Foye, P. E., Racke, M., Slone, A. L., Siegel, B. W., Danielson, P. E., Sutcliffe, J. G., & Erlander, M. G. (1993). A novel adenylyl cyclase-activating serotonin receptor (5-HT7) implicated in the regulation of mammalian circadian rhythms. *Neuron*, *11*(3), Article 3. https://doi.org/10.1016/0896-6273(93)90149-L

Lucki, I. (1998). The spectrum of behaviors influenced by serotonin. *Biological Psychiatry*, *44*(3), Article 3. https://doi.org/10.1016/s0006-3223(98)00139-5

Łukasiewicz, S., Błasiak, E., Szafran-Pilch, K., & Dziedzicka-Wasylewska, M. (2016). Dopamine D_2 and serotonin 5-HT $_{1A}$ receptor interaction in the context of the effects

of antipsychotics—*In vitro* studies. *Journal of Neurochemistry*, *137*(4), 549–560. https://doi.org/10.1111/jnc.13582

Luttrell, L. M., Ferguson, S. S., Daaka, Y., Miller, W. E., Maudsley, S., Della Rocca, G. J., Lin, F., Kawakatsu, H., Owada, K., Luttrell, D. K., Caron, M. G., & Lefkowitz, R. J. (1999). Beta-arrestin-dependent formation of beta2 adrenergic receptor-Src protein kinase complexes. *Science (New York, N.Y.)*, *283*(5402), 655–661. https://doi.org/10.1126/science.283.5402.655

Madshus, I. H. (1988). Regulation of intracellular pH in eukaryotic cells. *Biochemical Journal*, *250*(1), 1–8. https://doi.org/10.1042/bj2500001

Mahon, M. J. (2011). pHluorin2: An enhanced, ratiometric, pH-sensitive green florescent protein. *Advances in Bioscience and Biotechnology (Print)*, *2*(3), Article 3. https://doi.org/10.4236/abb.2011.23021

Maickel, R. P., Cox, R. H., Saillant, J., & Miller, F. P. (1968). A method for the determination of serotonin and norepinephrine in discrete areas of rat brain. *International Journal of Neuropharmacology*, *7*(3), 275–281. https://doi.org/10.1016/0028-3908(68)90034-8

Malik, R. U., Ritt, M., DeVree, B. T., Neubig, R. R., Sunahara, R. K., & Sivaramakrishnan, S. (2013). Detection of G protein-selective G protein-coupled receptor (GPCR) conformations in live cells. *The Journal of Biological Chemistry*, *288*(24), Article 24. https://doi.org/10.1074/jbc.M113.464065

Mann, D. A., & Oakley, F. (2013). Serotonin paracrine signaling in tissue fibrosis. *Biochimica et Biophysica Acta*, *1832*(7), Article 7. https://doi.org/10.1016/j.bbadis.2012.09.009

Markstein, R., Hoyer, D., & Engel, G. (1986). 5-HT1A-receptors mediate stimulation of adenylate cyclase in rat hippocampus. *Naunyn-Schmiedeberg's Archives of Pharmacology*, *333*(4), Article 4. https://doi.org/10.1007/BF00500006

Maruyama, Y., & Takemori, A. E. (1971). New gas chromatographic method for the analysis of 5-hydroxytryptamine and 5-hydroxyindoleacetic acid in the brain. *Biochemical Pharmacology*, *20*(8), 1833–1841. https://doi.org/10.1016/0006-2952(71)90381-9

Marvin, J. S., Borghuis, B. G., Tian, L., Cichon, J., Harnett, M. T., Akerboom, J., Gordus, A., Renninger, S. L., Chen, T.-W., Bargmann, C. I., Orger, M. B., Schreiter, E. R., Demb, J. B., Gan, W.-B., Hires, S. A., & Looger, L. L. (2013). An optimized fluorescent probe for visualizing glutamate neurotransmission. *Nature Methods*, *10*(2), Article 2. https://doi.org/10.1038/nmeth.2333

Marvin, J. S., Shimoda, Y., Magloire, V., Leite, M., Kawashima, T., Jensen, T. P., Kolb, I., Knott, E. L., Novak, O., Podgorski, K., Leidenheimer, N. J., Rusakov, D. A., Ahrens, M. B., Kullmann, D. M., & Looger, L. L. (2019). A genetically encoded fluorescent sensor for in vivo imaging of GABA. *Nature Methods*, *16*(8), 763–770. https://doi.org/10.1038/s41592-019-0471-2

Maswood, N., Caldarola-Pastuszka, M., & Uphouse, L. (1998). Functional integration among 5-hydroxytryptamine receptor families in the control of female rat sexual behavior. *Brain Research*, *802*(1–2), 98–103. https://doi.org/10.1016/S0006-8993(98)00554-X

Mauler, M., Bode, C., & Duerschmied, D. (2016). Platelet serotonin modulates immune functions. *Hämostaseologie*, *36*(1), Article 1. https://doi.org/10.5482/HAMO-14-11-0073

Maurel, J. L., Autin, J.-M., Funes, P., Newman-Tancredi, A., Colpaert, F., & Vacher, B. (2007). High-Efficacy 5-HT $_{1A}$ Agonists for Antidepressant Treatment: A Renewed Opportunity. *Journal of Medicinal Chemistry*, *50*(20), 5024–5033. https://doi.org/10.1021/jm070714l

Mena, M. A., Treynor, T. P., Mayo, S. L., & Daugherty, P. S. (2006). Blue fluorescent proteins with enhanced brightness and photostability from a structurally targeted library. *Nature Biotechnology*, *24*(12), 1569–1571. https://doi.org/10.1038/nbt1264

Mengod, G., Cortés, R., Vilaró, M. T., & Hoyer, D. (2010). Distribution of 5-HT Receptors in the Central Nervous System. In *Handbook of Behavioral Neuroscience* (Vol. 21, pp. 123–138). Elsevier. https://doi.org/10.1016/S1569-7339(10)70074-6

Miczek, K. A., Hussain, S., & Faccidomo, S. (1998). Alcohol-heightened aggression in mice: Attenuation by 5-HT 1A receptor agonists. *Psychopharmacology*, *139*(1–2), 160–168. https://doi.org/10.1007/s002130050701

Milligan, G., & Kostenis, E. (2006). Heterotrimeric G-proteins: A short history: Heterotrimeric G-proteins: a short history. *British Journal of Pharmacology*, *147*(S1), S46–S55. https://doi.org/10.1038/sj.bjp.0706405

Millón, C., Flores-Burgess, A., Narváez, M., Borroto-Escuela, D. O., Santín, L., Gago, B., Narváez, J. A., Fuxe, K., & Díaz-Cabiale, Z. (2016). Galanin (1-15) enhances the antidepressant effects of the 5-HT1A receptor agonist 8-OH-DPAT: Involvement of the raphe-hippocampal 5-HT neuron system. *Brain Structure & Function*, *221*(9), 4491–4504. https://doi.org/10.1007/s00429-015-1180-y

Mukherjee, S., Jansen, V., Jikeli, J. F., Hamzeh, H., Alvarez, L., Dombrowski, M., Balbach, M., Strünker, T., Seifert, R., Kaupp, U. B., & Wachten, D. (2016). A novel biosensor to study cAMP dynamics in cilia and flagella. *ELife*, *5*, e14052. https://doi.org/10.7554/eLife.14052

Muller, A., Joseph, V., Slesinger, P. A., & Kleinfeld, D. (2014). Cell-based reporters reveal in vivo dynamics of dopamine and norepinephrine release in murine cortex. *Nature Methods*, *11*(12), Article 12. https://doi.org/10.1038/nmeth.3151

Müller, C. P., & Homberg, J. R. (2015). The role of serotonin in drug use and addiction. *Behavioural Brain Research*, *277*, 146–192. https://doi.org/10.1016/j.bbr.2014.04.007

Muto, A., Ohkura, M., Kotani, T., Higashijima, S., Nakai, J., & Kawakami, K. (2011). Genetic visualization with an improved GCaMP calcium indicator reveals spatiotemporal activation of the spinal motor neurons in zebrafish. *Proceedings of the National Academy of Sciences*, *108*(13), 5425–5430. https://doi.org/10.1073/pnas.1000887108

Nagai, T., Ibata, K., Park, E. S., Kubota, M., Mikoshiba, K., & Miyawaki, A. (2002). A variant of yellow fluorescent protein with fast and efficient maturation for cell-biological applications. *Nature Biotechnology*, *20*(1), 87–90. https://doi.org/10.1038/nbt0102-87

Nakai, J., Ohkura, M., & Imoto, K. (2001). A high signal-to-noise Ca2+ probe composed of a single green fluorescent protein. *Nature Biotechnology*, *19*(2), 137–141. https://doi.org/10.1038/84397

Nelson, C. D., Perry, S. J., Regier, D. S., Prescott, S. M., Topham, M. K., & Lefkowitz, R. J. (2007). Targeting of Diacylglycerol Degradation to M1 Muscarinic Receptors by ß-Arrestins. *Science*, *315*(5812), 663–666. https://doi.org/10.1126/science.1134562

Neumeister, A., Nugent, A. C., Waldeck, T., Geraci, M., Schwarz, M., Bonne, O., Bain, E. E., Luckenbaugh, D. A., Herscovitch, P., Charney, D. S., & Drevets, W. C. (2004). Neural and behavioral responses to tryptophan depletion in unmedicated patients with remitted major depressive disorder and controls. *Archives of General Psychiatry*, *61*(8), Article 8. https://doi.org/10.1001/archpsyc.61.8.765

Nguyen, A. W., & Daugherty, P. S. (2005). Evolutionary optimization of fluorescent proteins for intracellular FRET. *Nature Biotechnology*, *23*(3), Article 3. https://doi.org/10.1038/nbt1066

Nguyen, Q.-T., Schroeder, L. F., Mank, M., Muller, A., Taylor, P., Griesbeck, O., & Kleinfeld, D. (2010). An in vivo biosensor for neurotransmitter release and in situ receptor activity. *Nature Neuroscience*, *13*(1), 127–132. https://doi.org/10.1038/nn.2469

Niino, Y., Hotta, K., & Oka, K. (2010). Blue fluorescent cGMP sensor for multiparameter fluorescence imaging. *PloS One*, *5*(2), e9164. https://doi.org/10.1371/journal.pone.0009164

Oakley, R. H., Laporte, S. A., Holt, J. A., Barak, L. S., & Caron, M. G. (1999). Association of β-Arrestin with G Protein-coupled Receptors during Clathrin-mediated Endocytosis Dictates the Profile of Receptor Resensitization. *Journal of Biological Chemistry*, *274*(45), 32248–32257. https://doi.org/10.1074/jbc.274.45.32248

Odaka, H., Arai, S., Inoue, T., & Kitaguchi, T. (2014). Genetically-Encoded Yellow Fluorescent cAMP Indicator with an Expanded Dynamic Range for Dual-Color Imaging. *PLoS ONE*, *9*(6), e100252. https://doi.org/10.1371/journal.pone.0100252

Ohkura, M., Sasaki, T., Kobayashi, C., Ikegaya, Y., & Nakai, J. (2012). An Improved Genetically Encoded Red Fluorescent Ca2+ Indicator for Detecting Optically Evoked Action Potentials. *PLoS ONE*, *7*(7), e39933. https://doi.org/10.1371/journal.pone.0039933

Ohta, Y., Furuta, T., Nagai, T., & Horikawa, K. (2018). Red fluorescent cAMP indicator with increased affinity and expanded dynamic range. *Scientific Reports*, *8*(1), Article 1. https://doi.org/10.1038/s41598-018-20251-1

Okada, S., Ota, K., & Ito, T. (2009). Circular permutation of ligand-binding module improves dynamic range of genetically encoded FRET-based nanosensor: Circularly Permutated PBP for FRET Nanosensor. *Protein Science*, *18*(12), 2518–2527. https://doi.org/10.1002/pro.266

Okaty, B. W., Commons, K. G., & Dymecki, S. M. (2019). Embracing diversity in the 5-HT neuronal system. *Nature Reviews Neuroscience*, *20*(7), 397–424. https://doi.org/10.1038/s41583-019-0151-3

Okaty, B. W., Freret, M. E., Rood, B. D., Brust, R. D., Hennessy, M. L., deBairos, D., Kim, J. C., Cook, M. N., & Dymecki, S. M. (2015). Multi-Scale Molecular Deconstruction

of the Serotonin Neuron System. *Neuron*, *88*(4), 774–791. https://doi.org/10.1016/j.neuron.2015.10.007

Okumoto, S., Looger, L. L., Micheva, K. D., Reimer, R. J., Smith, S. J., & Frommer, W. B. (2005). Detection of glutamate release from neurons by genetically encoded surface-displayed FRET nanosensors. *Proceedings of the National Academy of Sciences of the United States of America*, *102*(24), Article 24. https://doi.org/10.1073/pnas.0503274102

Ormö, M., Cubitt, A. B., Kallio, K., Gross, L. A., Tsien, R. Y., & Remington, S. J. (1996). Crystal Structure of the *Aequorea victoria* Green Fluorescent Protein. *Science*, *273*(5280), Article 5280. https://doi.org/10.1126/science.273.5280.1392

Papoucheva, E., Dumuis, A., Sebben, M., Richter, D. W., & Ponimaskin, E. G. (2004). The 5-hydroxytryptamine(1A) receptor is stably palmitoylated, and acylation is critical for communication of receptor with Gi protein. *The Journal of Biological Chemistry*, *279*(5), Article 5. https://doi.org/10.1074/jbc.M308177200

Park, J.-Y., Myung, S.-W., Kim, I.-S., Choi, D.-K., Kwon, S.-J., & Yoon, S.-H. (2013). Simultaneous Measurement of Serotonin, Dopamine and Their Metabolites in Mouse Brain Extracts by High-Performance Liquid Chromatography with Mass Spectrometry Following Derivatization with Ethyl Chloroformate. *Biological and Pharmaceutical Bulletin*, *36*(2), 252–258. https://doi.org/10.1248/bpb.b12-00689

Patriarchi, T., Cho, J. R., Merten, K., Howe, M. W., Marley, A., Xiong, W.-H., Folk, R. W., Broussard, G. J., Liang, R., Jang, M. J., Zhong, H., Dombeck, D., von Zastrow, M., Nimmerjahn, A., Gradinaru, V., Williams, J. T., & Tian, L. (2018). Ultrafast neuronal imaging of dopamine dynamics with designed genetically encoded sensors. *Science*, *360*(6396), Article 6396. https://doi.org/10.1126/science.aat4422

Patriarchi, T., Mohebi, A., Sun, J., Marley, A., Liang, R., Dong, C., Puhger, K., Mizuno, G. O., Davis, C. M., Wiltgen, B., von Zastrow, M., Berke, J. D., & Tian, L. (2020). An

expanded palette of dopamine sensors for multiplex imaging in vivo. *Nature Methods*, *17*(11), 1147–1155. https://doi.org/10.1038/s41592-020-0936-3

Penington, N. J., & Kelly, J. S. (1990). Serotonin receptor activation reduces calcium current in an acutely dissociated adult central neuron. *Neuron*, *4*(5), Article 5. https://doi.org/10.1016/0896-6273(90)90201-p

Perroy, J., Pontier, S., Charest, P. G., Aubry, M., & Bouvier, M. (2004). Real-time monitoring of ubiquitination in living cells by BRET. *Nature Methods*, *1*(3), Article 3. https://doi.org/10.1038/nmeth722

Perry, S. J., Baillie, G. S., Kohout, T. A., McPhee, I., Magiera, M. M., Ang, K. L., Miller, W. E., McLean, A. J., Conti, M., Houslay, M. D., & Lefkowitz, R. J. (2002). *Targeting of Cyclic AMP Degradation to* NL *2-Adrenergic Receptors by* NL *-Arrestins*. *298*, 3.

Peterson, Y. K., & Luttrell, L. M. (2017). The Diverse Roles of Arrestin Scaffolds in G Protein–Coupled Receptor Signaling. *Pharmacological Reviews*, *69*(3), 256–297. https://doi.org/10.1124/pr.116.013367

Piatkevich, K. D., Jung, E. E., Straub, C., Linghu, C., Park, D., Suk, H.-J., Hochbaum, D. R., Goodwin, D., Pnevmatikakis, E., Pak, N., Kawashima, T., Yang, C.-T., Rhoades, J. L., Shemesh, O., Asano, S., Yoon, Y.-G., Freifeld, L., Saulnier, J. L., Riegler, C., … Boyden, E. S. (2018). A robotic multidimensional directed evolution approach applied to fluorescent voltage reporters. *Nature Chemical Biology*, *14*(4), Article 4. https://doi.org/10.1038/s41589-018-0004-9

Placidi, G. P. A., Oquendo, M. A., Malone, K. M., Huang, Y.-Y., Ellis, S. P., & Mann, J. J. (2001). Aggressivity, suicide attempts, and depression: Relationship to cerebrospinal fluid monoamine metabolite levels. *Biological Psychiatry*, *50*(10), 783–791. https://doi.org/10.1016/S0006-3223(01)01170-2

Politis, M., & Niccolini, F. (2015). Serotonin in Parkinson's disease. *Behavioural Brain Research*, *277*, 136–145. https://doi.org/10.1016/j.bbr.2014.07.037

Prasad, R., Paila, Y. D., Jafurulla, Md., & Chattopadhyay, A. (2009). Membrane cholesterol depletion from live cells enhances the function of human serotonin1A receptors. *Biochemical and Biophysical Research Communications*, *389*(2), 333–337. https://doi.org/10.1016/j.bbrc.2009.08.148

Prasher, D. C., Eckenrode, V. K., Ward, W. W., Prendergast, F. G., & Cormier, M. J. (1992). Primary structure of the Aequorea victoria green-fluorescent protein. *Gene*, *111*(2), 229–233. https://doi.org/10.1016/0378-1119(92)90691-H

Pugh, E. N., & Lamb, T. D. (2000). Chapter 5 Phototransduction in vertebrate rods and cones: Molecular mechanisms of amplification, recovery and light adaptation. In *Handbook of Biological Physics* (Vol. 3, pp. 183–255). Elsevier. https://doi.org/10.1016/S1383-8121(00)80008-1

Qin, Y., Sammond, D. W., Braselmann, E., Carpenter, M. C., & Palmer, A. E. (2016). Development of an Optical Zn $^{2+}$ Probe Based on a Single Fluorescent Protein. *ACS Chemical Biology*, *11*(10), 2744–2751. https://doi.org/10.1021/acschembio.6b00442

Rapport, M. M. (1949). Serum vasoconstrictor (serotonin) the presence of creatinine in the complex; a proposed structure of the vasoconstrictor principle. *The Journal of Biological Chemistry*, *180*(3), Article 3.

Rapport, M. M., Green, A. A., & Page, I. H. (1948a). Crystalline Serotonin. *Science (New York, N.Y.)*, *108*(2804), Article 2804. https://doi.org/10.1126/science.108.2804.329

Rapport, M. M., Green, Arda. Alden., & Page, I. H. (1948b). PARTIAL PURIFICATION OF THE VASOCONSTRICTOR IN BEEF SERUM. *Journal of Biological Chemistry*, *174*(2), 735–741. https://doi.org/10.1016/S0021-9258(18)57355-5

Rasmussen, S. G. F., DeVree, B. T., Zou, Y., Kruse, A. C., Chung, K. Y., Kobilka, T. S., Thian, F. S., Chae, P. S., Pardon, E., Calinski, D., Mathiesen, J. M., Shah, S. T. A., Lyons, J. A., Caffrey, M., Gellman, S. H., Steyaert, J., Skiniotis, G., Weis, W. I., Sunahara, R. K., & Kobilka, B. K. (2011). Crystal structure of the β2 adrenergic

receptor–Gs protein complex. *Nature*, *477*(7366), 549–555. https://doi.org/10.1038/nature10361

Raymond, J. R., Fargin, A., Middleton, J. P., Graff, J. M., Haupt, D. M., Caron, M. G., Lefkowitz, R. J., & Dennis, V. W. (1989). The human 5-HT1A receptor expressed in HeLa cells stimulates sodium-dependent phosphate uptake via protein kinase C. *The Journal of Biological Chemistry*, *264*(36), Article 36.

Renner, U., Zeug, A., Woehler, A., Niebert, M., Dityatev, A., Dityateva, G., Gorinski, N., Guseva, D., Abdel-Galil, D., Fröhlich, M., Döring, F., Wischmeyer, E., Richter, D. W., Neher, E., & Ponimaskin, E. G. (2012). Heterodimerization of serotonin receptors 5-HT1A and 5-HT7 differentially regulates receptor signalling and trafficking. *Journal of Cell Science*, jcs.101337. https://doi.org/10.1242/jcs.101337

Riad, M., Garcia, S., Watkins, K. C., Jodoin, N., Doucet, E., Langlois, X., el Mestikawy, S., Hamon, M., & Descarries, L. (2000). Somatodendritic localization of 5-HT1A and preterminal axonal localization of 5-HT1B serotonin receptors in adult rat brain. *The Journal of Comparative Neurology*, *417*(2), 181–194.

Roberts, J. G., & Sombers, L. A. (2018). Fast-Scan Cyclic Voltammetry: Chemical Sensing in the Brain and Beyond. *Analytical Chemistry*, *90*(1), 490–504. https://doi.org/10.1021/acs.analchem.7b04732

Ross, E. M., & Wilkie, T. M. (2000). GTPase-Activating Proteins for Heterotrimeric G Proteins: Regulators of G Protein Signaling (RGS) and RGS-Like Proteins. *Annual Review of Biochemistry*, *69*(1), 795–827. https://doi.org/10.1146/annurev.biochem.69.1.795

Ruat, M., Traiffort, E., Leurs, R., Tardivel-Lacombe, J., Diaz, J., Arrang, J. M., & Schwartz, J. C. (1993). Molecular cloning, characterization, and localization of a high-affinity serotonin receptor (5-HT7) activating cAMP formation. *Proceedings of the National Academy of Sciences of the United States of America*, *90*(18), Article 18. https://doi.org/10.1073/pnas.90.18.8547

Sabatini, B. L., & Tian, L. (2020). Imaging Neurotransmitter and Neuromodulator Dynamics In Vivo with Genetically Encoded Indicators. *Neuron*, *108*(1), 17–32. https://doi.org/10.1016/j.neuron.2020.09.036

Saito, K., Chang, Y.-F., Horikawa, K., Hatsugai, N., Higuchi, Y., Hashida, M., Yoshida, Y., Matsuda, T., Arai, Y., & Nagai, T. (2012). Luminescent proteins for high-speed single-cell and whole-body imaging. *Nature Communications*, *3*(1), 1262. https://doi.org/10.1038/ncomms2248

Sakaue-Sawano, A., Yo, M., Komatsu, N., Hiratsuka, T., Kogure, T., Hoshida, T., Goshima, N., Matsuda, M., Miyoshi, H., & Miyawaki, A. (2017). Genetically Encoded Tools for Optical Dissection of the Mammalian Cell Cycle. *Molecular Cell*, *68*(3), Article 3. https://doi.org/10.1016/j.molcel.2017.10.001

Salomon, R. M., Miller, H. L., Krystal, J. H., Heninger, G. R., & Charney, D. S. (1997). Lack of behavioral effects of monoamine depletion in healthy subjects. *Biological Psychiatry*, *41*(1), 58–64. https://doi.org/10.1016/0006-3223(95)00670-2

Sasa, Suleiman., & Blank, C. LeRoy. (1977). Determination of serotonin and dopamine in mouse brain tissue by high performance liquid chromatography with electrochemical detection. *Analytical Chemistry*, *49*(3), 354–359. https://doi.org/10.1021/ac50011a008

Sasaki, K., Ito, T., Nishino, N., Khochbin, S., & Yoshida, M. (2009). Real-time imaging of histone H4 hyperacetylation in living cells. *Proceedings of the National Academy of Sciences*, *106*(38), 16257–16262. https://doi.org/10.1073/pnas.0902150106

Sato, M., Ueda, Y., & Umezawa, Y. (2006). Imaging diacylglycerol dynamics at organelle membranes. *Nature Methods*, *3*(10), Article 10. https://doi.org/10.1038/nmeth930

Seletti, B., Benkelfat, C., Blier, P., Annable, L., Gilbert, F., & de Montigny, C. (1995). Serotonin1A receptor activation by flesinoxan in humans. Body temperature and neuroendocrine responses. *Neuropsychopharmacology: Official Publication of the*

American College of Neuropsychopharmacology, *13*(2), 93–104. https://doi.org/10.1016/0893-133X(95)00025-9

Shenker, A., Maayani, S., Weinstein, H., & Green, J. P. (1985). Two 5-HT receptors linked to adenylate cyclase in guinea pig hippocampus are discriminated by 5-carboxamidotryptamine and spiperone. *European Journal of Pharmacology*, *109*(3), Article 3. https://doi.org/10.1016/0014-2999(85)90408-X

Shenoy, S. K., McDonald, P. H., Kohout, T. A., & Lefkowitz, R. J. (2001). Regulation of Receptor Fate by Ubiquitination of Activated β $_2$ -Adrenergic Receptor and β-Arrestin. *Science*, *294*(5545), 1307–1313. https://doi.org/10.1126/science.1063866

Shenoy, S. K., Modi, A. S., Shukla, A. K., Xiao, K., Berthouze, M., Ahn, S., Wilkinson, K. D., Miller, W. E., & Lefkowitz, R. J. (2009). Beta-arrestin-dependent signaling and trafficking of 7-transmembrane receptors is reciprocally regulated by the deubiquitinase USP33 and the E3 ligase Mdm2. *Proceedings of the National Academy of Sciences of the United States of America*, *106*(16), 6650–6655. https://doi.org/10.1073/pnas.0901083106

Shenoy, S. K., Xiao, K., Venkataramanan, V., Snyder, P. M., Freedman, N. J., & Weissman, A. M. (2008). Nedd4 Mediates Agonist-dependent Ubiquitination, Lysosomal Targeting, and Degradation of the β2-Adrenergic Receptor. *Journal of Biological Chemistry*, *283*(32), 22166–22176. https://doi.org/10.1074/jbc.M709668200

Shikanai, H., Yoshida, T., Konno, K., Yamasaki, M., Izumi, T., Ohmura, Y., Watanabe, M., & Yoshioka, M. (2012). Distinct Neurochemical and Functional Properties of GAD67-Containing 5-HT Neurons in the Rat Dorsal Raphe Nucleus. *Journal of Neuroscience*, *32*(41), 14415–14426. https://doi.org/10.1523/JNEUROSCI.5929-11.2012

Shimomura, O., Johnson, F. H., & Saiga, Y. (1962). Extraction, Purification and Properties of Aequorin, a Bioluminescent Protein from the Luminous

Hydromedusan,Aequorea. *Journal of Cellular and Comparative Physiology*, *59*(3), Article 3. https://doi.org/10.1002/jcp.1030590302

Simon, M. I., Strathmann, M. P., & Gautam, N. (1991). Diversity of G Proteins in Signal Transduction. *Science*, *252*(5007), 802–808. https://doi.org/10.1126/science.1902986

Smrcka, A. V. (2008). G protein βγ subunits: Central mediators of G protein-coupled receptor signaling. *Cellular and Molecular Life Sciences*, *65*(14), 2191–2214. https://doi.org/10.1007/s00018-008-8006-5

Somers, R. L., & Klein, D. C. (1984). Rhodopsin Kinase Activity in the Mammalian Pineal Gland and Other Tissues. *Science*, *226*(4671), 182–184. https://doi.org/10.1126/science.6091271

St-Pierre, F., Marshall, J. D., Yang, Y., Gong, Y., Schnitzer, M. J., & Lin, M. Z. (2014). High-fidelity optical reporting of neuronal electrical activity with an ultrafast fluorescent voltage sensor. *Nature Neuroscience*, *17*(6), 884–889. https://doi.org/10.1038/nn.3709

Sugiyama, M., Sakaue-Sawano, A., Iimura, T., Fukami, K., Kitaguchi, T., Kawakami, K., Okamoto, H., Higashijima, S., & Miyawaki, A. (2009). Illuminating cell-cycle progression in the developing zebrafish embryo. *Proceedings of the National Academy of Sciences*, *106*(49), Article 49. https://doi.org/10.1073/pnas.0906464106

Sun, F., Zeng, J., Jing, M., Zhou, J., Feng, J., Owen, S. F., Luo, Y., Li, F., Wang, H., Yamaguchi, T., Yong, Z., Gao, Y., Peng, W., Wang, L., Zhang, S., Du, J., Lin, D., Xu, M., Kreitzer, A. C., … Li, Y. (2018). A Genetically Encoded Fluorescent Sensor Enables Rapid and Specific Detection of Dopamine in Flies, Fish, and Mice. *Cell*, *174*(2), Article 2. https://doi.org/10.1016/j.cell.2018.06.042

Sun, X., Deng, J., Liu, T., & Borjigin, J. (2002). Circadian 5-HT production regulated by adrenergic signaling. *Proceedings of the National Academy of Sciences*, *99*(7), 4686–4691. https://doi.org/10.1073/pnas.062585499

Szlachta, M., Kuśmider, M., Pabian, P., Solich, J., Kolasa, M., Żurawek, D., Dziedzicka-Wasylewska, M., & Faron-Górecka, A. (2018). Repeated Clozapine Increases the Level of Serotonin 5-HT1AR Heterodimerization with 5-HT2A or Dopamine D2 Receptors in the Mouse Cortex. *Frontiers in Molecular Neuroscience*, *11*, 40. https://doi.org/10.3389/fnmol.2018.00040

Tena-Campos, M., Ramon, E., Borroto-Escuela, D. O., Fuxe, K., & Garriga, P. (2015). The zinc binding receptor GPR39 interacts with 5-HT1A and GalR1 to form dynamic heteroreceptor complexes with signaling diversity. *Biochimica Et Biophysica Acta*, *1852*(12), 2585–2592. https://doi.org/10.1016/j.bbadis.2015.09.003

Tenner, B., Zhang, J. Z., Kwon, Y., Pessino, V., Feng, S., Huang, B., Mehta, S., & Zhang, J. (2021). FluoSTEPs: Fluorescent biosensors for monitoring compartmentalized signaling within endogenous microdomains. *Science Advances*, *7*(21), eabe4091. https://doi.org/10.1126/sciadv.abe4091

Toyama, Y., Kano, H., Mase, Y., Yokogawa, M., Osawa, M., & Shimada, I. (2017). Dynamic regulation of GDP binding to G proteins revealed by magnetic field-dependent NMR relaxation analyses. *Nature Communications*, *8*(1), 14523. https://doi.org/10.1038/ncomms14523

Tsien, R. Y. (1998). THE GREEN FLUORESCENT PROTEIN. *Annual Review of Biochemistry*, *67*(1), Article 1. https://doi.org/10.1146/annurev.biochem.67.1.509

Twarog, B. M., & Page, I. H. (1953). Serotonin Content of Some Mammalian Tissues and Urine and a Method for Its Determination. *American Journal of Physiology-Legacy Content*, *175*(1), 157–161. https://doi.org/10.1152/ajplegacy.1953.175.1.157

Tyas, L., Brophy, V. A., Pope, A., Rivett, A. J., & Tavaré, J. M. (2000). Rapid caspase‑3 activation during apoptosis revealed using fluorescence‑resonance energy transfer. *EMBO Reports*, *1*(3), 266–270. https://doi.org/10.1093/embo-reports/kvd050

Umbriaco, D., Garcia, S., Beaulieu, C., & Descarries, L. (1995). Relational features of acetylcholine, noradrenaline, serotonin and GABA axon terminals in thestratum

radiatum of adult rat hippocampus (CA1). *Hippocampus*, *5*(6), 605–620. https://doi.org/10.1002/hipo.450050611

Unger, E. K., Keller, J. P., Altermatt, M., Liang, R., Matsui, A., Dong, C., Hon, O. J., Yao, Z., Sun, J., Banala, S., Flanigan, M. E., Jaffe, D. A., Hartanto, S., Carlen, J., Mizuno, G. O., Borden, P. M., Shivange, A. V., Cameron, L. P., Sinning, S., … Tian, L. (2020). Directed Evolution of a Selective and Sensitive Serotonin Sensor via Machine Learning. *Cell*, *183*(7), 1986-2002.e26. https://doi.org/10.1016/j.cell.2020.11.040

van Meer, G., Voelker, D. R., & Feigenson, G. W. (2008). Membrane lipids: Where they are and how they behave. *Nature Reviews Molecular Cell Biology*, *9*(2), 112–124. https://doi.org/10.1038/nrm2330

Vasudeva, R. K., Lin, R. C. S., Simpson, K. L., & Waterhouse, B. D. (2011). Functional organization of the dorsal raphe efferent system with special consideration of nitrergic cell groups. *Journal of Chemical Neuroanatomy*, *41*(4), 281–293. https://doi.org/10.1016/j.jchemneu.2011.05.008

Veetil, J. V., Jin, S., & Ye, K. (2010). A glucose sensor protein for continuous glucose monitoring. *Biosensors and Bioelectronics*, *26*(4), 1650–1655. https://doi.org/10.1016/j.bios.2010.08.052

Venter, J. C., Adams, M. D., Myers, E. W., Li, P. W., Mural, R. J., Sutton, G. G., Smith, H. O., Yandell, M., Evans, C. A., Holt, R. A., Gocayne, J. D., Amanatides, P., Ballew, R. M., Huson, D. H., Wortman, J. R., Zhang, Q., Kodira, C. D., Zheng, X. H., Chen, L., … Zhu, X. (2001). The Sequence of the Human Genome. *THE HUMAN GENOME*, *291*, 49.

Vialli, M., & Erspamer, V. (1937). Ricerche sul secreto delle cellule enterocromaffini. *Zeitschrift für Zellforschung und Mikroskopische Anatomie*, *27*(1), Article 1. https://doi.org/10.1007/BF00391792

Vilardaga, J.-P., Bünemann, M., Krasel, C., Castro, M., & Lohse, M. J. (2003). Measurement of the millisecond activation switch of G protein-coupled receptors in living cells. *Nature Biotechnology*, *21*(7), Article 7. https://doi.org/10.1038/nbt838

Walther, D. J., Peter, J.-U., Bashammakh, S., Hörtnagl, H., Voits, M., Fink, H., & Bader, M. (2003). Synthesis of Serotonin by a Second Tryptophan Hydroxylase Isoform. *Science*, *299*(5603), 76–76. https://doi.org/10.1126/science.1078197

Wan, J., Peng, W., Li, X., Qian, T., Song, K., Zeng, J., Deng, F., Hao, S., Feng, J., Zhang, P., Zhang, Y., Zou, J., Pan, S., Shin, M., Venton, B. J., Zhu, J. J., Jing, M., Xu, M., & Li, Y. (2021). A genetically encoded sensor for measuring serotonin dynamics. *Nature Neuroscience*, *24*(5), 746–752. https://doi.org/10.1038/s41593-021-00823-7

Wang, J., Karpus, J., Zhao, B. S., Luo, Z., Chen, P. R., & He, C. (2012). A Selective Fluorescent Probe for Carbon Monoxide Imaging in Living Cells. *Angewandte Chemie International Edition*, *51*(38), Article 38. https://doi.org/10.1002/anie.201203684

Watson, J., Collin, L., Ho, M., Riley, G., Scott, C., Selkirk, J. V., & Price, G. W. (2000). 5-HT$_{1A}$ receptor agonist-antagonist binding affinity difference as a measure of intrinsic activity in recombinant and native tissue systems: PK$_i$ difference may predict intrinsic activity. *British Journal of Pharmacology*, *130*(5), 1108–1114. https://doi.org/10.1038/sj.bjp.0703394

Wedegaertner, P. B., Wilson, P. T., & Bourne, H. R. (1995). Lipid Modifications of Trimeric G Proteins. *Journal of Biological Chemistry*, *270*(2), 503–506. https://doi.org/10.1074/jbc.270.2.503

Weiss, E. R., Raman, D., Shirakawa, S., Ducceschi, M. H., Bertram, P. T., Wong, F., Kraft, T. W., & Osawa, S. (1998). The cloning of GRK7, a candidate cone opsin kinase, from cone- and rod-dominant mammalian retinas. *Molecular Vision*, *4*, 27.

Weiss, S., Sebben, M., Kemp, D. E., & Bockaert, J. (1986). Serotonin 5-HT1 receptors mediate inhibition of cyclic AMP production in neurons. *European Journal of Pharmacology*, *120*(2), 227–230. https://doi.org/10.1016/0014-2999(86)90544-3

Welford, R. W. D., Vercauteren, M., Trébaul, A., Cattaneo, C., Eckert, D., Garzotti, M., Sieber, P., Segrestaa, J., Studer, R., Groenen, P. M. A., & Nayler, O. (2016). Serotonin biosynthesis as a predictive marker of serotonin pharmacodynamics and disease-induced dysregulation. *Scientific Reports*, *6*, 30059. https://doi.org/10.1038/srep30059

Weller, M., Virmaux, N., & Mandel, P. (1975). Light-stimulated phosphorylation of rhodopsin in the retina: The presence of a protein kinase that is specific for photobleached rhodopsin. *Proceedings of the National Academy of Sciences*, *72*(1), 381–385. https://doi.org/10.1073/pnas.72.1.381

Wingler, L. M., & Lefkowitz, R. J. (2020). Conformational Basis of G Protein-Coupled Receptor Signaling Versatility. *Trends in Cell Biology*, *30*(9), Article 9. https://doi.org/10.1016/j.tcb.2020.06.002

Witherow, D. S., Garrison, T. R., Miller, W. E., & Lefkowitz, R. J. (2004). Beta-Arrestin inhibits NF-kappaB activity by means of its interaction with the NF-kappaB inhibitor IkappaBalpha. *Proceedings of the National Academy of Sciences of the United States of America*, *101*(23), 8603–8607. https://doi.org/10.1073/pnas.0402851101

Yaginuma, H., Kawai, S., Tabata, K. V., Tomiyama, K., Kakizuka, A., Komatsuzaki, T., Noji, H., & Imamura, H. (2014). Diversity in ATP concentrations in a single bacterial cell population revealed by quantitative single-cell imaging. *Scientific Reports*, *4*(1), Article 1. https://doi.org/10.1038/srep06522

Yamauchi, J. G., Nemecz, Á., Nguyen, Q. T., Muller, A., Schroeder, L. F., Talley, T. T., Lindstrom, J., Kleinfeld, D., & Taylor, P. (2011). Characterizing Ligand-Gated Ion Channel Receptors with Genetically Encoded Ca++ Sensors. *PLoS ONE*, *6*(1), e16519. https://doi.org/10.1371/journal.pone.0016519

Yang, F., Moss, L. G., & Phillips, G. N. (1996). The molecular structure of green fluorescent protein. *Nature Biotechnology*, *14*(10), Article 10. https://doi.org/10.1038/nbt1096-1246

Yang, T.-T., Sinai, P., Green, G., Kitts, P. A., Chen, Y.-T., Lybarger, L., Chervenak, R., Patterson, G. H., Piston, D. W., & Kain, S. R. (1998). Improved Fluorescence and Dual Color Detection with Enhanced Blue and Green Variants of the Green Fluorescent Protein. *Journal of Biological Chemistry*, *273*(14), Article 14. https://doi.org/10.1074/jbc.273.14.8212

Yang, Y., Cui, Y., Sang, K., Dong, Y., Ni, Z., Ma, S., & Hu, H. (2018). Ketamine blocks bursting in the lateral habenula to rapidly relieve depression. *Nature*, *554*(7692), 317–322. https://doi.org/10.1038/nature25509

Yohn, C. N., Gergues, M. M., & Samuels, B. A. (2017). The role of 5-HT receptors in depression. *Molecular Brain*, *10*(1), Article 1. https://doi.org/10.1186/s13041-017-0306-y

Yoshida, T., Kakizuka, A., & Imamura, H. (2016). BTeam, a Novel BRET-based Biosensor for the Accurate Quantification of ATP Concentration within Living Cells. *Scientific Reports*, *6*, 39618. https://doi.org/10.1038/srep39618

Yoshizaki, H., Aoki, K., Nakamura, T., & Matsuda, M. (2006). Regulation of RalA GTPase by phosphatidylinositol 3-kinase as visualized by FRET probes. *Biochemical Society Transactions*, *34*(5), 851–854. https://doi.org/10.1042/BST0340851

Zacharias, D. A., Violin, J. D., Newton, A. C., & Tsien, R. Y. (2002). Partitioning of Lipid-Modified Monomeric GFPs into Membrane Microdomains of Live Cells. *Science*, *296*(5569), Article 5569. https://doi.org/10.1126/science.1068539

Zgombick, J. M., Beck, S. G., Mahle, C. D., Craddock-Royal, B., & Maayani, S. (1989). Pertussis toxin-sensitive guanine nucleotide-binding protein(S) couple adenosine A1 and 5-hydroxytryptamine1A receptors to the same effector systems in rat

hippocampus: Biochemical and electrophysiological studies. *Molecular Pharmacology*, *35*(4), Article 4.

Zhang, J., Ma, Y., Taylor, S. S., & Tsien, R. Y. (2001). Genetically encoded reporters of protein kinase A activity reveal impact of substrate tethering. *Proceedings of the National Academy of Sciences*, *98*(26), Article 26. https://doi.org/10.1073/pnas.211566798

Zhang, W. H., Herde, M. K., Mitchell, J. A., Whitfield, J. H., Wulff, A. B., Vongsouthi, V., Sanchez-Romero, I., Gulakova, P. E., Minge, D., Breithausen, B., Schoch, S., Janovjak, H., Jackson, C. J., & Henneberger, C. (2018). Monitoring hippocampal glycine with the computationally designed optical sensor GlyFS. *Nature Chemical Biology*, *14*(9), Article 9. https://doi.org/10.1038/s41589-018-0108-2

Zhao, X., Haeseleer, F., Fariss, R. N., Huang, J., Baehr, W., Milam, A. H., & Palczewski, K. (1997). Molecular cloning and localization of rhodopsin kinase in the mammalian pineal. *Visual Neuroscience*, *14*(2), 225–232. https://doi.org/10.1017/S0952523800011366

Zhao, Y., Araki, S., Wu, J., Teramoto, T., Chang, Y.-F., Nakano, M., Abdelfattah, A. S., Fujiwara, M., Ishihara, T., Nagai, T., & Campbell, R. E. (2011). An Expanded Palette of Genetically Encoded Ca $^{2+}$ Indicators. *Science*, *333*(6051), 1888–1891. https://doi.org/10.1126/science.1208592

Zhao, Y., Jin, J., Hu, Q., Zhou, H.-M., Yi, J., Yu, Z., Xu, L., Wang, X., Yang, Y., & Loscalzo, J. (2011). Genetically Encoded Fluorescent Sensors for Intracellular NADH Detection. *Cell Metabolism*, *14*(4), Article 4. https://doi.org/10.1016/j.cmet.2011.09.004

Zheng, Z., Im, S. H., Lee, B. H., Seo, H., Bae, M. A., & Ahn, S.-H. (2015). In vitro permeability, pharmacokinetics and brain uptake of WAY-100635 and FCWAY in rats using liquid chromatography electrospray ionization tandem mass

spectrometry. *Archives of Pharmacal Research*, *38*(6), 1072–1079. https://doi.org/10.1007/s12272-014-0369-6

Zhou, F., Filipeanu, C. M., Duvernay, M. T., & Wu, G. (2006). Cell-surface targeting of α2-adrenergic receptors—Inhibition by a transport deficient mutant through dimerization. *Cellular Signalling*, *18*(3), 318–327. https://doi.org/10.1016/j.cellsig.2005.05.014

6 Supplements

6.1 Primer Sequences

Primer name	Primer sequence (5' → 3')
N1 1A HIII F	CAGATCTCGAGCTCAAGCTTATGGATGTGCTCAGCCCTGG
1A N1 NI R	ATGATCTAGAGTCGCGGCCGCTCACTGGCGGCAGAACTTACAC
cpGFP F	AACGTCTATATCAAGGCCGACAAG
cpGFP R	GTTGTACTCCAGCTTGTGCCC
S1A Li 2AS M R	TCGGCCTTGATATAGACGTTMNNMNNTGAGCTCAGGAAGCGCGCAGCTCGG
S1A Li 2AS M F	GGCACAAGCTGGAGTACAACNNKNNKGACCAACTGCGAGAGAGGAAGACAGTGAAGACGC
1A Li cG DL1 M R	TCGGCCTTGATATAGACGTTMNNMNNTGAGCTCAGGCGGAAGCGCGCAGC
1A Li cG DL1 M F	GGCACAAGCTGGAGTACAACNNKNNKGACCAACTGGCCCGAGAGAGGAAGACAGT
2AS CF F	GGCACAAGCTGGAGTACAACTGTTTTGACCAACTGCGAGAGAGGAAGACAGTGAAGACGC
2AS CW F	GGCACAAGCTGGAGTACAACTGTTGGGACCAACTGCGAGAGAGGAAGACAGTGAAGACGC
M34 NG Mut R	CTTGATATAGACGTTCTTATAMNNMNNMNNGAAGCGCGCAGCTCG
M34 NG Mut F	AAGCTGGAGTACAACTGTTTTNNKNNKNNKCGAGAGAGGAAGACAGTGAAGAC
M34 sfGFP R	TCCTCGCCCTTGCTCACCATCTTATATGAGCTCAGGAAGCGCG
M34 sfGFP F	GCATGGACGAGCTGTACAAGTGTTTTGACCAACTGCGAGAGA
FP F	ATGGTGAGCAAGGGCGAG
FP R	CTTGTACAGCTCGTCCATGCC
sfcpGFP F	AACGTCTATATCACCGCCGAC
sfcpGFP R	GTTGTACTCCAGCTTGTGCCC
M34KDMut1 F	CTCATGGTGTCGGTGTTGGT
M34KDMut1 R	ACCAACACCGACACCATGAGGTTGGTGACCGCCAAAGAGCC
M34KDMut2 F	GTGCTGTGCTGCACCTCA
M34KDMut2 R	GATGAGGTGCAGCACAGCACGTTGAGGGCGATGAACAGGTCG
M34KDMut3 F	ACCTTTGGAGCTTTCTACATCCC
M34KDMut3 R	ATGTAGAAAGCTCCAAAGGTGGCATAGATAGTGTAGCCATGATCCTTGC
For-pAAV-5-HT1As	CGAACATCGATTGAATTCATGGATGTGCTCAGCCCTGG
S1A3LcG VI FL R	TCGGCCTTGATATAGACGTTGCCGCCGCCGCCGCCGCCCTTGGGCTGCGGGGC
S1A3LcG VI FL F	GGCACAAGCTGGAGTACAACGGCGGCGGCGGCGGCGGCGGTCCTACCCCTTGTGCCC
5HT1Ae-Rev-pAAV	TGCTCGAGGCAAGCTTTCACTGGCGGCAGAACTT
S1A3LcG IV R	TCGGCCTTGATATAGACGTTCCTGCTCCCCGACTCTCC
S1A3LcG IV F	GGCACAAGCTGGAGTACAACAAAGAGCACTTGCCTCTGCC
S1A3LcG IV FL R	TCGGCCTTGATATAGACGTTGCCGCCGCCGCCGCCGCCAGCCTTGCTCTCCACGCC
S1A3LcG IV FL F	GGCACAAGCTGGAGTACAACGGCGGCGGCGGCGGCGGCGTGATCGAGGTGCACCGAGT
S1A3LcGIII R	TCGGCCTTGATATAGACGTTAGCCTTGCTCTCCACGCC

S1A3LcGIII F	GGCACAAGCTGGAGTACAACGTGATCGAGGTGCACCGAG
S1A3LsplitG II dou FL 1AFP 2 R	TCGGCCTTGATATAGACGTTGCCGCCGCCGCCGCCGCCCTGGCGGCAGAACTTACACT
S1A3LcGIII FL R	TCGGCCTTGATATAGACGTTGCCGCCGCCGCCGCCGCCAGCCTTGCTCTCCACGCC
S1A3LsplitcG I FL F	GCATGGACGAGCTGTACAAGGGCGGCGGCGGCGGCGGCGTGATCGAGGTGCACCGAG
S1A3LsplitcG IdouFL R	TCCTCGCCCTTGCTCACCATGCCGCCGCCGCCGCCGCCCTGGCGGCAGAACTTACACT
hacpGFP-pAAV	CTGCTCGAGGCAAGCTTTCAGTTGTACTCCAGCTTGTGCCC
S1A3LsplitG II FL R	TCCTCGCCCTTGCTCACCATGCCGCCGCCGCCGCCGCCAGCCTTGCTCTCCACGCC
S1A3LcGIII FL F	GGCACAAGCTGGAGTACAACGGCGGCGGCGGCGGCGGCGTGATCGAGGTGCACCGAG
GFP paaV R	CTGCTCGAGGCAAGCTTTCACTTGTACAGCTCGTCCATGCC
sfcpGFP builder F	GGCATGGACGAGCTGTACAAGGGCGGTACCGGAGGGAGCATGGTGAGCAAGGGCGAG

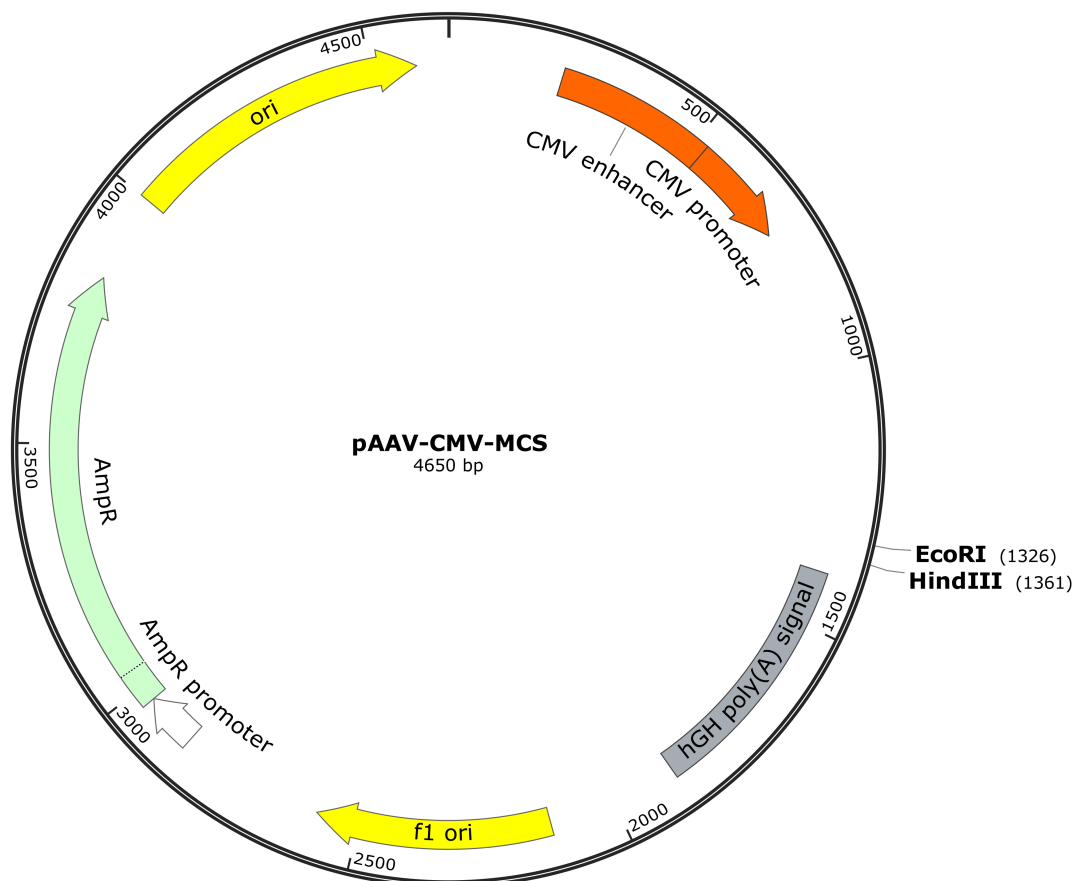## 6.2   Vectormaps of plasmid backbones

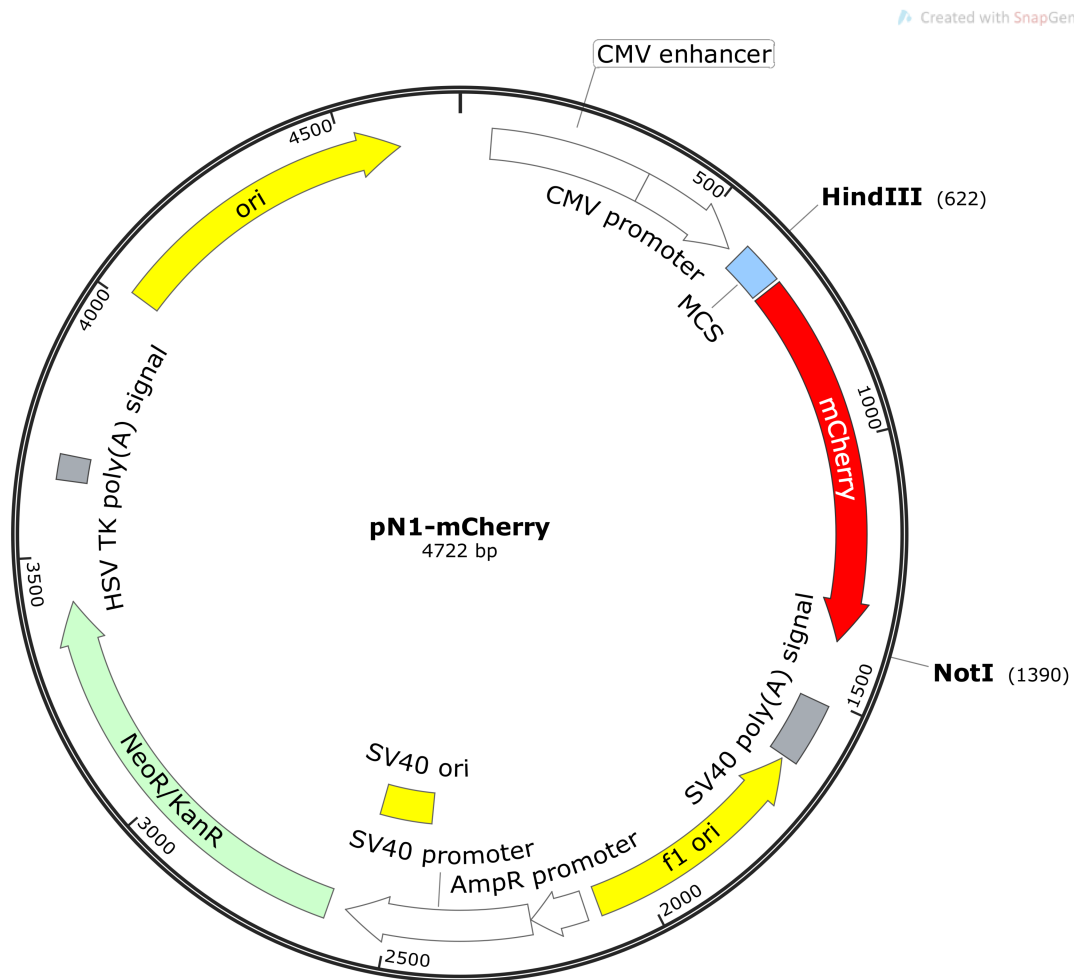*Figure 40: pAAV-CMV-MCS vector*

Figure 41: pN1-mCherry vector
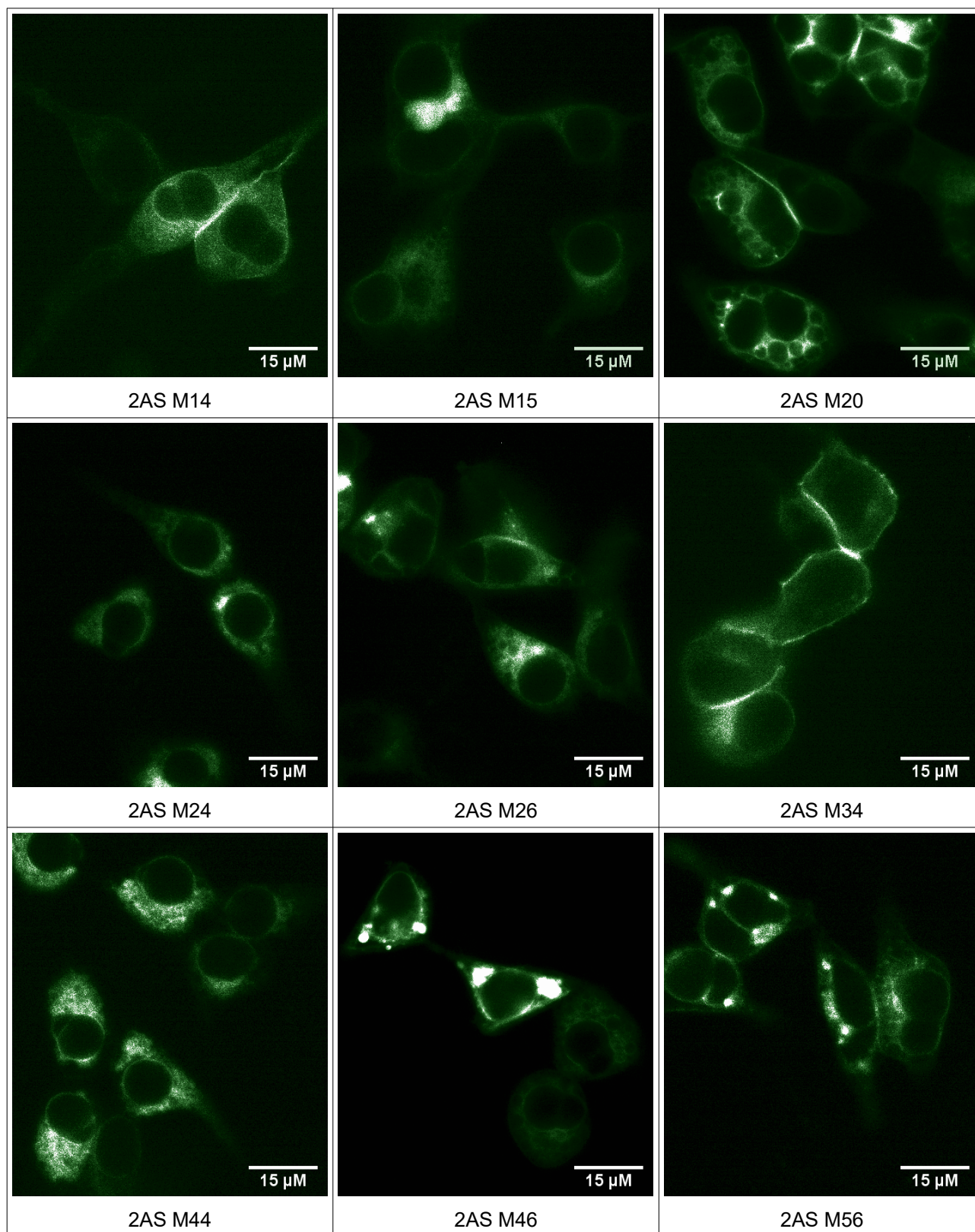
6.3 Example fluorescence profiles

Figure 42: Example fluorescence profiles of different mutants within the 2AS mutant family